K_v2.1 Clustering and Spatial Patterning of Exocytosis in Human Pancreatic β-cells

by

Jianyang Fu

A thesis submitted in partial fulfillment of the requirements for the degree of

Doctor of Philosophy

Department of Pharmacology
University of Alberta

ABSTRACT

K_v2.1 Clustering and Spatial Patterning of Exocytosis in Human Pancreatic β-Cells

PhD Thesis 2018, Jianyang Fu

Department of Pharmacology, University of Alberta

Diabetes is a common metabolic disorder, which is characterized by peripheral insulin resistance and a relative insufficiency of insulin secretion from human pancreatic β-cells. Recent insights indicate that impaired insulin secretion is a key determining factor in type 2 diabetes mellitus (T2D). Thus, a better understanding of the mechanisms mediating granule exocytosis events underlying insulin secretion from human single β-cells is essential.

This present thesis investigates an ion channel, K_v2.1, which regulates the electrical firing of isolated pancreatic β-cells from both non-diabetic and T2D donors. My studies show that expression of K_v2.1 is downregulated in T2D donors. In insulin secreting cells, including pancreatic β-cells, K_v2.1 is compartmentalized in clusters and colocalized with insulin granules. Overexpression of K_v2.1 and restoration of K_v2.1 clusters can rescue pancreatic β-cell exocytotic function.

Similar to compartmentalization of K_v2.1, this present work indicates that exocytotic sites themselves are compartmentalized at "hotspots" in β-cells, and this spatial patterning is impaired in T2D β-cells. K_v2.1 clusters contribute to this compartmentalized exocytosis, in a process that can be regulated by post-translational SUMOylation at the exocytotic site directly.

This work contributes to a novel knowledge of spatial patterning in human pancreatic β-cells and suggests that K_v2.1 clusters and SUMOylation can be potentially important in the pathogenesis of T2D (208 words).

PREFACE

This thesis is an original work by Jianyang Fu. All research work received research ethics approval from the University of Alberta Animal Ethics Board, protocols AUP00000291 and AUP00000405, and the Human Ethics Board, protocols Pro00013094 and Pro00001754.

A version of Chapter 2 has been published as JY. Fu, XQ Dai, G Plummer, K Suzuki, A Bautista, J. M. Githaka, L. Senior, M. Jensen, D Greitzer-Antes, J E. Manning Fox, H Y. Gaisano, C. B. Newgard, N. Touret and P. E. MacDonald. (2017) K_v2.1 Clustering Contributes to Insulin Exocytosis and Rescues Human β-Cell Dysfunction. *Diabetes*, **66**(7), 1890-1900. I was responsible for the majority of the data collection, data analysis, and manuscript composition. X. Dai, G. Plummer, K. Suzuki, A. Bautista, J.M. Githaka, L. Senior and J.E. Manning Fox contributed to data collection as outlined in the figure legends in Chapter 2. P.E. MacDonald was the supervisory author and was involved with concept formation and editing of the manuscript.

A version of Chapter 3 is to be submitted as JY Fu, XQ Dai, G. Plummer, K. Suzuki, J. M Githaka, M. Jensen, D. Greitzer-Antes, J. E Manning Fox, H. Y. Gaisano, C. B. Newgard, N Touret, P.E. MacDonald (2018). K_v2.1 Clustering Contributes to Exocytosis Hotspots and Rescues Human β-Cell Dysfunction. I was responsible for the majority of the data collection, analysis, and manuscript composition. X. Dai, G. Plummer, J.M. Githaka, and J.E. Manning Fox contributed to data collection as outlined in the figure legends in Chapter 3. P.E. MacDonald was the supervisory author and was involved with concept formation and editing of the manuscript. In Chapter 4, I was responsible for the majority of the data collection and analysis. K. Suzuki, D. Greitzer-Antes and M. Jensen prepared plasmids. P.E. MacDonald was the supervisory authority and was involved in concept formation.

ACKNOWLEDGEMENTS

First of all, I would like to offer my utmost gratitude to my supervisor, Dr. Patrick MacDonald for giving me an opportunity six years ago. Thank you for your generous support, excellent guidance, continuous support throughout my education. Your knowledge and enthusiasm for diabetes and electrophysiology helped me developing the ability of critical thinking and problem solving. I owe you big thanks!

I am also sincerely grateful to my supervisory committee membranes, Dr. Xing-Zhen Chen and Dr. Peter Light. Thanks a lot for asking questions, providing suggestions and discussing projects together with me. I really appreciate that. Thanks Dr. Chen for inviting me to join your lab party especially when I first arrived in Canada. Your patience and kindness eliminated my fear towards a brand-new living and studying environment. Thanks Dr. Light for providing me many suggestions and advices for my future care. Your professional guidance and recommendations help me a lot for embracing the future. I would also like to thank Dr. Herbert Gaisano at the University of Toronto for allowing me to study time-lapse live cell imaging in his laboratory.

I would like to thank the past and present members of the MacDonald lab, including Xiaoqing Dai, Joss Manning Fox, Mourad Ferdaoussi, Greg Plummer, James Lyon, Aliya Spigelman, Nancy Smith, Jelena Kolic and Cathy Pretzlaw. Especially thanks to Xiaoqing for helping me with patch clamp. Thanks Greg for guiding with me with imaging and western blot. Thanks Jelena for all your help and encouragement. I will always be grateful.

Last but not least, I owe my greatest gratitude to my family and my friends for their love and support during these years. I owe a great deal to my wife Tammy, who sacrifices a lot for her career and our coming son. I cannot make this journey without your accompaniment.

TABLE OF CONTENTS

LIST OF FIGURES

Chapter 1. Introduction

Chapter 2. K_v2.1 clustering contributes to insulin exocytosis and rescues β-cell dysfunction

Chapter 4. $K_v2.1$ Clustering Regulates Exocytosis Spatial Pattern In Human Pancreatic β-cells

LIST OF TABLES

ABBREVIATIONS

2, 3-BPG	2, 3-Bis-Phosphoglycerate
2-ME	2-mercaptoethanol
4-AP	4-aminopyridine
ADP	Adenosine diphosphate
ANOVA	Analysis of Variance
ATP	Adenosine triphosphate
ATPase	Adenosine Triphosphatase
AU	Arbitrary Unit
BK channel	Big voltage-dependent K^+ channel
BMI	Body Mass Index
cAMP	Cyclic Adenosine Monophosphate
CAMs	Cell-adhesion Molecules
CAZ	Cytomatrix assembled at the active zone
CHO	Chinese hamster ovary
DAG	Diacylglycerol
DM	Diabetes mellitus
DMEM	Dulbecco's Modified Eagle's medium
DMSO	Dimethyl sulfoxide
DTSSP	3,3'-dithiobis(sulfosuccinimidyl propionate
ECM	Extracellular matrix
EGFP	Enhanced green fluorescent protein
ELEC	Electrostatic
FBS	Fetal bovine serum
FFAs	Fee fatty acids
FPG	Fasting plasma glucose
GDM	Gestational diabetes
GIP	Glucose-dependent insulinotropic peptide
GLP-1	Glucagon-like peptide-1
GLP-2	Glucagon-like peptide-2
GLUT	Glucose transporter
GPCR	G-protein-coupled receptor
GRPP	Glicentin-related pancreatic polypeptide
GSIS	Glucose-stimulated insulin secretion
HbA1C	Hemoglobin A1c
HCN	Hyperpolarization-activated cyclic nucleotide gated channels
HEK	Human embryonic kidney cell
IFG	Impaired fasting blood glucose
IGT	Impaired glucose tolerance
IK channel	Intimidate Ca^{2+} activated K^+ channel

INS-1	Rat Insulinoma Cell Line
IP-1	Intervening peptide-1
IP-2	Intervening peptide-2
IPGTT	Intraperitoneal glucose tolerance test
IR	Insulin Receptor
IRS	Insulin receptor substrate
K_{ATP}	ATP-sensitive K^+ channels
K_{Ca}	Ca^{2+}-activated K^+ channels
Kir	Potassium inward rectifier
K_v	Voltage-gated potassium channels
LDCVs	Large dense-core vesicles
MAG	Myelin-associated glycoprotein
MAP-Kinase	Mitogen-activated Protein Kinase
min	Minute
mRNA	Messenger RNA
ms	Milliseconds
Munc	Mammalian uncoordinated- homology protein
NADH	Nicotinamide adenine dinucleotide
NADPH	Nicotinamide adenine dinucleotide phosphate
Na_v	Voltage-dependent Na^+ channels
NBD	Nucleotide-binding domain
ND	Non-diabetic
NF-κβ	Nuclear factor kappa-light-chain-enhancer of activated B cells
NPY	Neuropeptide Y
OGTT	Oral glucose tolerance test
P2K1	Two-pore-domain potassium channels
PA	photoactivatable
PALM	Photo-activated localization microscopy
PC1/2	prohormone convertases 1/2
PDB	Protein Data Bank
PDK1	Phosphoinositide-Dependent Kinase-1
PDX-1	Pancreatic duodenal homeobox 1
PI-3K	Phosphoinositide 3-kinase
PIP2	Phosphatidylinositol 4, 5-bisphosphate
PKD	Protein Kinase D
PP Cell	Pancreatic polypeptide cells
PRC	Proximal restriction and clustering in C-terminus
RBC	Red blood cells
RER	Rough endoplasmic reticulum
RIM 2	Regulating synaptic membrane exocytosis protein 2

RIP	Rat Insulin Promoter
RP	Reserve Pool
RRP	Ready Release Pool
SENPs	Sentrin/SUMO-specific proteases
SG	Secretory granules
shRNA	Short Hairpin Ribonucleic Acid
SK channel	Small Ca^{2+} activated K^+ channel
SLVs	Synaptic-like vesicles
SM	Sec1/Munc18-like
SNAP	Synaptosomal-associated protein
SNAP-25	Synaptosomal-associated protein 25
SNARE	Soluble N-ethylmaleimide-sensitive factor attachment protein receptor
STED	Stimulated emission depletion microscopy
Stx	Syntaxin
STX	Stromatoxin
SUMO	Small ubiquitin-like modifier
SUR	Sulfonylurea receptor
Syt	Synaptotagmin
T2D	Type 2 diabetes mellitus
TASK	Twik-related acid-sensitive K^+ channels
TCA	Tricarboxylic acid cycle
TEA	Tetraethyl ammonium
TIRF	Total internal reflection fluorescence
TMD	Transmembrane domain
TPeA	Tetrapentylammonium
TRP	Transient receptor potential
t-SNARE	Target-membrane SNARE proteins
UV	Ultraviolet
V	Voltage
VAMP	Vesicle-associated membrane protein
VDCC	Voltage-gated calcium channels
VDW	Van Der Waals
Vm	Membrane Potential
VSAC	Volume-sensitive anion channels
v-SNARE	Vesicle-associated SNARE protein
WT	Wide Type
Z-FIX	Zinc Formalin Fixative
µg	Microgram
µL	Microliter
µM	Micromolar

CHAPTER 1

Introduction

1.1 DIABETES AND INSULIN SECREION FROM BETA CELLS

1.1.1 Diabetes mellitus

Diabetes mellitus (DM) is a disease whose symptoms have been recorded in the annals of history ever since the earliest reports of the presence of glycosuria in 1500 BC (Brunton, 1874). Nowadays, according to International Diabetes Federation, diabetes is defined as a chronic disease in which the body cannot produce or respond to insulin properly, resulting in abnormal metabolism of elevated level of blood glucose. Diabetes can cause serious complications, such as heart disease, blindness and kidney failure.

Across the globe, including in Canada, the economic burden of diagnosed diabetes is enormous and growing. In 2018, the International Diabetes Federation estimated that in 2017 there were 451 million (age 18-99 years) people with diabetes worldwide. This number is expected to increase to 693 million by 2045. It was estimated that almost half of all people (49.7%) living with diabetes are undiagnosed. In 2017, around 5 million deaths worldwide were attributable to diabetes in the 20-99 years age range. The global healthcare expenditure on people with diabetes was estimated to be 850 billion USD in 2017 (Cho et al., 2018). In Canada, there are 11 million Canadians living with diabetes or prediabetes. Every three minutes, another Canadian is diagnosed. In Alberta, there are around 1 million people diagnosed with diabetes or prediabetes in 2016. This number was expected to increase to 1.3 million by 2026, according to Diabetes Canada latest report. Total health care costs attributable to diabetes in Canada during the last 10 years were $7.55 billion for females and $7.81 billion for males ($15.36 billion total) (Anja & Laura, 2017). Clearly, diabetes represents a heavy health care burden in Alberta, Canada and around the world.

There are three major types of diabetes. Type 1 DM, sometimes referred to "insulin-dependent diabetes mellitus", when the pancreas cannot produce enough insulin because of auto-immune destruction of the β-cells in the islets. T2D, previously regarded as "non-insulin dependent diabetes mellitus", has been characterized as primarily driven by insulin resistance. However, it is more clear these days that defective insulin secretion from β-cells is a major contributing factor to the development of T2D (Prentki & Nolan, 2006). Gestational diabetes (GDM) is a temporary diabetic condition that occurs during pregnancy because the pancreas cannot secrete enough insulin to counterbalance the effect of pregnancy hormones. Between three to 20 per cent of pregnant women develop gestational diabetes. Women who have had GDM have a substantially increased risk for development of T2D, even though ~96% women return to a euglycaemic state shortly after delivery (Kampmann et al., 2015). There are also other forms of diabetes that result from rare genetic mutations, drug side effects or complications associated with other diseases.

The precursor stage before diabetes mellitus, in which not all of the symptoms required to diagnose diabetes are present, but blood sugar is abnormally high, is regarded as pre-diabetes. There are two forms of prediabetes, impaired fasting blood glucose and impaired glucose tolerance. Although they are similar in clinical definition (glucose levels too high for their context), the pathophysiologic mechanisms that contribute to these disturbances in glucose homeostasis are different (Festa et al., 2004; Hanefeld et al., 2003). Impaired fasting blood glucose (IFG) is characterized by fasting glucose consistently above the normal range, but below the diagnostic cut-off for a formal diagnosis of diabetes mellitus while impaired glucose tolerance (IGT) is characterized by the body becoming less sensitive to the effects of insulin (Aguiree et al., 2017).

Based on International Diabetes Federation's newest report in 2017, both diabetes and pre-diabetes can be diagnosed based on plasma glucose criteria, either the fasting plasma glucose (FPG) or the 2-hours plasma glucose (2-h PG) value during a 75-g oral glucose tolerance test (OGTT), or hemoglobin A1c (HbA1C) criteria (Table 1). Clinically, diabetes mellitus is diagnosed as the fasting plasma glucose level higher than 7.0 mmol/L and higher than 11.1 mmol/L two hours after a 75-g oral glucose load in a glucose tolerance test. Another criterion of diabetes mellitus is random plasma glucose greater than 11.1 mmol/L or HbA1C greater than 48 mmol/mol. Pre-diabetes should be diagnosed if both of the following criteria are met. IFG is diagnosed as the fasting plasma glucose level lower than 7.0 mmol/L, but between 7.8 and 11.1mmol/L 2-hours after a 75-g oral glucose load. Alternatively, IGF is defined as the fasting plasma glucose level between 6.1 and 6.9 while it is lower than 7.8 mmol/L two hours after a 75g oral glucose load.

Table 1

Criteria	Diabetes[1]	Pre-Diabetes[2]	
		Impaired glucose tolerance (IGF)	Impaired fasting glucose (IFG)
Fasting plasma glucose	>7.0 mmol/L	<7.0 mmol/L	6.1-6.9 mmol/L
2-hour plasma glucose following 75g oral glucose	>11.1 mmol/L[3]	7.8-11.1 mmol/L	<7.8 mmol/L

1. Diabetes should be diagnosed if one or more of the above criteria are met
2. Pre-diabetes should be diagnosed if both above criteria are met
3. Another criteria of diabetes is when random glucose >11.1 mmol/L or HbA1C > 48mmol/mol (equivalent to 6.5%)

Table 1 diabetes diagnosis criteria according to International Diabetes Federation, 2017.

1.1.2 Glucose homeostasis

Under physiological conditions, plasma glucose is constantly under homeostasis. To ensure the normal body function, it is essential to have a tight control of the blood glucose level (Röder, Wu, Liu, & Han, 2016). Break down of glucose homeostatic control leads to diabetes.

Why is glucose homeostasis so important? The major reason is that both the brain and red blood cells (RBCs) require a constant glucose supply to maintain their basic functions. In the brain, nervous tissues, such as neurons and glial cells, use glucose as the major energy substrate. Under hypoglycemic conditions, ketone bodies can replace 20% of the glucose requirement. Since there are no mitochondria in mature RBCs, anaerobic glycolysis is essential to provide energy for a period ranging from 10 seconds to 2 minutes. In red blood cells, 2, 3-bis-phosphoglycerate (2, 3-BPG) is required for effective transport of oxygen (Paolisso, Scheen, d'Onofrio, & Lefebvre, 1990).

The brain is important for glucose homeostasis, since it functions as an insulin sensitive tissue. Evidence of insulin action in the brain was shown 40 years ago (Woods, Lotter, McKay, & Porte, 1979). Neuronal systems sense and respond to hormonal inputs such as insulin, glucagon and leptin that are secreted from pancreatic islet and body fat tissues, and from the metabolism of circulating glucose and free fatty acids (FFAs). The brain, specifically the hypothalamus, can respond to feedback and make adaptive changes occur in energy intake, expenditure and hepatic glucose production (Schwartz & Porte, 2005). In these regions, there are glucose-excited or inhibited neurons and glucose sensing glial cells that function together to sense glucose and maintain plasma glucose homeostasis by regulating glucose production *in vivo* (Routh, Hao, Santiago, Sheng, & Zhou, 2014).

The liver has a unique role in the regulation of blood glucose to maintain glucose homeostasis. First of all, the liver can both produce and store glucose. Second, the insulin concentration in the liver is 3 to 10 times higher than that in systemic circulation. Third, liver is the only site of the glucose regulation by secreted glucagon (Sherwin, 1980). Last but not the least, the gut-brain-liver axis controls glucose homeostasis (Scarlett & Schwartz, 2015). In short, the liver has the ability to store glucose as glycogen when plasma glucose is elevated. When hypoglycemia happens, gluconeogenesis in the liver turns the glycogen into glucose to maintain glucose homeostasis.

The gastrointestinal tract has a crucial role in the control of glucose homeostasis through its role in the digestion, absorption, and assimilation of ingested nutrients, which is associated with secretion of multiple gut hormones. Incretin hormones, including gastrointestinal hormones such as glucose-dependent insulinotropic peptide (GIP) and glucagon-like peptide-1 (GLP-1), can promote insulin biosynthesis and secretion, and islet β cell survival (Drucker, 2007).

Last and foremost, islets play an essential role in the regulation of nutrient metabolism and glucose homeostasis by secreting various pancreatic hormones. The total number of islets in a human pancreas is around 3.2 to 14.8 million, with a total islet volume of 0.5 to 2.0 cm^3 (HELLMAN, 1959; Ionescu-Tirgoviste et al., 2015; Kim et al., 2009; Saito, Iwama, & Takahashi, 1978). Within one human islet, there are 30-50% glucagon-producing α-cells, 50-60% insulin-producing β-cells and ~10% of other cells, including somatostatin-producing δ-cells, γ-cells, ghrelin-producing ε-cells and pancreatic polypeptide-producing (PP) cells (In't Veld & Marichal, 2010). Among them, both insulin from β-cells and glucagon from α-cells are essential for glucose homeostasis.

Insulin is a hormone produced, stored and secreted from pancreatic β-cells, in the islets of Langerhans. In 1869, Paul Langerhans first discovered the cells that secrete insulin, named after him as the islets of Langerhans. In 1889, Oscar Minkowski and Joseph von Mering first discovered the role of the pancreas in diabetes from dog experiments. In 1921, insulin was first discovered and extracted at the University of Toronto by Frederick Banting and John Macleod, who won the Nobel Prize in Physiology or Medicine in 1923. Insulin was refined and purified to a form which permitted clinical by James Collip from University of Alberta. Since then, commercial production of insulin has helped patients living with diabetes (Quianzon & Cheikh, 2012). The insulin signaling cascade and insulin secretion pattern will be discussed in the next section. For Type-1 diabetes patients, insulin therapy is the first and the major treatment.

Glucagon was first reported as a second substance in aqueous extractions with insulin (Kimball & Murlin, 1923). Contrary to insulin, glucagon is known to elevate plasma glucose by promoting gluconeogenesis and glycogenolysis to keep glucose homeostasis. Glucagon was discovered as a major hormone produced from pancreatic α-cells in 1948 and further confirmed by immunocytochemistry in 1962 (Baum, Simons Jr, Unger, & Madison, 1962; Sutherland, 1948). Human glucagon has 29 amino acids, with 3.49 KDa in size. Glucagon is first produced as pro-glucagon. In pancreatic α-cells, after cleavage by prohormone convertase-2 (PC2), glucagon, glicentin-related pancreatic polypeptide (GRPP), intervening peptide-1 (IP-1) and major pro-glucagon fragment are produced (Rouille, Martin, & Steiner, 1995), whereas in L cells of the small intestine and the brain, pro-glucagon is cleaved by PC1/3 into oxyntomodulin, intervening peptide-2 (IP-2), GLP-1, and glucagon-like peptide-2 (GLP-2) (Bell, Santerre, & Mullenbach, 1983). GLP-1 can inhibit glucagon secretion and promote insulin secretion (Orskov & Orskov, 1992). Thus, GLP-1 analogues are developed as another treatment of type 2 diabetes.

1.1.3 Insulin, signaling cascade and secretion pattern

The hallmark of diabetes is a relative lack of insulin or the inability of the peripheral tissue to respond to insulin, leading to high levels of blood glucose (Aguiree et al., 2017). Impaired insulin secretion is required for both Type 1 diabetes (T1D) and T2D to develop. Thus, a better understanding of insulin itself, mechanisms of its action, and how it is secreted essential to facing this challenge of diabetes.

The human insulin (protein data bank (PDB): 1LPH) has 51 amino acids, with 5.8 KDa molecular mass. It is composed of an A-Chain (Green chain shown in Figure 1A) and a B-chain (Red chain shown in Figure 1A), linked together by disulfide bonds. Similar to the production of glucagon in pancreatic β-cells, insulin is first produced as a prepropeptide, pre-proinsulin. When translocated to the rough endoplasmic reticulum (RER), one 24-aa signal polypeptide is cleaved to form proinsulin (PDB: 2KQP). Different from the structure of insulin, proinsulin has C-peptide (cyan chain in Figure 1B), which is further cleaved by cellular endopeptidases known as prohormone convertases (PC2 & PC1/3), as well as the exoprotease carboxypeptidase E (Steiner & Oyer, 1967). Mature insulin is further packed in insulin granules, waiting for exocytosis upon stimulation.

When blood glucose increases, insulin is secreted to the circulation and binds with the insulin receptor (Figure 1C), which is a disulfide-linked $(\alpha\beta)_2$ receptor tyrosine kinase (Menting et al., 2014). Thus, insulin signaling will be activated, which includes two major branches of signaling cascade through insulin receptor substrate (IRS) proteins. Both phosphatidylinositol-3-kinase (PI-3K, Phosphoinositide 3-kinase) and mitogen-activated protein kinase (MAP-Kinase) pathways will be activated (White, 2003).

Figure 1

A.

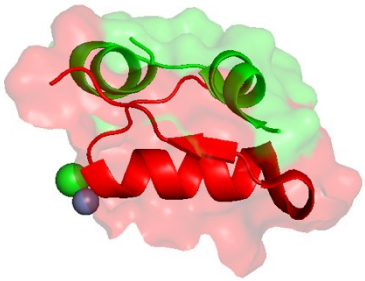

B.

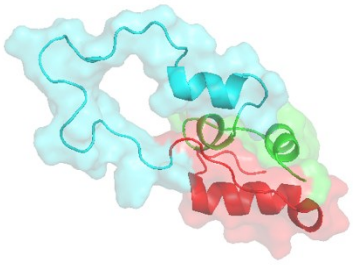

C.

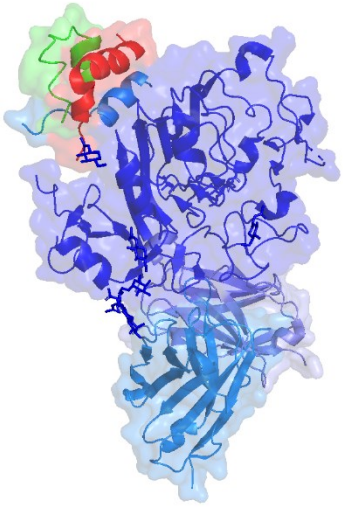

Figure 1. The structure of human insulin (A), proinsulin (B) and the interaction between insulin and insulin receptors (C).

The first signaling pathway can be explained as follows. Activation of PI-3K can trigger activation of 3'-phosphoinositide-dependent protein kinase 1 (PDK1). After that, the Akt cascade and the Grb2/SOS will be stimulated to trigger ras kinase cascade. This pathway is responsible for cell survival and proliferation, synthesis of proteins and the distribution of glucose.

The second signal cascade can be explained as follows. Activation of the receptors for insulin and IGF1 results in tyrosine phosphorylation of the IRS proteins, which bind PI3K (p85/p110) and Grb2/SOS. The Grb2/SOS complex promotes GDP/GTP exchange on p21 ras, which activates the ras→RAF→MEK→ERK1/2 cascade. This pathway is essential for mitogenic functions such gene transcription and cell growth.

Clearly, a better understanding of insulin signaling pathways impacting on diabetes can improve our understanding of insulin action and insulin resistance at the cellular level. However, another direction is focusing on insulin secretion itself. Under physiological conditions, pancreatic β-cells secrete insulin in a biphasic manner, called first and second phase insulin secretion (Cheng, Andrikopoulos, & E Gunton, 2013). This characteristic biphasic pattern was first demonstrated by Dr. Grodsky around 40 years ago (O'Connor, Landahl, & Grodsky, 1980). In vivo, first phase insulin secretion starts within ~2 minutes of nutrition ingestion from diet and lasts for 10~15 minutes. In contrast, the second phase of insulin secretion is prolonged and sustained, lasting around 5~60 minutes, after which secretion reaches a plateau.

In vitro, first phase of insulin secretion is characterized as the exocytosis from the ready release pool (RRP) of granules; a small fraction of docked granules that are primed and thus immediately available for release on stimulation. Since the insulin granules in RRP are associated with the plasma membrane, it takes less time to release under an acute calcium-dependent stimulation. Within the RRP, there are around 1~5% of all insulin granules, which is

around 20~100 granules depending on the experimental conditions (Gromada et al., 1999; Renstrom, Eliasson, & Rorsman, 1997). There are about 40 granules undergoing exocytosis during the first phase insulin secretion per pancreatic β-cell (Patrik Rorsman et al., 2000). Since docking granules in RRP will be depleted, the insulin granules inside of the cell will be recruited and start to undergo exocytosis. Thus, the second phase of insulin secretion starts.

The second phase of insulin secretion is characterized by the fusion events from reserve pool (RP), where a large amount (up to 99%) of insulin granules sit further beneath the surface of cell membrane. Since it requires the trafficking of the reserved granule pool to the plasma membrane, the second phase of insulin secretion is much slower and long-lasting. Different from the first phase, newcomer secretory granules (SG), other than depletion of docking granules, account for subsequent insulin release (Gaisano, 2014; Shibasaki et al., 2007).

In type 2 diabetes, diminution of first-phase insulin release is the earliest detectable and an independent predictor of impaired of β-cell function (Gerich, 2002). Thus, focusing on insulin granules and the associated exocytotic proteins within the pancreatic β-cells, including docked granules and newcomer SGs, is becoming a novel target for diabetes for diabetes prevention and remediation (Aslamy & Thurmond, 2017).

1.1.4 Insulin secretion from pancreatic β-cells

Pancreatic β-cells are electrically excitable, able to sense and respond quickly to postprandial increases of blood glucose. When blood glucose is less than 5 mM (Dean & Matthews, 1970), rodent β-cells are electrically silent, with a resting membrane potential around -70 mV due to a high resting K^+ conductance (Matthews & Sakamoto, 1975; Meissner, Henquin, & Preissler, 1978; Meissner & Schmelz, 1974).

When plasma glucose concentration elevates after food intake, membrane depolarization of pancreatic β-cells happens. Glucose enters through a "liver type" glucose transporter (GLUT). As opposed to Glut2 in rodents, human pancreatic β-cells express Glut1 (De Vos et al., 1995; Fukumoto et al., 1988). This is important for glucose-stimulated insulin secretion, after which glucokinase plays a central role as glucose sensor by regulating glucose phosphorylation and glycolysis in both human and rodent cells (De Vos et al., 1995; Meglasson & Matschinsky, 1984). Pyruvate is produced and enters the mitochondria and is decarboxylated to acetyl-CoA, which enters the tricarboxylic acid cycle (TCA), resulting in the production of nicotinamide adenine dinucleotide (NADH) and $FADH_2$. These reducing balance are oxidized in the respiratory chain to produce ATP (P. E. MacDonald, Joseph, & Rorsman, 2005).

As a result, the intracellular ATP/ADP ratio increases. ATP-sensitive K^+ (K_{ATP}) channels will close to depolarize the cell membrane and activate the voltage-gated calcium channels (VDCC), which triggers exocytosis of insulin granules. After that, voltage-gated K^+ (K_v) channels start to open to mediate repolazation. Action potentials are terminated by the opening of K_v channels, which limit Ca^{2+} entry and insulin secretion (Dean and Matthews 1970; Pace and Price 1972). Thus, ion channels play an essential role in insulin granule coupling and insulin secretion (Figure 2).

Figure 2. Insulin secretion from pancreatic β-cells

Figure 2 presents a classic model for glucose-dependent insulin secretion from pancreatic β-cells. After transport into pancreatic β-cells via a GLUT transporter and metabolism by the mitochondria to increase ATP/ADP ratio, glucose triggers a depolarization through the closure of ATP-sensitive K^+ (K_{ATP}) channels. Membrane depolarization triggers voltage-dependent Ca^{2+} channel (VDCC) opening, followed by the entry of Ca^{2+}. Elevated Ca^{2+} concentration will lead to insulin granule exocytosis. Voltage-dependent K^+ (K_v) channels act to repolarize the β-cell plasma membrane.

Figure 2

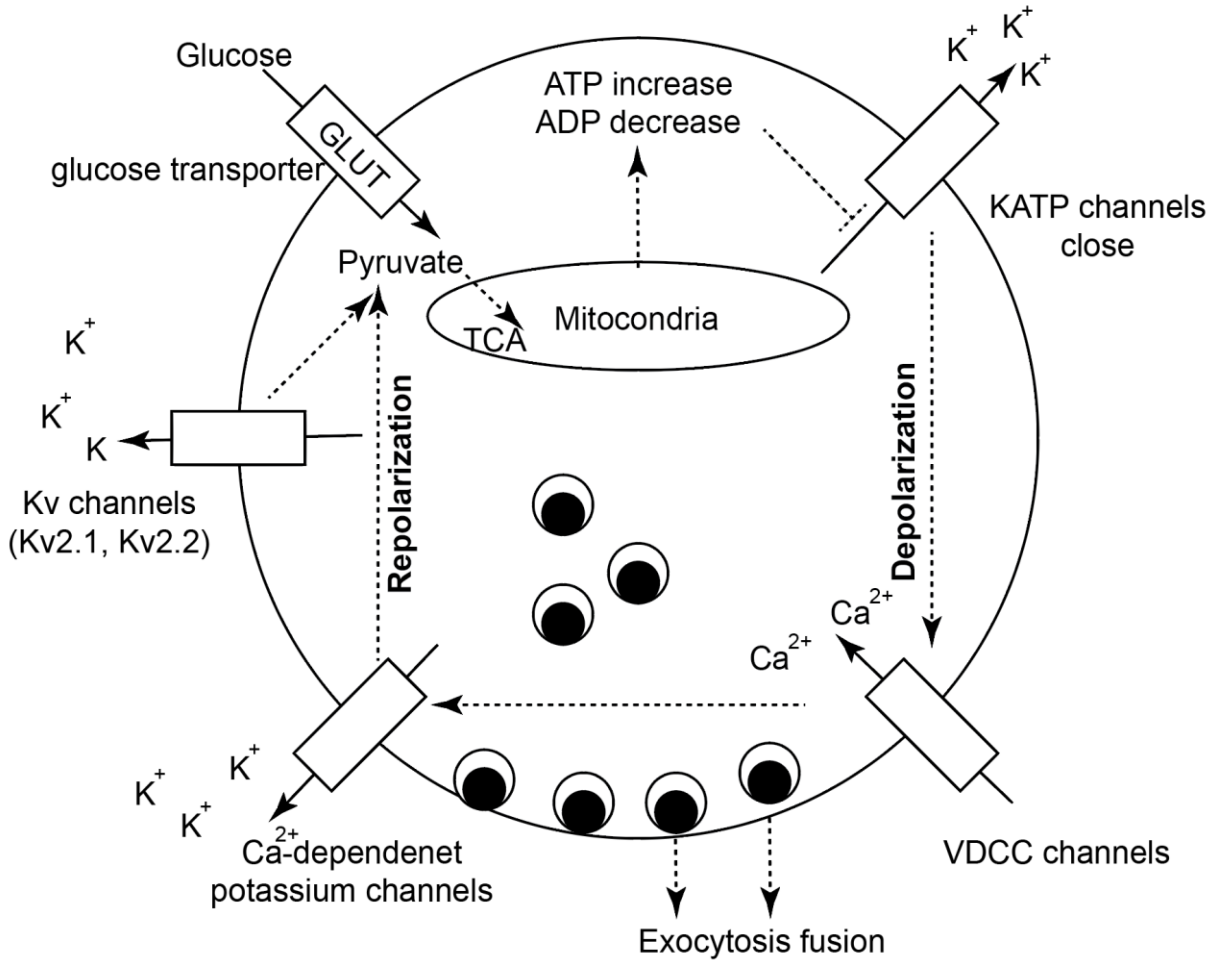
Glucose
GLUT
glucose transporter
ATP increase
ADP decrease
K+ K+
K+
KATP channels
close
Pyruvate
TCA
Mitocondria
K+
K+
K
Kv channels
(Kv2.1, Kv2.2)
Repolarization
Depolarization
Ca2+
Ca2+
K+ K+
K+
Ca2+-dependenet
potassium channels
VDCC channels
Exocytosis fusion

1.2 ION CHANNELS ON PANCREATIC BETA-CELLS

On the cell membrane of pancreatic β-cells, there are more than 16 ion channel families, including about 50 different type of ion channels that contribute to electrical firing (F M Ashcroft & Rorsman, 1989; Drews, Krippeit-Drews, & Dufer, 2010). Among them, ATP-sensitive K^+ (K_{ATP}) channels, voltage-dependent Ca^{2+} channels (VDCCs), Ca^{2+}-activated K^+ (K_{Ca}) channels, voltage-dependent Na^+ (Na_v) channels and voltage-dependent K^+ (K_v) channels, play central roles in electrical activity and regulating glucose-dependent insulin secretion (Fig 3).

1.2.1 ATP-sensitive potassium channel (K_{ATP} channel)

K_{ATP} channels were first discovered in cardiac myocytes in 1983 (Noma, 1983). One year later, both a glucose-sensitive K^+ channel (Frances M Ashcroft, Harrison, & Ashcroft, 1984) and an ATP-sensitive channel (Cook & Hales, 1984) were reported in pancreatic β-cells. This channel is active at resting membrane potentials and can be inhibited by glucose. Moreover, it links metabolism and membrane K^+ permeability. In 1985, it was determined that these were the same channel, known as the K_{ATP} channel today (P Rorsman & Trube, 1985). It suggests that glucose can depolarize the pancreatic β-cells by increasing the cytoplasmic concentration of ATP. These days, K_{ATP} is identified as widely distributed and present in a number of tissues including muscle, pancreatic β-cells and the brain (Tinker, Aziz, & Thomas, 2014).

The K_{ATP} channel consists of four pore-forming subunits (potassium inward rectifier 6, Kir 6.x) and four regulatory subunits (Sulfonylurea receptor, SURx). In mammalian cells, there are two Kir 6.x genes and two SURx genes, including Kir 6.1 (*KCNJ8*), Kir 6.2 (*KCNJ11*), SUR1 (*ABCC8*) and SUR2 (*ABCC9*). In pancreatic β-cells, K_{ATP} channels are composed of Kir 6.2 and SUR1 subunits (Kir6.2/SUR1). Kir6.2 has two transmembrane helices (M1 and M2) and

intracellular N- and C-terminus tails. Each SUR1 subunit contains one five-helix transmembrane domain (TMD0), two six-helix transmembrane domains (TMD1 and TMD2), two nucleotide-binding domains (NBD1 and NBD2) and extracellular N- and intracellular C-termini (Aguilar-Bryan & Bryan, 1999; F M Ashcroft & Gribble, 2000; Tucker et al., 1998).

K_{ATP} channels can sense intracellular ATP/ADP through an interaction with ATP directly. ATP binds Kir6.2 to inhibit the channel while MgADP and MgATP could bind with NBD 1 and NBD 2 separately in SUR1 subunits to activate this channel (F M Ashcroft & Gribble, 2000). MgADP binding to NBD more likely induces a conformational change at NBD2 that transduces another conformational change in NBD1 to stabilize ATP binding at NBD1 (Ueda, Komine, Matsuo, Seino, & Amachi, 1999).When the ATP/MgADP ratio increases, MgADP unbinding initiates a conformational change to the closed state in K_{ATP} channels (F M Ashcroft & Gribble, 2000). K_{ATP} channels are a major target for the treatment of type 2 diabetes and neonatal diabetes. However, the use of sulfonylurea class of drugs inhibits K_{ATP} channels to depolarize pancreatic β-cells and trigger insulin secretion.

Figure 3. Summary diagram of the ionic currents in human pancreatic β-cell

Major transmembrane currents are:

$\boldsymbol{I}_{CaP}$ is the voltage-gated P-type Ca^{2+} current, which is also responsible for insulin release. $\boldsymbol{I}_{CaL}$ is the voltage-gated L-type Ca^{2+} current, $\boldsymbol{I}_{CaT}$ is the voltage-gated T-type Ca^{2+} current.

$\boldsymbol{I}_{Na}$, voltage-gated Na^{+} current; $\boldsymbol{I}_{Nab}$, Na^{+} background current

$\boldsymbol{I}_{KDr}$, delayed rectifier K^{+} current; $\boldsymbol{I}_{KCaB}$, Ca^{2+} and big voltage-dependent K^{+} (BK channel) current; $\boldsymbol{I}_{KCa}$, small Ca^{2+} activated K^{+} (SK channel) current; $\boldsymbol{I}_{Kher}$ is the human-ERG K^{+} channel current and $\boldsymbol{I}_{KATP}$, ATP-sensitive K^{+} channels current.

Figure 3

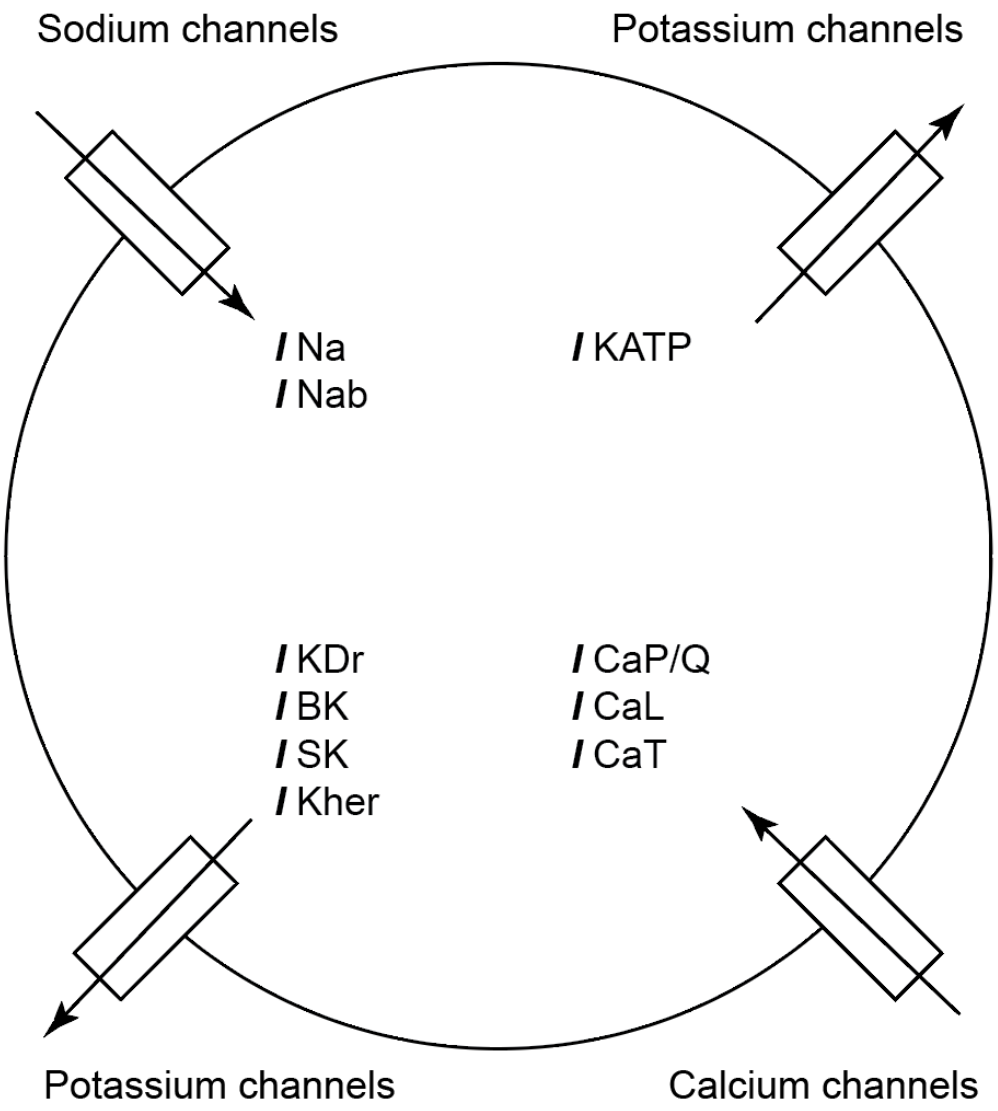
Sodium channels
Potassium channels
I Na
I Nab
I KATP
I KDr
I BK
I SK
I Kher
I CaP/Q
I CaL
I CaT
Potassium channels
Calcium channels

1.2.2 Voltage-dependent calcium channels (Ca_v channels)

Ca^{2+} currents are essential for depolarization, electrical firing, and insulin secretion from β-cells. Thus, the activity and density of Ca_v channels in pancreatic β-cells are decisive for appropriate insulin secretion. Ca_v channels are composed of a pore-forming α1 subunit and auxiliary β, γ and α2δ subunits. While the α1 subunit forms the Ca^{2+}-conducting pore and voltage sensor, the auxiliary subunits modulates the activation, inactivation and current amplitude of the channel (Arikkath & Campbell, 2003). Recently, it is reported that the auxiliary α2δ subunits can regulate channel trafficking via its interaction between the α1 and protein-binding domains in α2δ subunits (Davies et al., 2007).

In pancreatic islet cells, Dr. Milner and Dr. Hales first showed that Ca^{2+} influx is important for insulin secretion in vitro (Milner & Hales, 1967). Moreover, Ca^{2+} current can initiate the action potential in rodent β-cells (Dean & Matthews, 1970; P Rorsman & Trube, 1985). In human β-cells, voltage-activated Ca^{2+} currents were first reported by Dr. Ashcroft in 1991 (Kelly, Sutton, & Ashcroft, 1991). There are three types of Ca_v channels, L-type ($Ca_v1.2$, $Ca_v1.3$), P/Q-type (Ca_v 2.1, $Ca_v2.2$, $Ca_v2.3$) and T-type ($Ca_v3.1$, $Ca_v3.2$) with no N- or R-type of Ca_v channel expressed in human pancreatic β-cells. Although insulin secretion requires various types of Ca_v channels, L-type Ca_v channels play an important role for Ca^{2+} influx, action potential and exocytosis. While L-type Ca_v channels contribute for ~30% of Ca^{2+} current, ~45% of human β-cells Ca_v current have been identified as P/Q-type Ca_v current (Braun et al., 2008). It is suggested that exocytosis of insulin-containing granules is principally triggered by Ca^{2+} influx through P/Q-type Ca^{2+} channels. T-type channels are important at basal glucose conditions since they may increase the spontaneous Ca^{2+} currents, resulting in insulin secretion in non-stimulatory conditions (Ming Li, 2015).

1.2.3 Ca^{2+}-activated K^+ channels (K_{Ca})

While Ca^{2+} mediates the depolarization of the membrane potential, K^+ mediates the down-stroke of the action potential, which is called repolarization. The efflux of K^+ through Ca^{2+}-activated K^+ channels leads to the repolarization phase of the action potential. By patch clamp, Ca^{2+}-activated K^+ channels can be classified into three different channels, big channels (BK), small channels (SK) and intimidate channels (IK), according to different voltage dependence, Ca^{2+} sensitivity and conductance. Both BK and SK channels are expressed in pancreatic β-cells (D A Jacobson & Philipson, 2007).

BK channels are expressed in insulinoma tumor cells (X.-M. Xia, Ding, & Lingle, 1999), human pancreatic islet (Ferrer, Wasson, Salkoff, & Permutt, 1996) and primary β-cells (X.-M. Xia et al., 1999). BK channels are required for rapid membrane repolarization in pancreatic β-cells, and BK channels antagonists increase to insulin secretion (Braun et al., 2008). Although BK channels cannot mediate firing frequency, BK channels play an essential role in regulating the action potential amplitude (David A Jacobson et al., 2010) , action potential duration and insulin secretion (M Dufer et al., 2011).

SK channels are expressed in mouse islets (Tamarina et al., 2003), insulinoma cells and human pancreatic β-cells and responds to glucose stimulation (Tamarina et al., 2003), which indicates that SK channels may control action potential and mediating insulin secretion (David A Jacobson et al., 2010; Patrik Rorsman & Braun, 2013). SK-channels are essential for rapid bursting (Riz, Braun, & Pedersen, 2014), and control action potential duration and firing frequency (Martina Dufer et al., 2009).

1.2.4 Voltage-gated sodium channels (Na_v channels)

Na_v channels are responsible for Na^+ current that underlies the rapid upstroke of the action potential in nerves, muscle fibers and pancreatic β-cells (Kasimova, Granata, & Carnevale, 2016). Since first cloned in 1984 (Noda et al., 1984), Na_v channels are characterized by their marked voltage sensitivity. At resting potential, Na_v channels are closed. When depolarization happens, Na_v channels will start to open quickly (less than 1 mills second, ms) after a short latency and inactivate until the membrane is hyperpolarized. As a result, inward Na^+ current can quickly reach the peak (activation) but slowly time-dependent decline (inactivation). Thus, this channel plays an important role in determining cellular excitability (Godazgar, Zhang, Chibalina, & Rorsman, 2018).

Na_v channels are usually composed of one α-subunit and one or more smaller β-subunits (Catterall, 1986). Functionally, α-subunits, which have around 2000 amino acid residues, contribute to pore formation and electrical sensation while the β-subunits modify the gating properties and enhance the Na^+ current amplitude (Isom et al., 1992).

In pancreatic β-cells, Na_v channels play a vital role during voltage-dependent steady-state inactivation. Specifically, confirmed by RT-PCR, there are $Na_v1.3$, $Na_v1.6$ and $Na_v1.7$ expressed in β-cells and islets (Cox et al., 2006). Knocking out $Na_v1.3$ can reduce glucose stimulated insulin-secretion in mice (Salunkhe et al., 2015). In $Na_v1.7$ knockout mice, the insulin content of islet β-cells is elevated (Szabat et al., 2015). Carbamazepine, a Na^+ channel antagonist, has been confirmed as a positive modulator and has protective effects in mouse pancreatic β-cells (Szabat et al., 2015; Y. H. C. Yang, Vilin, Roberge, Kurata, & Johnson, 2014).

1.2.5 Voltage-gated potassium channels (K_v channels)

Repolarization of pancreatic β-cell action potentials is also largely mediated by the activation of delayed rectifying channels. The first K_v channels was cloned in late 1980's. In 1987, *Shaker* K_v channels were cloned and identified from *Drosophila melanogaster* (Kamb, Tseng-Crank, & Tanouye, 1988). One year later, the first mammalian K_v channels homologous to *Shaker* were cloned from mouse (Kamb et al., 1988) and rat brain (Christie, Adelman, Douglass, & North, 1989). Currently, there are now at least 12 subfamilies of mammalian K_v channels (K_v1-12), including 40 different K_v ion channels (Gutman et al., 2005). These channels are originally classified into four classes, *Shaker* (K_v1.x), *Shab* (K_v2.x), *Shaw* (K_v3.x) and *Shal* (K_v4.x) according to homology to different *Drosophila* genes. There are also various related families (EAG related, KCNQ or K_vLQT) reported. K_v channels not only mediate the electrical function and firing pattern of action potentials, but also regulate the cell cycle, proliferation and migration (Urrego, Tomczak, Zahed, Stühmer, & Pardo, 2014).

The structure of K_v channels is composed of four homo- or hetero- pore-forming α-subunits and auxiliary β-subunits, which could regulate the channel function and localization. Within each α-subunit, K_v channels contains six-transmembrane domains, S1-S6 (Figure 4A). While the first four transmembrane domains (S1-S4) contain the voltage sensor, the last two transmembrane domains (S5-P-S6) form a pore loop function as the pore domain for K^+ efflux (Figure 4B). Four monomers of K_v2.1 chains assemble into one functional tetramer (Figure 4C).

In pancreatic β-cells, there are K_v1.4, K_v1.5, K_v1.6, K_v2.1, K_v2.2, K_v3.2, K_v6.2 and K_v9.3 expressed based on PCR, in situ hybridization and immunoblot studies (D A Jacobson & Philipson, 2007). Among them, K_v2.1 channels, encoded by KCNB1, are the most abundant and play a predominant role in mediating the delayed rectifier K^+ current. Thus, K_v2.1 serves as a

brake for insulin secretion (Patrick E. MacDonald, Salapatek, & Wheeler, 2003). $K_v2.2$ is also highly expressed in pancreatic islets. Although $K_v2.2$ channels may play an essential role in regulating somatostatin release from pancreatic δ-cells (X. N. Li et al., 2013), both transcriptomic analysis (Blodgett et al., 2015) and experimental studies from purified primary mouse cells (Jensen et al., 2013) confirm that $K_v2.2$ is highly expressed in pancreatic β-cells. Since the relative contribution of $K_v2.1$ versus $K_v2.2$ was not fully investigated, electrophysiology and PCR experiments were performed in this present thesis (Fu et al., 2017).

The primary function of K_v channels is repolarization. S4 segment in K_v channel can sense the voltage change. When depolarization happens, S4 segment is displaced outward across the plasma membrane, giving rise to a gating current and triggering the conformational change in the adjacent S5-P-S6 helices, that open the channel pore to let K^+ pass (Larsson, Baker, Dhillon, & Isacoff, 1996). Thus, activation of K_v channels can return the depolarized cell back to a resting state. There are two main types of inactivation of K_v channels; fast mode and slow mode. Fast inactivation of K_v channels happens from the inner mouth of the electrical pore by part of the N terminus of the channel while the slow inactivation happens at the external mouth of the electrical pore by C terminus domains (Liu, Holmgren, Jurman, & Yellen, 1997; McCoy & Nimigean, 2012). Moreover, Phosphatidylinositol 4, 5-bisphosphate (PIP_2), a membrane phospholipid (Delgado-Ramirez et al., 2018) and SUMOylation (Dai, Kolic, Marchi, Sipione, & MacDonald, 2009; Plant, Dowdell, Dementieva, Marks, & Goldstein, 2011) are also reported to modulate $K_v2.1$ inactivation and have an influence on the excitability of pancreatic β-cells. Aside from the classic electrical function, recent works have demonstrated that $K_v2.1$ channels, similarly to other ion channels, can themselves directly influence biochemical events and facilitate exocytosis in ways independent of its channel activity (Lori, Dafna, Uri, & Ilana,

2009). This pore-independent function is discussed as non-electrical function in this present thesis. $K_v2.1$ can interact with SNARE proteins (Greitzer-Antes et al., 2018; Leung et al., 2003), SUMOylated (Dai et al., 2009; Plant et al., 2011) and compartmentalized on plasma membrane (Deutsch et al., 2012; Fox, Loftus, & Tamkun, 2013; Lim, Antonucci, Scannevin, & Trimmer, 2000; O'Connell, Loftus, & Tamkun, 2010). Thus, I will show these non-electrical functions of $K_v2.1$ in the following chapters respectively.

1.2.6 Transient receptor potential channels (TRP channels)

Besides the channels mentioned before, there are also transient receptor potential (TRP) channels (including TRPM2 (Togashi et al., 2006), TRPV4 (Casas, Novials, Reimann, Gomis, & Gribble, 2008) and TRPM3 (Wagner et al., 2008)), twik-related acid-sensitive K^+ (TASK) channels (Dadi, Vierra, & Jacobson, 2014; Patrick E. MacDonald, 2014), volume-sensitive anion channels (VSAC) channels (Best, 2005), human-ERG K^+ channels (Hardy et al., 2009) and hyperpolarization-activated cyclic nucleotide gated (HCN) channels (Yi Zhang et al., 2009) expressed and involved in action potential regulation and electrophysiology in pancreatic β-cells.

Figure 4 Structure of K_v 2.1 channels

A. Scheme of a single α-subunit of the K_v 2.1 channel. Transmembrane segments S1-S6 and pore-forming P-loop are marked. S4 segment is voltage-sensing segment.

B. Crystal structure of a single α-subunit of the K_v2.1 channel. Dash lines indicate the cell membrane. Four subunits of K_v2.1 form one functional ion channel.

C. Crystal structure of the Kv2.1 tetramer channel in a complex with the β-subunit.

Figure 4

A

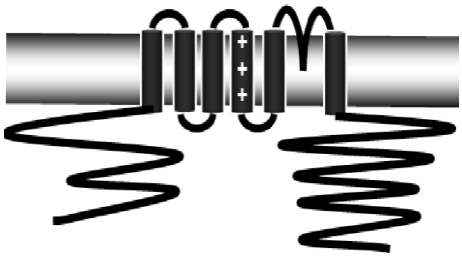

B.

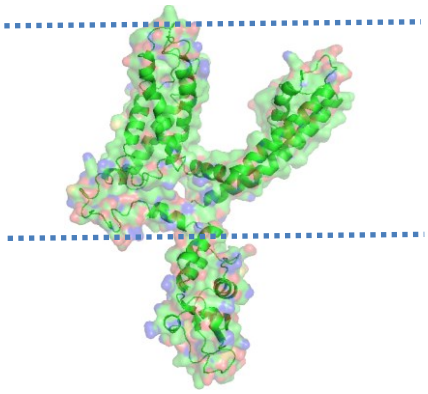

C.

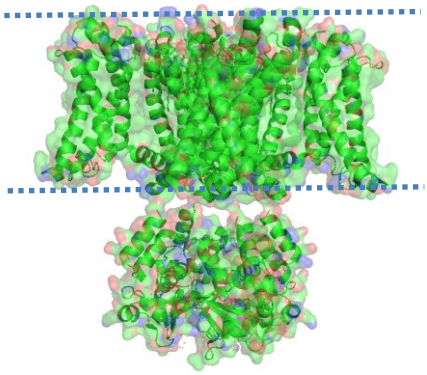

1.3 SNARE PROTEINS OF PANCREATIC BETA CELLS

Both insulin secretion and glucose uptake are mediated by SNARE (soluble N-ethylmaleimide-sensitive factor attachment protein receptor) proteins. SNARE protein can interact with ion channels to "tether" insulin granules close to exocytotic sites (Aslamy & Thurmond, 2017; Gaisano, 2017). Thus, SNARE proteins are important for mediating vesicle fusion, exocytosis, and insulin secretion. The SNARE proteins consist of more than 60 members in yeast and mammalian cells, including neuron cells, mast cells, endocrine cells and more (Ungar & Hughson, 2003). These proteins can be classified into two categories, vesicle-associated (v-SNARE) proteins and target-membrane (t-SNARE) proteins. In β-cell lines and pancreatic islets, there are Synaptobrevin family (part of vesicle-associated membrane protein (VAMP) family) and Synaptotagmin (Syt) family expressed. For t-SNARE proteins, there are three subfamilies: the SNAP family (Synaptosomal-associated protein, SNAP 23, SNAP 25, and SNAP 29), the Munc family (Mammalian uncoordinated- homology, Munc 18 and Munc 13) and the Syntaxin family (Stx 1A, Stx2, Stx3 and Stx4) (Wheeler et al., 1996). When exocytosis occurs, Ca^{2+} could come inside of cell membrane and stimulate granule fusion via biding with Synaptotagmin. SNARE complexes, formed by three SNARE proteins on the vesicle and target membrane, can bridge the two membranes (Südhof & Rothman, 2009). Thus, SNARE proteins constitute the core fusion machinery. Different SNARE complexes are involved with different types of exocytosis (Figure 4) (Duman & Forte, 2003; Gaisano, 2014).

1.3.1 Exocytosis of pre-docked insulin granules (Primary exocytosis)

SNARE proteins can mediate docking granules sitting on the cell membrane to constitute the readily releasable pools (RRP). It is believed that SNARE proteins and ion channels can

interact together to "tether" pre-docking granules close to the sites of Ca^{2+} influx. This complex, termed the "excitosome", includes SNARE (Munc18a/Syntaxin-1A/SNAP25/VAMP-2) complex proteins, $Ca_v1.2$ and other ion channels (such $K_v2.1$). Thus, "excitosome" can coordinate signaling, excitability and optimizes the Ca^{2+} entry to the sites of exocytosis (Wiser et al., 1999). Moreover, it is reported that another SNARE complex (Munc18c/Syntaxin 4/SNAP25/VAMP-2&-8) also contributes to pre-docked granule exocytosis.

1.3.2 Exocytosis of newcomer insulin granules (Newcomer granule exocytosis)

Newcomer insulin secretion is characterized as exocytosis rapidly with minimal or no residence time on the plasma membrane before fusion. It is thought that newcomer insulin granules are account for the substantial portion of first phase of glucose-stimulated insulin secretion (GSIS). Currently, there are two major SNARE complexes that mediate newcomer exocytosis. Munc18b/Syntaxin 3/SNAP25/VAMP-8 and Munc18c/Styntaxin-4/SNAP25/VAMP-2, -8. It is suggested that syntaxin1A interacts with VAMP8 may mediate the newcomer granule exocytosis as well (Liang et al., 2017).

1.3.3 Exocytosis from compound insulin granules (Compound exocytosis)

Compound exocytosis is different from full fusion of single secretory granules. It is characterized by granules that are located at intracellular locations distal to the plasma membrane undergoing fusion with each other in the cytosol first before fusing with the plasma membrane. Compound exocytosis is therefore considered the most extensive mode of cargo release. This type of exocytosis occurs in both exocrine and endocrine cells and in immune cells including eosinophils and neutrophils (Lacy & Eitzen, 2008). Munc18b/Syntaxin-3/SNAP25/VAMP-8

complex plays an essential role in compound exocytosis. Moreover, Rab5 and SNAP23 are also reported to be important in regulating granule-granule fusion (Klein et al., 2017). Since there is more insulin secreted from compound exocytosis, understanding the molecules involved in regulating this type of exocytosis can be novel strategy for understanding or treating T2D. For example, it is reported that Carbachol (M B Hoppa et al., 2012) and glucagon-like peptide 1 (GLP-1) (Kwan & Gaisano, 2005) can stimulate compound exocytosis in rat β-cells.

1.3.4 Exocytosis from compound insulin granules (Kiss-and-Run exocytosis)

Secretory vesicles can be recycled by kiss-and-run exocytosis, where fusion with the plasma membrane is only transient (Rutter & Tsuboi, 2004). It is reported that kiss-and-run of synaptic-like vesicles (SLVs) and large dense-core vesicles (LDCVs) in endocrine and neuroendocrine may serve the disparate purposes of rapid vesicle recycling and selective release of small molecule transmitters, respectively in pancreatic β-cells (Patrick E MacDonald, Braun, Galvanovskis, & Rorsman, 2006). Different than other type of exocytosis, it remains controversial whether "kiss-and-run" exocytosis really exists since only a minor fraction of fusion events has been shown to be kiss-and-run determined by imaging and electro-physiological studies (L. He & Wu, 2007). Another major reason for this controversy is the SNARE complex. It is thought that the SNARE complex should be dissociated after exocytosis. However, if "kiss-and-run" exocytosis happens, it suggests that the SNARE complex can form and dissociate quickly and reversibly (Palfrey & Artalejo, 2003). However, the newest TIRF microscopy data reveals that "kiss-and-run" exocytosis happens and play an important role in synaptic exocytosis and endocytosis at photoreceptor ribbon synapses (Wen, Saltzgaber, & Thoreson, 2017).

Figure 5 Different types of exocytosis

1) Primary exocytosis. An insulin granule is docked on the plasma membrane, becomes primed, and sits on the plasma membrane until Ca^{2+} influx mediates its fusion with the plasma membrane to release insulin.

2) Newcomer granule exocytosis. These insulin granules undergo fusion with minimal or no residence time on the plasma membrane.

3) Compound exocytosis. Several insulin granule first undergo fusion with each other inside the cytoplasm, then one large granules fuses with the plasma membrane to release massive amounts of insulin from the compound granule.

4) Kiss-and-Run exocytosis. Insulin granules exocytosis and endocytosis very transiently, back and forth, on the cell membrane (<6 ms).

Figure 5

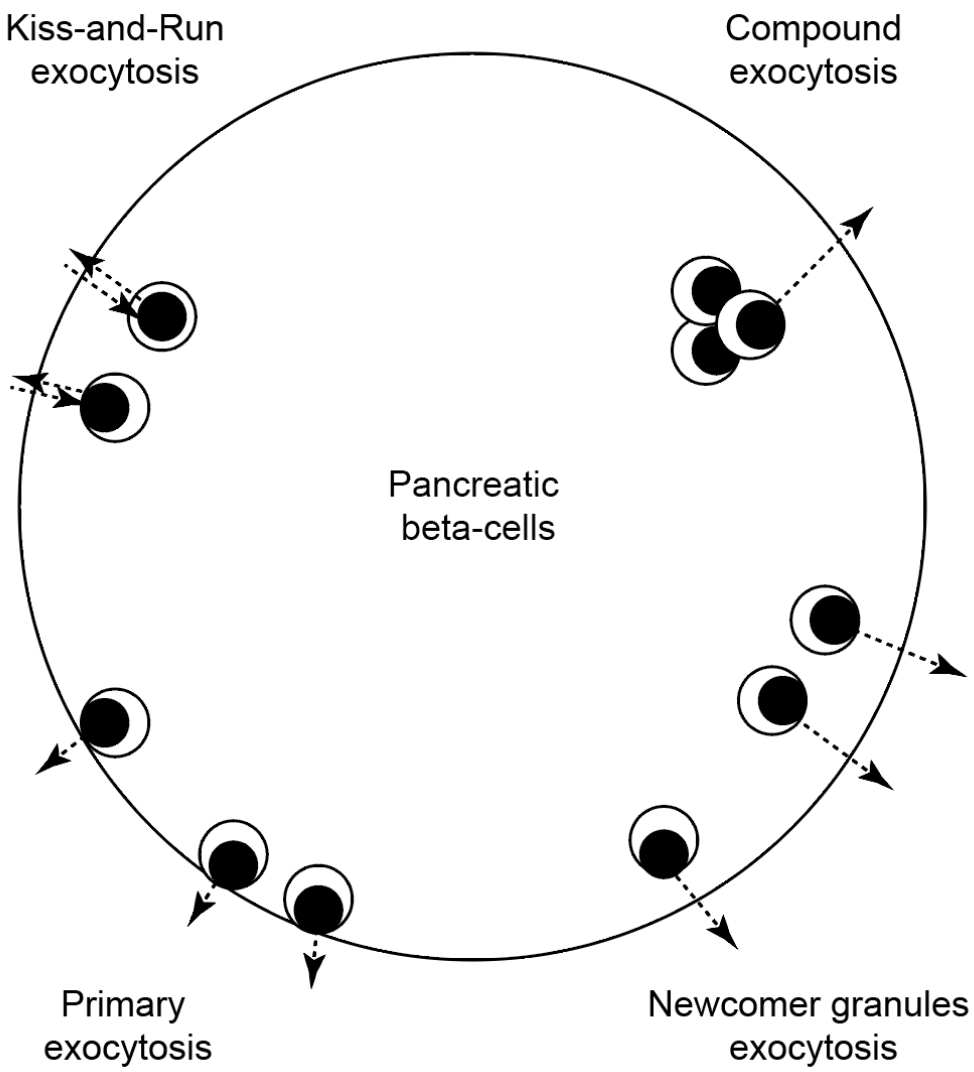
Kiss-and-Run
exocytosis
Compound
exocytosis
Pancreatic
beta-cells
Primary
exocytosis
Newcomer granules
exocytosis

1.4 SUMOYLATION OF ION CHANNELS AND SNARE PROTEINS

1.4.1 Introduction of SUMOylation

Similar to ubiquitin, Small ubiquitin-like modifier (SUMO) can covalently attach to target proteins. However, this post-translational attachment, called SUMOylation, does not necessarily target proteins for degradation. Instead, SUMOylation can modify a protein's localization, interactions, stability and/or activity and function in a readily reversible manner (Mahajan, Gerace, & Melchior, 1998; Manning Fox, Hajmrle, & Macdonald, 2012).

SUMOylation is highly conserved within the trans-activation domain of ATF6 protein of human, mouse, or rat specie and is essential for the regulation of various cellular process. There are four known functional SUMO isoforms (SUMO1, SUMO2, SUMO 3 and SUMO4) present in mammals. SUMOylation of targeted proteins requires sequential enzymatic action of E1 enzyme (SAE1/SAE2 heterodimer), E2 enzyme (Ubc9) and one of several E3 ligases (Mustfa et al., 2017). This process is reversible by the sentrin/SUMO-specific proteases (SENPs), including SENP1 to 3 and SENP 5 to 7. While SUMO2/3 can be deconjugated by SENP3 and SENP5 (Gong & Yeh, 2006), SUMO1 is preferentially deconjugated by SENP1 (Sharma, Yamada, Lualdi, Dasso, & Kuehn, 2013).

SUMOylation is important in pancreatic β-cells. Expression of SUMO1 in both mouse and human islets (which consist of 50%–80% β-cells), as well as the insulinoma cell line, INS-1 832/13, has been demonstrated (Xiao Qing Dai et al., 2011; Vergari, Plummer, Dai, & MacDonald, 2012). Mutation of SUMO4 is linked with type 1 diabetes by increasing β-cell death through NF-κβ (nuclear factor kappa-light-chain-enhancer of activated B cells) pathway.

Moreover, glucose stimulation can induce SUMOylation of PDX-1 (pancreatic duodenal homeobox 1) and MafA in β-cells, regulating their localization and activity and recruiting

histone acetylase p300. While SUMOylation is implicated in transcription factor targeting and cell signing in the nucleus, it is also reported that SUMOylation is essential for maintaining β-cell functionality (X. He et al., 2018) and SUMOylation plays an important role regulating transmembrane proteins, such as receptors, the SNARE complex (Ferdaoussi et al., 2017), and ion channel functions (Plant et al., 2010, 2011; Plant, Marks, & Goldstein, 2016). Thus, SUMOylation can mediate electrical activity and Ca^{2+}-dependent exocytosis in β-cells directly.

1.4.2 SUMOylation in ion channels

Voltage-dependent K^+ channels are the major ion channels which can be SUMOylated in pancreatic β-cells. Over-expression or infusion of SUMO-1 can inhibit recombinant and native $K_v2.1$ current in INS-1 831/13 cells and human β-cells. Mechanistically, this is due to a SUMO-dependent increase in the rate of K_v current inactivation. Overexpression of SUMO can prolong the action potential while decreasing electrical firing frequency in INS-1 cells (Dai et al., 2009). Directly SUMOylation of $K_v2.1$ is on the lysine residue K470 in heterologous expressed $K_v2.1$. Moreover, up to 2 of the 4 $K_v2.1$ subunits could be modified by SUMO-1 and SUMO can produce a graded shift in half maximal activation voltage (Plant et al., 2011).

Two-pore-domain K^+ (P2K1) channels belong to the family of background K^+ channels. It is reported that in pancreatic β-cells, P2K1 (coded by *TWIK1* gene) inactivation can cause hyperpolarization of the resting membrane potential (Chatelain et al., 2012). SUMO-1 can assemble with K2P1 on plasma membrane and modify its lysine residue K274 (Rajan, Plant, Rabin, Butler, & Goldstein, 2005). Besides, one SUMO is sufficient to silence the electrical function of P2K1 channels and this SUMOylation could be reversed with SENP1 in live Chinese hamster ovary (CHO) cells. (Plant et al., 2010).

1.4.3 SUMOylation in SNARE proteins

SUMOylation at the exocytotic site is a key regulator of secretory function in pancreatic β-cells. Since SNARE proteins, which are around 100 amino acids in length and 12 KDa in mass, are essential to form "excitosome" complexes at the exocytotic site, SUMOylation of SNARE proteins can directly regulate target protein function and protein-protein interaction. Synaptotagmin VII co-immunoprecipates following pull-down of SUMO-1 from human islet extracts confirm that SUMO-1 has Ca^{2+}-independent inhibitory effects on exocytosis (Xiao Qing Dai et al., 2011). Moreover, SUMO-1 can interact with Synapsin 1A at lysine residue K27 (Tang, Craig, & Henley, 2015) and this can reduce its interaction with other SNARE proteins and disrupts the balance of endocytosis-exocytosis coupling (Craig, Anderson, Evans, Girach, & Henley, 2015). SUMOylation of tomosyn1 at K298 can also affect its interaction with Syntaxin1A. Thus, SUMOylation can help pancreatic β-cells response to Ca^{2+} stimulation and is required for insulin granule trafficking and exocytosis downstream of Ca^{2+} influx (Ferdaoussi et al., 2017).

Figure 6. Proposed model for the regulation of SUMO at the exocytotic site

Metabolically derived reducing equivalents, in the form of NADPH, are proposed to amplify insulin exocytosis in part by promoting deSUMOylation of several targets at the exocytotic site via the SUMO protease SENP1. Potential targets include Syntaxin 1A, Synaptotagmin VII, and the voltage-dependent K^+ channel $K_V2.1$ (Vergari et al., 2012).

Figure 6.

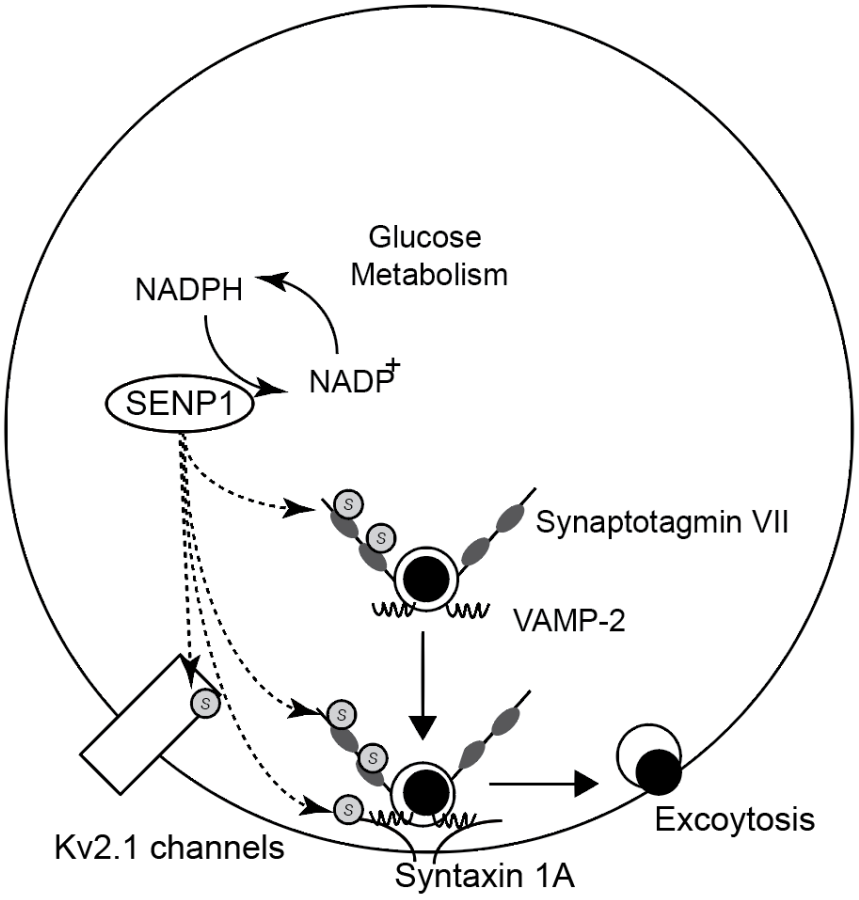
Glucose
Metabolism
NADPH
NADP+
SENP1
Synaptotagmin VII
VAMP-2
Kv2.1 channels
Syntaxin 1A
Excoytosis

1.5 COMPARTMENTALIZATION OF EXOCYTOSIS.

1.5.1 Compartmentalization on the cell membrane

In the last thirty years the "lipid raft" theory indicates that the proteins on the cell membrane are not randomly distributed but associate to micro-domains enriched in cholesterol and sphingolipids. Since lipid rafts may contain many signaling molecules, they may serve as organizing 'hub' or 'hotspots' for signal transition, receptor trafficking and neurotransmission regulation (Korade & Kenworthy, 2008). Thus, the spatial pattern and distribution of moleculars on the cell membrane itself is becoming a "hotspot" and drawing attentions of investigators in the field of biomedical and biological sciences (F. Xia et al., 2004, 2008).

In neuronal synapses, neurotransmitter release is compartmentalized at the active zone of the presynaptic nerve terminus. However, β-cells lack ultra-structurally identifiable active zones. Since active zones in neuronal synapses are composed of conserved protein complexes containing ion channels and SNARE proteins similar to β-cells, such as Munc13, RIM2 (regulating synaptic membrane exocytosis protein 2) (Yasuda et al., 2010) and Ca_v channels (Gandasi et al., 2017). Areas analogous to active zones may also exist and contribute to regulated exocytosis in pancreatic β-cells.

1.5.2 Compartmentalization of exocytosis

The spatial pattern of insulin exocytosis across the cell surface has been less investigated. It is reported that individual exocytosis events are coordinated spatially and temporally in isolated human islets. Under glucose stimulation, exocytosis events are progressively localized to preferential release sites. Moreover, neighboring β-cells are compartmentalized as functional clusters (Almaca et al., 2015). This subcellular spatial pattern of

insulin secretion maybe associated with vascular interactions. In response to glucose, insulin granule fusion happens at asymmetric, non-random sites, towards the vasculature (Low et al., 2014). Within single pancreatic β-cells, the spatial occurrence of the fusion events is not well explored due to the lack of sensitive and objective analysis methods. However, it is reported that in insulin-secreting cells exocytosis is compartmentalized at "hotspots". In insulinoma cells, individual vesicle fusion events are not random, and this spatial pattern will be impaired upon the disruption of cytoskeleton network (Yuan, Lu, Zhang, Zhang, & Chen, 2015).

1.5.3 Compartmentalization of SNARE complexes

In presynaptic nerve terminus compartmentalized exocytosis happens at the active zones, which exert significant functional effects by regulating the formation and dissociation of SNARE complexes. Thus, SNARE proteins are also compartmentalized at active zones. It is reported that Syntaxin1A is compartmentalized as clusters at sites of secretory granule docking and exocytosis in pancreatic β-cells (Barg, Knowles, Chen, Midorikawa, & Almers, 2010a). Sytaxin1A interacts with Munc18 to form clusters. Since this pre-exiting syntaixn1A clusters cannot be observed, it suggests that these syntaxin1A clusters maybe induced by insulin granule contact. Moreover, syntaxin1A can interact with the strongly anionic lipid phosphatidylinositol-4,5-bisphosphate (PIP2) to form distinct nanoscale regions at the granule docking site as well (Aoyagi et al., 2005; van den Bogaart et al., 2011). Similarly, SNAP-25 assembles into clusters on plasma membrane. Most importantly, these clusters are co-localized with syntaxin1A clusters and insulin granules in normal primary rat pancreatic β-cells and insulinoma MIN6 cells. In diabetic β-cells, consistent with the recently reported reduction of docked insulin granules (Gandasi et al., 2018), both SNAP-25 and Syntaxin1A clusters are impaired (M Ohara-Imaizumi et al., 2004). Thus,

compartmentalization of SNARE proteins is highly associated with fusion events from previously docked insulin granules (M Ohara-Imaizumi et al., 2004).

1.5.4 Compartmentalization of ion channels

Another important role of the active zone is recurring Ca^{2+} channels to exocytosis sites (Südhof, 2012) and tuning Ca^{2+} channel-vesicle coupling (Bohme et al., 2016). Thus, ion channel compartmentalization may also be important for exocytosis in pancreatic β-cells.

Compartmentalization of Ca^{2+} channels, particularly $Ca_v1.2$, is important because the docked insulin granules supposed to be exposed to micro-domains of high concentration of Ca^{2+} without the accumulation of the bulk cytosolic Ca^{2+} concentration inside the whole β-cells. Since membrane-proximal Ca^{2+} is localized into submicroscopic "hot spots", the Ca^{2+} increase in these micro-domains, not bulk Ca^{2+} increase, could be sufficient enough to support vesicle fusion (Omann & Axelrod, 1996). Thus, this compartmentalization can regulate the rapid release of insulin directly. However, in pancreatic β-cells from T2D donors, this rapid exocytosis function is impaired, which indicates that $Ca_v1.2$ clusters have altered (Gandasi et al., 2017). Similarly, chronic palmitate exposure could impair insulin secretion by dissociation of Ca_v channels from insulin granules in both mouse and human islets (Michael B Hoppa et al., 2009).

Although there is no Na_v channels clusters reported in pancreatic β-cells, $Na_v1.1$, $Na_v1.2$, $Na_v1.6$, $Na_v1.7$, $Na_v1.8$ and Na_v 1.9 have been reported to be compartmentalized at the nodes of Ranvier (Black, Frezel, Dib-Hajj, & Waxman, 2012; Chang & Rasband, 2013). Na_v is highly clustered here on the order of ~1200 channels/μm^2 (Rosenbluth, 1976), while each node has ~20-25 channels/μm^2 (Ritchie & Rogart, 1977). Functionally, compartmentalization of Na_v channels can ensure asymmetrical elevated concentration of Na^+ to regenerate the action potential,

resulting in improved energy efficiency in fast-spiking neurons (Freeman, Desmazieres, Fricker, Lubetzki, & Sol-Foulon, 2016; Waxman, Black, Kocsis, & Ritchie, 1989).

Similar to Na_v channels, K_v channels, which interact with cell-adhesion molecules (CAMs), cytoskeletal scaffolding proteins, and extracellular matrix (ECM) components, form clusters at the nodes of Ranvier (Chang & Rasband, 2013; Salzer, 2003), and on the surface of neurons or in transfected HEK cells (Tamkun, O'connell, & Rolig, 2007). It is reported that $K_v2.1$ can form 1-3 μm^2 clusters from neuronal electrophysiology. Mechanistically, these $K_v2.1$ clusters are formed by sub-membrane cytoskeletal structures that limit the lateral diffusion of only the sub-population of $K_v2.1$ channels carrying the modifications on the $K_v2.1$ C-terminus. A unique proximal restriction and clustering domain on the C-terminus (PRC) in $K_v2.1$ plays an essential role in the compartmentalization of the channels. Moreover, it is reported that in both primary neuronal cultures and transfected HEK cells, $K_v2.1$ clusters represent endoplasmic reticulum/plasma membrane (ER/PM) junctions that function as membrane trafficking hubs (Fox et al., 2015). Specifically, K_v2 channels interact with VAMP-associated proteins (VAPs) embedded in the ER membrane in rat hippocampal neuron (Johnson et al., 2018). Thus, $K_v2.1$-induced ER remodeling and VAP concentration at ER/PM contacts likely play a central role in neuronal physiology. Since $K_v2.1$ clusters are less investigated in pancreatic β-cells, I focus on this special character of $K_v2.1$ in insulin-secreting cells in this thesis.

1.6 GENERAL HYPOTHESIS

Although the electrical/non-electrical role of ion channels (such as $K_v2.1$) and the temporal analysis of exocytosis in insulin-secreted cells have been investigated, the spatial pattern of ion channels and exocytosis sites, especially in human pancreatic β-cells from non-diabetes and T2D donors, has not been reported before. Better understanding of the spatial patterning, compartmentalized ion channels and exocytosis discussed in the present dissertation, could provide a novel insights into the mechanisms of T2D. Further study on compartmentalized ion channels and exocytosis may prove to be a novel therapeutic treatment for T2D.

The hypothesis of this dissertation is that compartmentalized $K_v2.1$ clustering is required for insulin granule docking at the plasma membrane and priming for eventual Ca^{2+}-dependent exocytosis. Furthermore, regulated exocytosis in pancreatic β-cells is compartmentalized as well, and this spatial patterning is mediated in part by $K_v2.1$ channels and SUMOylation. This spatial pattern of $K_v2.1$ and regulated exocytosis is impaired in pancreatic β-cells from T2D.

1.7 SPECIFIC AIMS

1.7.1 AIM 1: Examine whether K_v2.1 and/or K_v2.2 are compartmentalized in human pancreatic β-cells, and their function in exocytosis and insulin secretion

The relative contribution of K_v2.1 and K_v2.2 to insulin secretion via electrical and non-electrical mechanisms was assessed using selective shRNA and duplex siRNA respectively. The existence of K_v2.1 clusters was confirmed in insulinoma cells and human pancreatic β-cells immunostaining and imaging. The importance of this spatial pattern was further investigated using truncated mutation that lacked the ability to form clusters.

1.7.2 AIM 2: Elucidate the spatial-temporal pattern of regulated exocytosis human pancreatic β-cells

Spatial-temporal analysis of exocytosis in human β-cell from both healthy and T2D donors under different stimulation conditions was investigated to evaluate the importance of compartmentalized exocytosis as hotspots. The importance of docking granules was assessed under single-case analysis. Mechanistically, the regulation by K_v2.1 clusters of docking granule density and exocytosis "hotspots" was examined.

1.7.3 AIM 3: Investigate the role and the mechanism of K_v2.1 SUMOylation in spatial-temporal pattern of regulated exocytosis

SUMOylation can exert a strong inhibitory action of electrical function on K_v2.1 and regulate cellular excitability in native β-cells. SUMOylation sites of K_v2.1 were examined. The mechanisms by which K_v2.1 SUMOylation regulates exocytosis was investigated spatially and temporally under time-lapse microscopy.

CHAPTER 2

$K_v2.1$ clustering contributes to insulin exocytosis and rescues β-cell dysfunction

The following chapter is adapted from work published in *Diabetes*. It is reprinted with the permission of the American Diabetes Association:

Fu J, Dai X, Plummer G, Suzuki K, Bautista A, Githaka JM, Senior L, Jensen M, Greitzer-Antes D, Manning Fox JE, Gaisano HY, Newgard CB, Touret N, MacDonald PE (2017). $K_v2.1$ clustering contributes to insulin exocytosis and rescues human β-cell dysfunction. *Diabetes*, **66**(7), 1890-1900.

2.1 ABSTRACT

Insulin exocytosis is regulated by ion channels that control excitability and Ca^{2+}-influx. Channels also play an increasingly appreciated role in micro-domain structure. Here I examine the mechanism by which the voltage-dependent K^+ (K_v) channel, K_v2.1 (KCNB1), facilitates depolarization-induced exocytosis in INS 832/13 cells and β-cells from human donors with and without type 2 diabetes (T2D). I find that K_v2.1, but not K_v2.2 (KCNB2), forms clusters of 6-12 tetrameric channels at the plasma membrane and facilitates insulin exocytosis. Knockdown of K_v2.1 expression reduces secretory granule targeting to the plasma membrane. Expression of the full-length channel (K_v2.1-WT) supports the glucose-dependent recruitment of secretory granules. However, a truncated channel (K_v2.1-ΔC318) that retains electrical function and syntaxin1A binding, but lacks the ability to form clusters, and does not enhance granule recruitment or exocytosis. Expression of KCNB1 appears reduced in T2D islets, and knockdown of KCNB1 does not inhibit K_v current in T2D β-cells. Up-regulation of K_v2.1-WT, but not K_v2.1-ΔC318, rescues the exocytotic phenotype in T2D β-cells and increases insulin secretion from T2D islets. Thus, the ability of K_v2.1 to directly facilitate insulin exocytosis depends on channel clustering. Loss of this structural role for the channel may contribute to impaired insulin secretion in diabetes.

2.2 INTRODUCTION

The regulated exocytosis of insulin containing secretory granules is critical for glucose homeostasis, and impaired insulin secretion from β-cells of the pancreatic islets of Langerhans is a key factor in the development of type 2 diabetes (T2D) (Kahn, Cooper, & Del Prato, 2014). In response to elevated plasma glucose, the mitochondrial generation of ATP within β-cells results in closure of ATP-dependent K^+ (K_{ATP}) channels, action potential firing, and activation of voltage-dependent Ca^{2+} channels (VDCCs); the subsequent entry of Ca^{2+} triggers exocytosis of insulin containing dense-core vesicles (reviewed in (Patrik Rorsman & Braun, 2013)).

The repolarization of β-cell action potentials is mediated by delayed rectifier K^+ channels, and in rodents this is largely mediated by the voltage-dependent K^+ (K_v) channel isoform $K_v2.1$ (David A Jacobson et al., 2007; Patrick E. MacDonald et al., 2003) However, even though human β-cells express abundant $K_v2.1$ channels encoded by *KCNB1* (Braun et al., 2008; Dai et al., 2012; Herrington et al., 2005; Yan et al., 2004), inhibition of these (and the related $K_v2.2$) has little effect on human β -cell electrical function and variable effects on insulin secretion from human islets (Braun et al., 2008; X. N. Li et al., 2013). Additionally, control of $K_v2.2$ expression may also contribute to the regulation of insulin secretion (Jensen et al., 2013) and recent transcriptomic analysis of purified β-cells suggests an ~10-fold higher expression of the $K_v2.2$ encoding gene *KCNB2* versus *KCNB1* (Blodgett et al., 2015). Thus, the role for $K_v2.1$ channels in insulin secretion, particularly in humans, remains unclear.

Interestingly, $K_v2.1$ may play a direct role in the exocytotic process, independent of its pore function, through an interaction with syntaxin 1A at the channel C-terminus (Singer-Lahat et al., 2007). Indeed, this is true in both rodent and human β-cells, where I demonstrated that disruption of the $K_v2.1$-syntaxin 1A interaction impairs depolarization-induced exocytosis and

insulin secretion (X. Q. Dai et al., 2012). Tetrameric $K_v2.1$ channels target to distinct membrane micro-domains or clusters, and this requires a C-terminus region of the channel (Baver & O'Connell, 2012; Lim et al., 2000; Tamkun et al., 2007) that does not overlap with the syntaxin-binding domain. A physiological role for $K_v2.1$ channel clusters, which may be electrically silent (O'Connell et al., 2010) due to increased channel density (Fox, Loftus, et al., 2013), is not readily apparent although they likely play a role in the exocytosis of GLUT4-containing vesicles (Deutsch et al., 2012) and appear to define regions of plasma membrane association with the cortical endoplasmic reticulum (Fox, Haberkorn, et al., 2013).

Here I have examined the role for K_v2 channels as facilitators of insulin exocytosis in pancreatic β-cells from human donors with and without T2D. I find that $K_v2.1$ and 2.2 both contribute to the delayed outward K^+ current, but that only $K_v2.1$ facilitates insulin exocytosis. Expression of *KCNB1* and *KCNB2* and the contribution of these channels to outward K^+ currents are reduced in islets from donors with T2D, where up-regulation of full-length $K_v2.1$ restores exocytotic function and increases insulin secretion. Mechanistically, tetrameric $K_v2.1$ channels cluster at the plasma membrane, and these are required for efficient insulin granule recruitment independent of the channel's ability to conduct K^+ or bind syntaxin1A. Thus, I demonstrate an important structural role for $K_v2.1$ at the plasma membrane of pancreatic β-cells, the loss of which may contribute to impaired insulin secretion in T2D.

2.3 MATERIALS AND METHODS

2.3.1 Cells and tissues

Human embryonic kidney (HEK) 293 cells were cultured in DMEM with 20 mM glucose, 10% FBS, 100 units/mL penicillin, and 100 mg/mL streptomycin at 37°C and 5% CO_2. The glucose responsive INS 832/13 insulinoma cell line (Hohmeier & Newgard, 2004) was cultured in RPMI-1640 with 11.1 mM glucose, 10% FBS, 10 mM HEPES, 0.29 mg/ml L-glutamine, 1 mM sodium pyruvate, 50 μM 2-mercaptoethanol, and 100 U/ ml penicillin/streptomycin. Human islets from the Clinical Islet Laboratory at the University of Alberta and the Alberta Diabetes Institute IsletCore (Lyon et al., 2016) were cultured in low-glucose (5.5 mM) DMEM with L-glutamine, 110 mg/l sodium pyruvate, 10% FBS, and 100 U/ml penicillin/streptomycin. Islets from 40 donors without diabetes and 15 T2D donors contributed to this work. All human islet studies were approved by the Human Research Ethics Board (Pro00001754) at the University of Alberta and all families of organ donors provided written informed consent.

2.3.2 Molecular biology

Knockdown of KCNB1 or KCNB2 expression in human cells was carried out using a mixture of 4 siRNA duplexes (QIAGEN, Toronto, ON, Canada), in which each recognizes different regions of the target gene. Transfected cells were identified by co-transfection with an Alexa Fluor 488-tagged duplex (Cat. # 1027292, Qiagen). Adenoviral shRNA constructs to knockdown rat Kcnb1 or Kcnb2 in INS 832/13 cells are described (Jensen et al., 2013). Knockdown of KCNB1 or KCNB2 in human islets was confirmed by qPCR using Taqman expression assays (Applied Biosystems/Thermo Fisher Scientific, MA USA). The cDNA

encoding wild type rat $K_v2.1$ or the truncated $K_v2.1$-ΔC318 ($K_v2.1$ Glu536_Ile853 del) was amplified by PCR using a pCDNA3-$K_v2.1$ plasmid as a template, and inserted between BsrG-I and Xho-I site of Cherry-LacRep plasmid (Dundr et al., 2007) (from Mirek Dundr: Addgene plasmid#18985) by Gibson Assembly to make pmCherry-$K_v2.1$-WT and pmCherry-$K_v2.1$-ΔC318.

To generate a photoactivatable (PA) construct for PALM, the mCherry cDNA in pmCherry-$K_v2.1$-WT was replaced with PAmCherry cDNA amplified by PCR from pPAmCherry1-C1 (Subach et al., 2009) (from Vladislav Verkhusha; Addgene plasmid # 31929) and inserted between Nhe-I and BsrG-I of the pmCherry-$K_v2.1$-WT plasmid. To generate Myc-tagged constructs, the cDNA encoding 5xMyc was inserted between Nhe-I and BsrG-I sites of the pmCherry-$K_v2.1$ WT and pmCherry-$K_v2.1$-ΔC318 expression vector by Gibson Assembly. The $K_v2.1$ pore mutant ($K_v2.1$W365C/Y380T) was described previously (X. Q. Dai et al., 2012; Singer-Lahat et al., 2007), and used to create the GFP-co-expressing adenovirus Ad-$K_v2.1$W365C/Y380T (Welgen Inc., Woster, MA). Adenovirus expressing GFP alone was a control (Ad-GFP; Welgen Inc.).

2.3.3 Electrophysiology and Insulin Secretion.

Patch-clamp measurement of K_v currents and exocytosis in single INS 832/13 or human β-cells, identified by positive insulin immunostaining following the experiment, were performed at 32-35ºC as described before. Insulin secretion was measured, 48 hours following adenoviral infection, in human islets by perifusion at 37°C in Krebs-Ringer buffer (KRB, in mM): 115 NaCl, 5 KCl, 24 $NaHCO_3$, 2.5 $CaCl_2$, 1 $MgCl_2$, 10 HEPES, and 0.1% BSA, pH 7.4. Twenty islets per lane were perifused (0.25 ml/min) with 1 mM glucose KRB for 24 minutes and then

with the indicated condition. Samples were collected over 2-minute intervals. Islets were lysed in acid/ethanol buffer (1.5% concentrated HCl, 23.5% acetic acid, and 75% ethanol) for total insulin content. Samples were assayed using the Insulin Detection Kit (Meso Scale Discovery).

2.3.4 TIRF and PALM Imaging

Imaging was performed on fixed cells, except for live-cell data in Fig. 21G-I, 36-48 hours after transduction with mCherry-tagged channel constructs and Venus- or EGFP-tagged NPY to mark secretory granules, or following immunostaining for $K_v2.1$ and insulin with antibodies diluted in 1:1000 monoclonal mouse anti-$K_v2.1$ (UC Davis/NIH NeuroMab Antibodies, CA, USA) and 1:1000 polyclonal guinea pig anti-insulin (Dako Canada, Burlington, Ontario, Canada) diluted in 5% goat serum or 2% donkey serum. Detection was with Alexa Fluor 488 or 594 conjugated secondary antibodies (Molecular Probes, Eugene, Oregon) diluted 1:2000 as above.

All TIRF imaging used a Cell-TIRF motorized system (IX83P2ZF, Olympus Canada) with a 100×/1.49 NA TIRFM objective, a Photometrics Evolve 512 camera (Photometrics), and Metamorph Imaging software (Molecular Devices). Stimulation was at 491 nm (LAS-491-50) and 561 nm (LAS-561-50, Olympus, Germany) with a quad filter passing through a major dichroic and band pass filter (405/488/561/640, Chroma Technology, Bellows Falls, VT). Penetration depth was set to 105 nm, calculated using existing angle of the laser and assuming a refractive index of 1.37. Emission was collected through bandpass filters of 525/25 nm and 605/26 nm for excitations of 488 and 561 nm, respectively. Images were acquired sequentially with single laser excitation to minimize potential bleed-through. Object-based co-localization was performed using Imaris Scientific 3D/4D Image Processing software (Bitplane, Zurich, Switzerland, v7.3.2) on top-hat filtered and background subtracted images. A Gaussian filter

assuming initial spot diameter of 0.3 μm was used to initially identify spots, and region growing was applied to ensure capture of clusters with differing sizes. The "Co-localize Spots" function, calculated by Matlab, r2013, was run with a center-to-center threshold value of 0.3 μm, which is <2 pixels and represents the minimum resolvable distance to distinguish two objects in our system. Live-cell acquisition was 5-Hz with a 200 ms exposure at 35°C. Before acquisition, cells were pre-incubated (30 mins) in bath containing (in mM) 138 NaCl, 5.6 KCl, 1.2 $MgCl_2$, 2.6 $CaCl_2$, 5 $NaHCO_3$, 1 glucose and 5 HEPES (pH 7.4 with NaOH) and then exposed to 5 mM glucose upon recording. Fusion events, indicated by abrupt brightening (ratio of peak fluorescence to background >1.3) and then disappearance of NPY-EGFP fluorescence, were selected and analyzed with computer-assisted analysis software and normalized to membrane area.

For PALM imaging (Betzig et al., 2006) cells were fixed on ice with 3% glytaraldehyde for 10 minutes followed by quenching with 0.1% sodium borohydride to minimize auto fluorescence by quenching free aldehyde groups. A low power (20 μW) 405 nm UV-laser (Spectral Applied Research, Richmond Hill, Canada) was used to photo-activate PAmCherry, of which the signal was acquired using a 605/20 nm bandpass filter after excitation with 1 mW of 561 nm laser (Spectral Applied Research) at 100 ms exposure time until all molecules were photo-bleached. Acquisition was with a 100x (1.45 NA) oil objective, a Hamamatsu EM-CDD camera (ImageEM91013, Hamamatsu), and Volocity software (PerkinElmer). To identify clusters, Spatial Pattern Analysis was computed as previously described with Gaussian-mixture-model fitting (Betzig et al., 2006; Jaqaman et al., 2008; Thomann, Rines, Sorger, & Danuser, 2002) To avoid potential molecule over-counting from emission by the same molecules, multi-appearance localizations were eliminated (Betzig et al., 2006). Cluster spatial maps were

generated by calculation of second order neighborhood local density value Li(r) for each coordinate. To obtain cluster properties, a robust and unbiased thresholding approach was applied to segment the local density spatial maps and identify regions from which cluster properties could be computed (Githaka et al., 2016; Williamson et al., 2011).

2.3.5 Extracellular crosslinking and immunoprecipitation

Cross-linking was performed with the membrane-impermeable thiol-cleavable cross-linker DTSSP (3, 3′dithiobis [sulfosuccinimidyl-propionate]; Thermo Fisher Scientific, MA, USA). INS 832/13 or HEK 293 cells (107 cells per reaction) were incubated with 25 mM DTSSP in distilled water at room temperature for 30 minutes. After the incubation, cells were washed two times with PBS, and remaining DTSSP was blocked by 15-minute incubation with 50 mM stop solution (1 M Tris, pH 7.5). Cell lysates were harvested in RIPA buffer, separated using SDS-PAGE, transferred to PVDF membrane, and probed with: mouse polyclonal anti-Myc antibody (1:2000; Merck Millipore, Billerica, MA, US); mouse anti-β-tubulin antibody (1:2000; Sigma-Aldrich. St. Louis, MO, USA); or mouse anti-K_v2.1 (1:1000 in 5% BSA; UC Davis/NIH NeuroMab Antibodies, CA, USA). Immunoprecipitation using Syntaxin 1A antibody (4E209, sc-73098) from Santa Cruz Biotechnology was as before (X. Q. Dai et al., 2012). Densitometry was performed using with ImageJ software.

2.3.6 Statistical analysis.

Data analysis was performed using FitMaster (HEKA Electronik), Origin Lab (v7.0) and GraphPad Prism (v6.0c). All data are shown as the mean ± SEM. Statistical outliers were identified by an unbiased ROUT (robust regression followed by outlier identification) test (Motulsky & Brown, 2006). Comparison of multiple groups was by ANOVA and Bonferroni post-test. When comparing two means only, data were analyzed by the 2-tailed Student's t test. A P-value less than 0.05 was considered significant.

2.4 RESULTS

2.4.1 K_v2.1 and 2.2 mediate outward K^+ currents in human β-cells, but only K_v2.1 facilitates exocytosis

Pharmacologic inhibitors of K_v2 channels and dominant-negative strategies which are not selective for K_v2.1 versus K_v2.2 enhance electrical excitability, prolong the action potential duration, increase intracellular Ca^{2+} responses, and enhance insulin secretion from rodent islets (Patrick E. MacDonald et al., 2001; Patrick E MacDonald, Sewing, et al., 2002). Although their role in insulin secretion from human islets is debated (Braun et al., 2008; X. N. Li et al., 2013), and I also find no effect of the K_v2 inhibitor stromatoxin on insulin secretion from human islets (Fig. 7), it is clear that human pancreatic β-cells express robust K_v2-mediated currents (Braun et al., 2008; Dai et al., 2012; Herrington et al., 2005; Yan et al., 2004). While often interpreted as an important role for K_v2.1, recent work in insulinoma cells suggests a key contribution of K_v2.2 (Jensen et al., 2013) and transcriptomic data demonstrate that purified β-cells express more KCNB2 than KCNB1 (Blodgett et al., 2015). Indeed, I find that in human islets KCNB2 expression is 8.7±2.0 fold higher than that of KCNB1 (Fig. 8A). Selective knockdown of KCNB1 or KCNB2 in human β-cells (Fig. 8B) demonstrates that each isoform contributes to the outward delayed rectifier current in these cells (Fig. 8C-D). However, knockdown of KCNB1, but not KCNB2, impairs depolarization-induced exocytosis in human β-cells (Fig. 7E-F) which is consistent with the divergent C-terminus homology and an inability of K_v2.2 to bind the syntaxin 1A/SNAP-25 complex (Wolf-Goldberg et al., 2006). Similar results were obtained upon knockdown of Kcnb1 and Kcnb2 in INS 832/13 insulinoma cells (Fig. 9).

Figure 7. Pharmacologic K_v2 inhibition does not enhance insulin secretion from human islets

Insulin secretion was measured from human islets at 1 or 16.7 mM glucose in the presence or absence of the $K_v2.1/2.2$ inhibitor stromatoxin (STX, 100 nM), or the non-selective K_v channel inhibitor tetraethyl ammonium TEA, 10 mM). Data are from 5 separate human islet donors. *$p<0.05$ compared with the 1 mM glucose condition, or as indicated. (All work by Aliya Spigelman).

Figure 7.

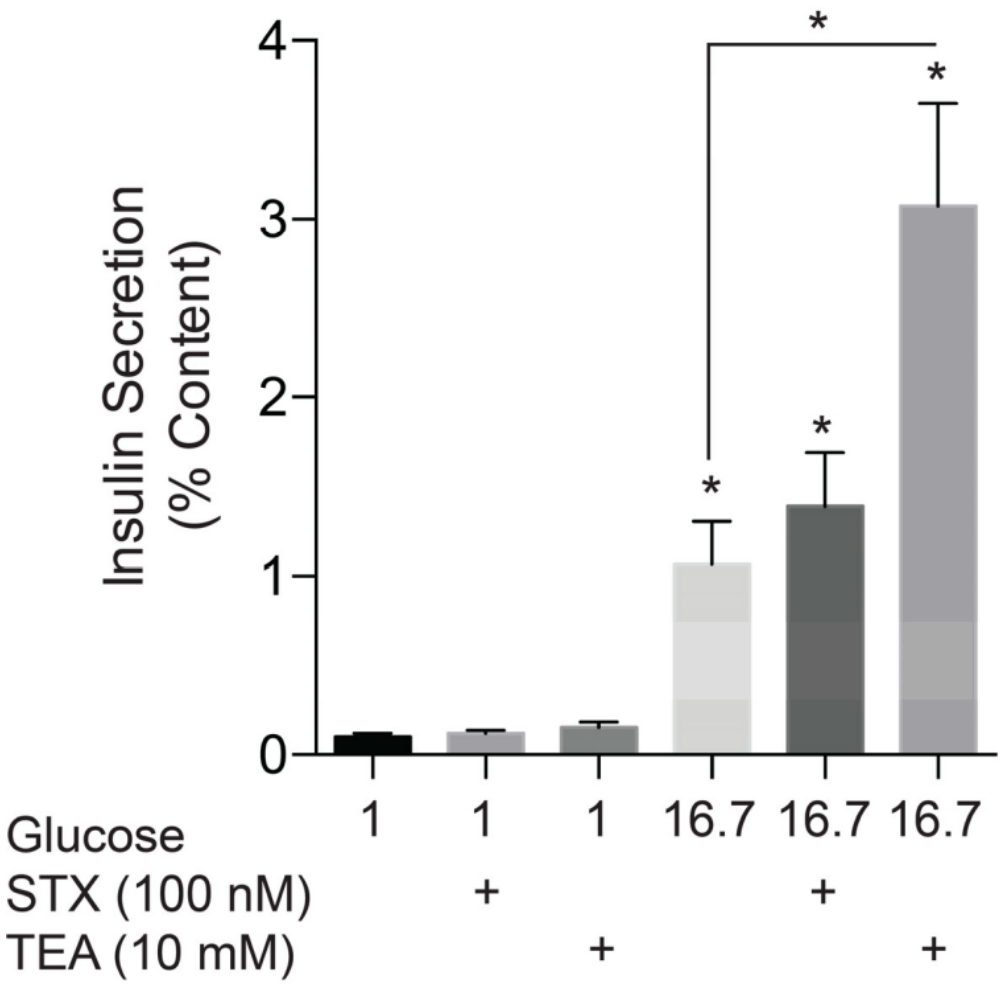
Insulin Secretion
(% Content)
4
3
2
1
0
*
*
*
*
Glucose
STX (100 nM)
TEA (10 mM)
1
1
1
16.7
16.7
16.7
+
+
+
+

Figure 8. K_v2.1, but not K_v2.2, controls exocytosis in human β-cells

A) Expression of mRNA encoding K_v2.1 (KCNB1) and K_v2.2 (KCNB2) in islets from human donors assessed by quantitative PCR (n=11 donors). B) Knockdown of KCNB1 and KCNB2 expression in human islet cells, assessed by quantitative PCR, following transfection with control siRNA duplexes (si-Scrambled) or siRNAs targeting K_v2.1 (si-K_v2.1) or K_v2.2 (si-K_v2.2) (n=6 donors). C-D) Representative traces (C) and averaged current-voltage relationships (D) of K_v currents recorded from human β-cells following transfection with si-Scrambled (grey squares), si-K_v2.1 (black circles), si-K_v2.2 (grey circles), or both (black squares) (n=20, 13, 21, 17 cells from 4 donors). E-F) Representative capacitance traces (E) and averaged cumulative exocytotic responses (F) of human β-cells to a series of membrane depolarizations following transfection with si-Scrambled, si-K_v2.1, or si-K_v2.2 (n=23, 32, 31 cells from 5 donors). *-$p<0.05$, **-$p<0.01$, and ***-$p<0.001$ compared with the K_v2.1 group (A) or Scrambled control (B-F). (all work by Fu J, except panels A and B by Manning Fox JE).

Figure 8

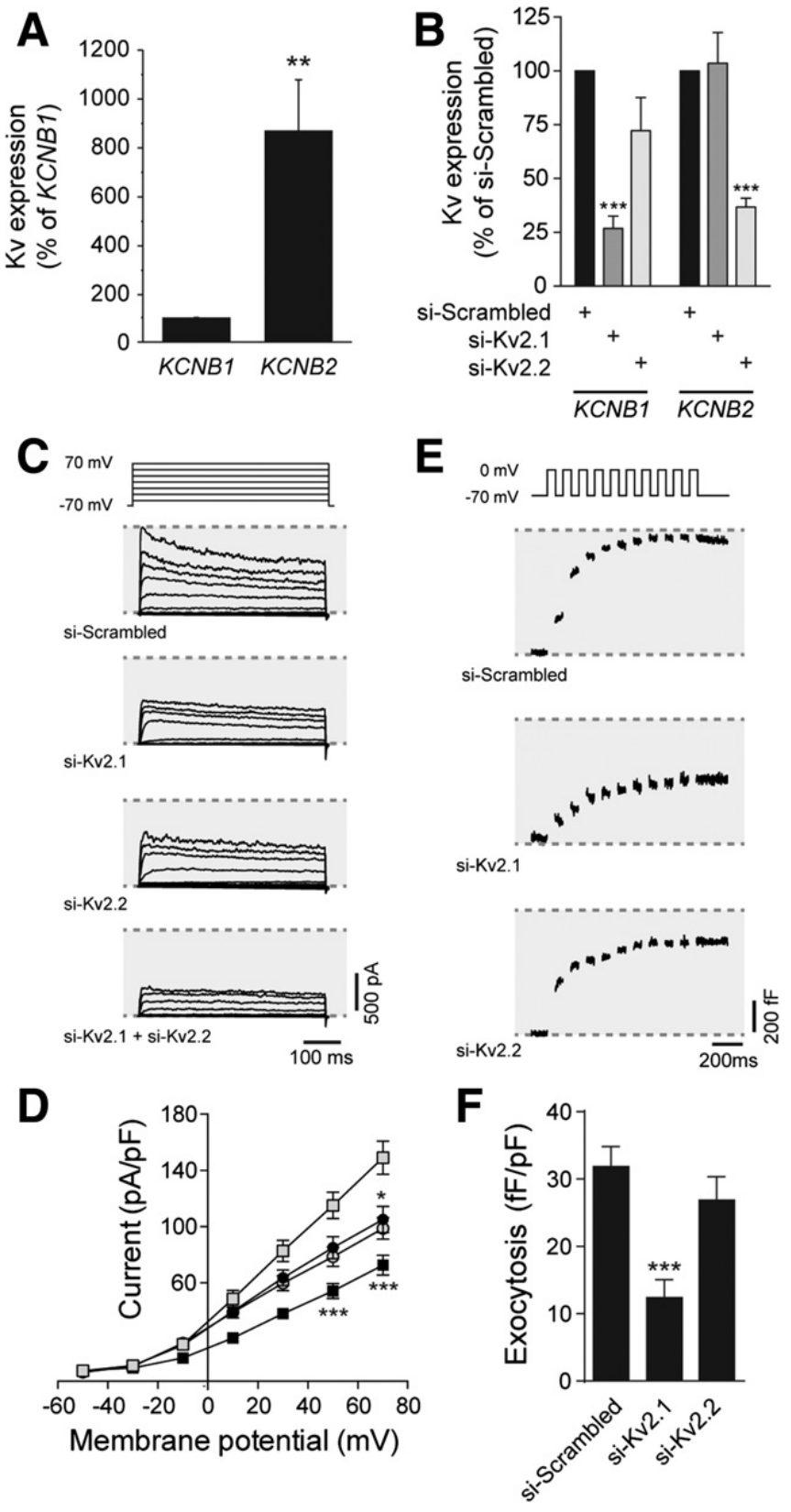
A
Kv expression (% of KCNB1)
1200
1000
800
600
400
200
0
**
KCNB1
KCNB2
B
Kv expression (% of si-Scrambled)
125
100
75
50
25
0
***
***
si-Scrambled
si-Kv2.1
si-Kv2.2
KCNB1
KCNB2
C
70 mV
-70 mV
si-Scrambled
si-Kv2.1
si-Kv2.2
si-Kv2.1 + si-Kv2.2
500 pA
100 ms
E
0 mV
-70 mV
si-Scrambled
si-Kv2.1
si-Kv2.2
200 fF
200ms
D
Current (pA/pF)
180
140
100
60
*
***
***
-60 -40 -20 0 20 40 60 80
Membrane potential (mV)
F
Exocytosis (fF/pF)
40
30
20
10
0
***
si-Scrambled
si-Kv2.1
si-Kv2.2

Figure 9. Knockdown of the K_v2.1 isoform selectively impairs depolarization-induced exocytosis in INS 832/13 cells

A) Expression of mRNA for K_v2.1 (Kcnb1) or K_v2.2 (Kcnb2) in INS 832/13 cells following infection with adenovirus expressing scrambled shRNA (Ad-shScrambled), or targeting K_v2.1 (Ad-shK_v2.1) or K_v2.2 (Ad-shK_v2.2). n=3 separate experiments.

B) Current-voltage-relationship of K_v currents recorded by whole-cell voltage-clamp from a holding potential of -70 mV in INS 832/13 cells transduced with adenovirus as indicated. n=27, 20, 18, 19 cells.

C) Cumulative exocytotic responses to a series of 10 membrane depolarizations from -70 to 0 mV by INS 832/13 cells transduced with adenovirus as indicated. n=15, 16, 11, 16 cells.

*-$p<0.05$, **-$p<0.01$, and ***-$p<0.001$ compared with Ad-sh-Scrambled. (all work by Fu J, except panels A by Manning Fox JE).

Figure 9.

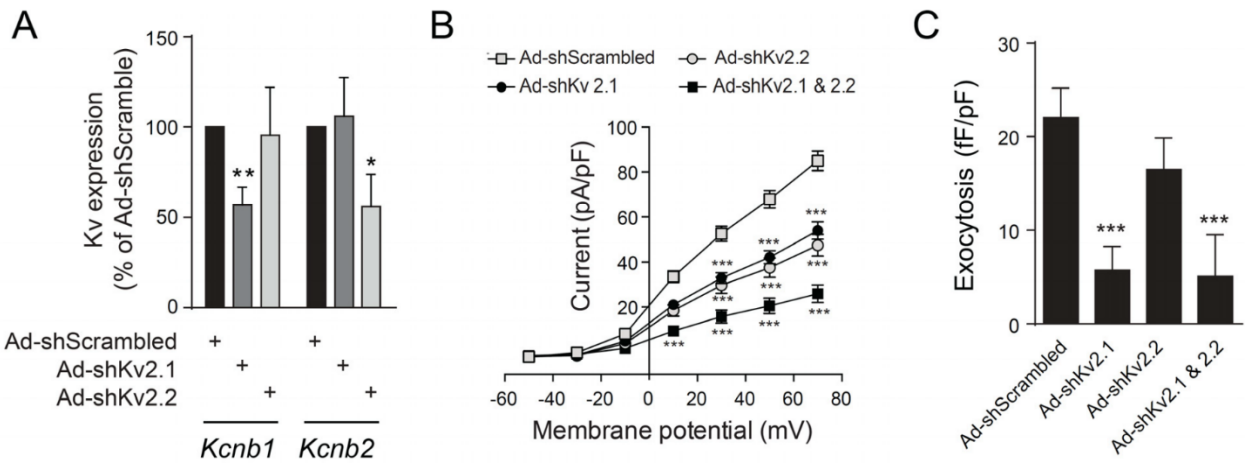
A
Kv expression (% of Ad-shScramble)
150
100
50
0
**
*
Ad-shScrambled
Ad-shKv2.1
Ad-shKv2.2
Kcnb1
Kcnb2
B
Ad-shScrambled
Ad-shKv2.2
Ad-shKv 2.1
Ad-shKv2.1 & 2.2
Current (pA/pF)
Membrane potential (mV)
C
Exocytosis (fF/pF)
30
20
10
0
***
Ad-shScrambled
Ad-shKv2.1
Ad-shKv2.2
Ad-shKv2.1 & 2.2

2.4.2 K_v2.1 clusters in β-cells

In human β-cells (Fig. 10A), and INS 832/13 cells (Fig. 10B) imaged by total internal reflected fluorescence (TIRF) microscopy to visualize fluorescence within 100 nm above the coverslip, endogenous K_v2.1 is not homogenously distributed. Using an object-based co-localization routine considering centers within 0.3 μm as co-localized, a portion of these (25.6+/3.1% in human β-cells, n=23 cells from 3 donors; 25.5+/-2.4% in INS 832/13, n=26 cells from 3 experiments) appear associated with an insulin granule. When expressed in INS 832/13 cells, a mCherry-tagged wild-type K_v2.1 (mCherry-K_v2.1-WT) also form membrane-localized clusters and can occasionally be seen to co-localize with secretory granules marked by NPY-Venus in fixed cells (Fig. 10C). Bleed through of the Venus signal into the red-channel does not account for the apparent co-localization (Fig. 12).

Using a photoactivatable (PA) mCherry-tagged channel (PAmCherry-K_v2.1-WT) I performed PALM imaging, and spatial pattern analysis (Williamson et al., 2011) of K_v2.1 clusters in HEK 293 and INS 832/13 cells. In both cell types, PAmCherry-K_v2.1-WT was non-homogenously distributed on the cell membrane (Fig. 11A-B) with 35-40% of tagged subunits being localized to clusters (Fig. 11C). Based on the average number molecules per cluster (~25-40; Fig. 11D), and assuming each tetrameric channel will have 3-4 detectable molecules, I estimate that K_v2.1 clusters contain 6-12 tetrameric channels on average. Extracellular cross-linking confirmed that these target to the plasma membrane where they form large macromolecular complexes corresponding to multi-channel clusters which barely migrate into the running gel (Fig. 11E). Following cleavage of the crosslink with 2-mercaptoethanol (2-ME) these appear as single monomeric subunits.

Figure 10. K_v2.1 forms clusters in insulin-secreting cells

A-B) Human β-cells (A) or INS 832/13 cells (B) were immune-stained with anti-K_v2.1 (red) and anti-insulin (green) antibodies and visualized by TIRF microscopy (representative of 23 cells from 3 donors and 26 cells in 3 experiments, respectively). C) INS 832/13 cell expressing mCherry-K_v2.1-WT (red) and NPY-Venus (green; 33 cells in 3 experiments).

Figure 10

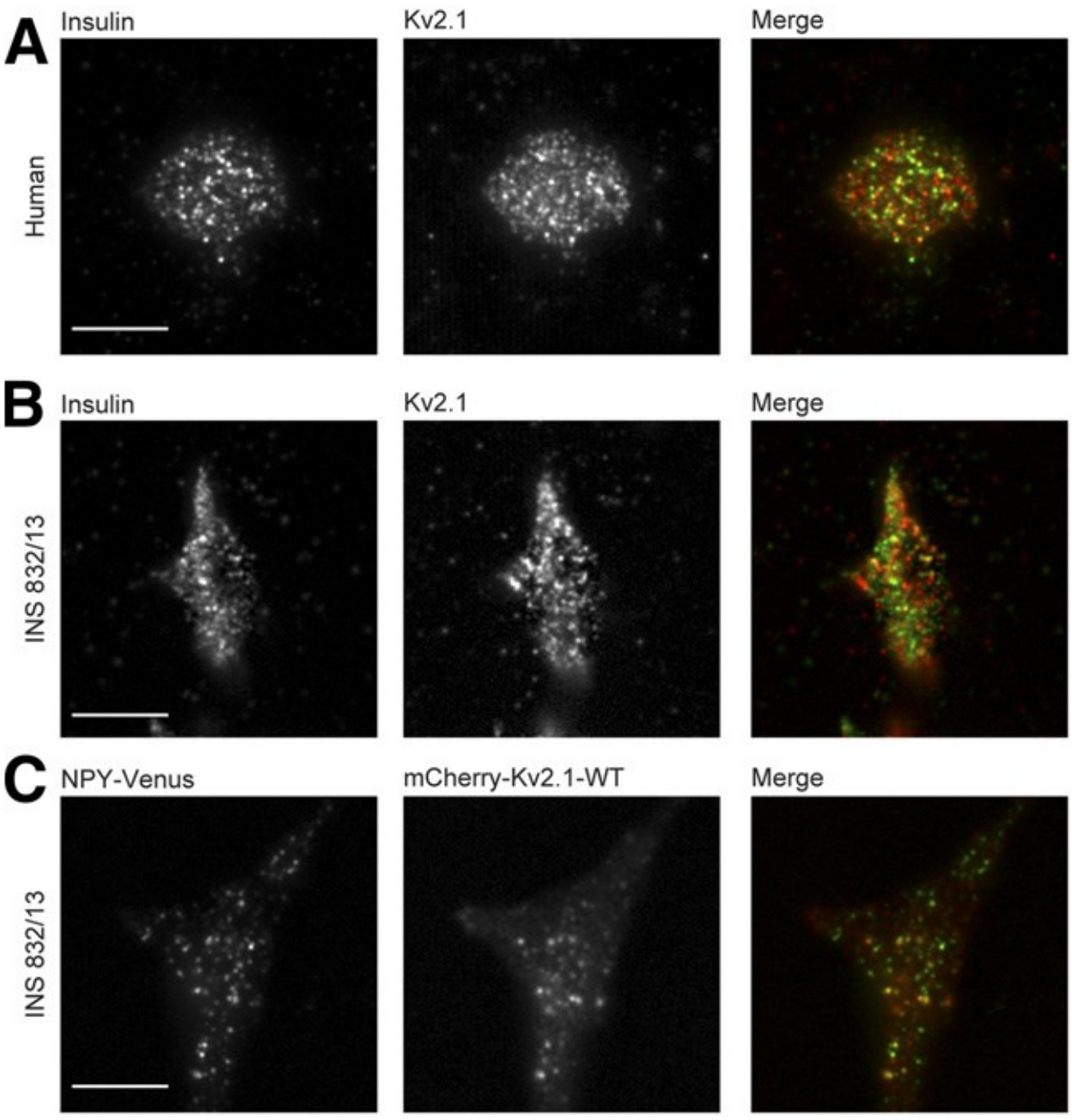
A
Insulin
Kv2.1
Merge
Human
B
Insulin
Kv2.1
Merge
INS 832/13
C
NPY-Venus
mCherry-Kv2.1-WT
Merge
INS 832/13

Figure 11. Super-resolution imaging of K_v2.1 clusters

A) PALM images of HEK 293 and INS 832/13 cells expressing PAmCherry-K_v2.1-WT (red). Inset zoom in area corresponds to the ROI. B) PAmCherry-K_v2.1-WT molecule coordinate plots for ROIs in panel A, with cluster regions determined by spatial pattern analysis, highlighted in red in the background. C-D) The percentage of PAmCherry-K_v2.1-WT molecules found within clustered domains (C) and the average number of molecules per cluster (D) in HEK 293 cells (n=22) and INS 832/13 cells (n=29). E) Extracellular cross-linking with DTSSP followed by blotting of protein lysates with anti-K_v2.1 antibody demonstrates that the tagged (PAmCherry-K_v2.1-WT) channels form large molecular weight complexes at the cell surface, consistent with channel clustering. Breakdown of crosslinks with 2-mercaptoethanol reveals the expression of channel monomers (representative of n=6 experiments). (Panels A-D by Githaka JM and panel E by Fu J)

Figure 11

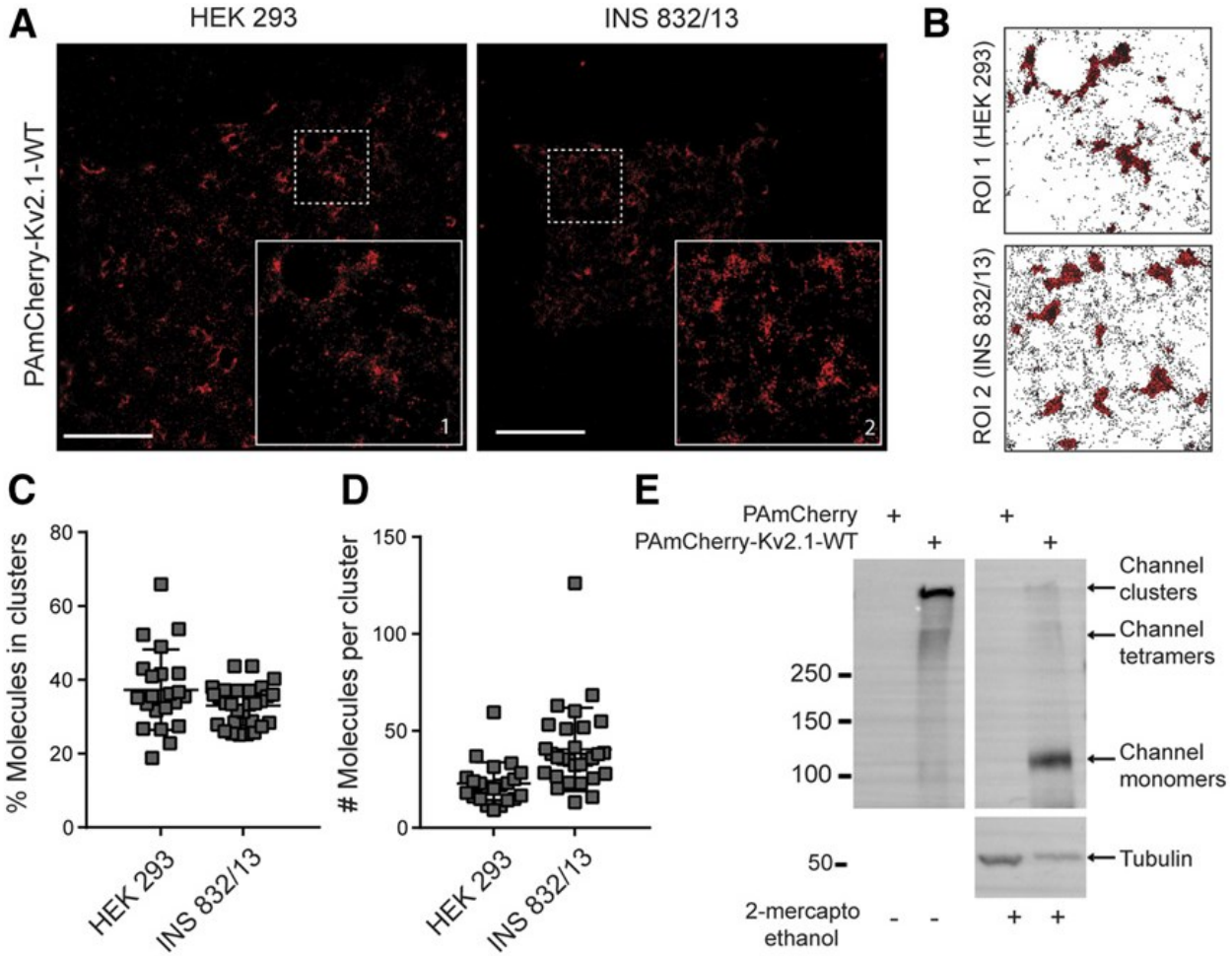
A
HEK 293
INS 832/13
PAmCherry-Kv2.1-WT
1
2
B
ROI 1 (HEK 293)
ROI 2 (INS 832/13)
C
% Molecules in clusters
80
60
40
20
0
HEK 293
INS 832/13
D
Molecules per cluster
150
100
50
0
HEK 293
INS 832/13
E
PAmCherry + +
PAmCherry-Kv2.1-WT + +
Channel clusters
Channel tetramers
250
150
100
Channel monomers
50
Tubulin
2-mercapto ethanol - - + +

Figure 12. Separation of mCherry-K_v2.1-WT and NPY-Venus signals

INS 832/13 cells were expressing either mCherry-K_v2.1-WT alone (red), NPY-Venus alone (green) or both, and imaged using TIRF microscopy as outlined in the Methods. Bleed through between channels was not detected. In the bottom example two cells transfected with NPY-Venus are shown, only one of which is co-expressing mCherry-K_v2.1-WT.

In some of these images (i.e. the negative green - top left -, and negative red - middle) I have increased the brightness relative to other images in order to detect possible bleed-through. (All panels by J Fu)

Figure 12.

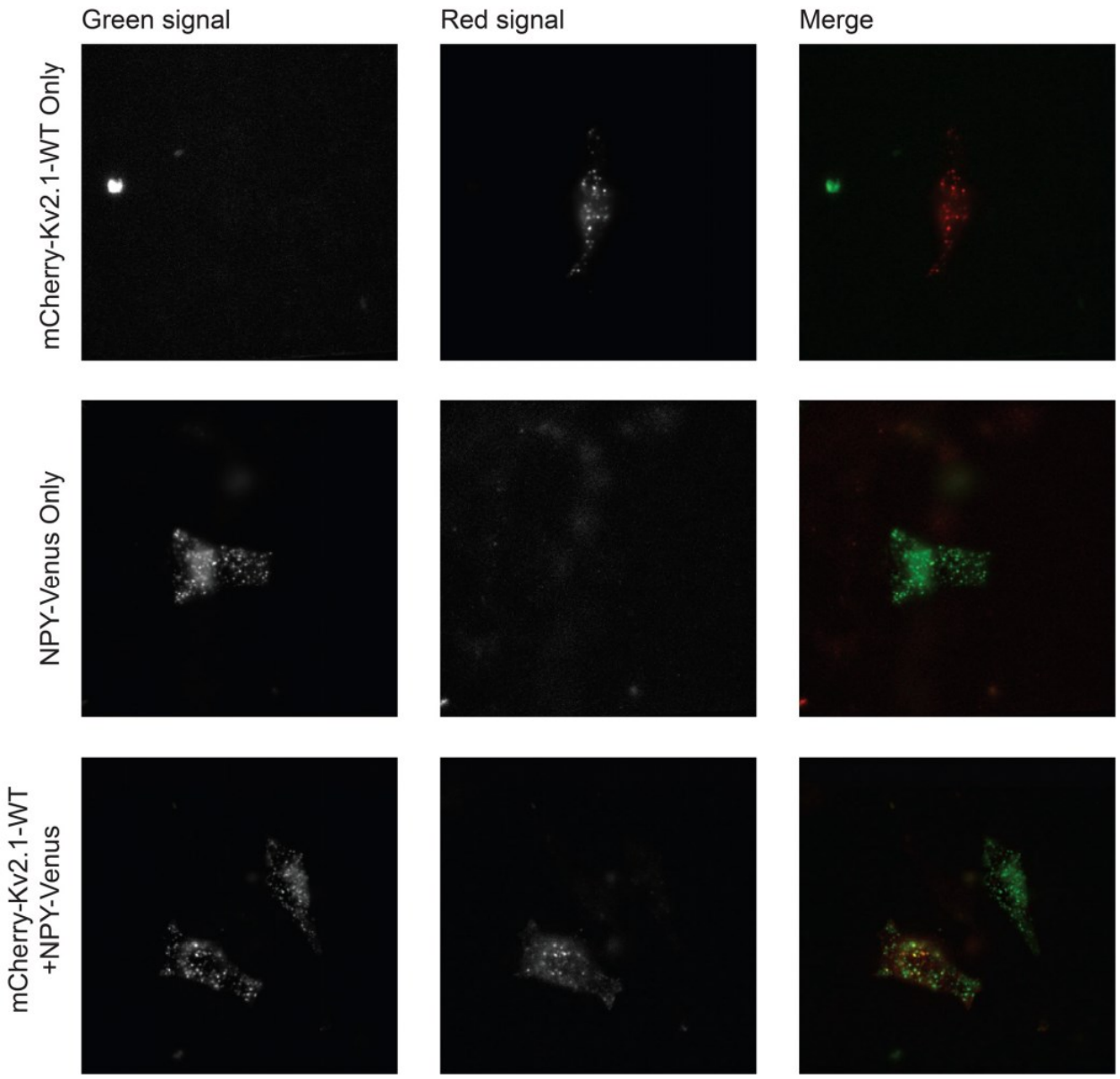
Green signal
Red signal
Merge
mCherry-Kv2.1-WT Only
NPY-Venus Only
mCherry-Kv2.1-WT
+NPY-Venus

2.4.3 Clusters of K_v2.1 promotes exocytosis

I generated clustering-deficient channels (mCherry-K_v2.1-ΔC318 and Myc-K_v2.1-ΔC318; Fig. 13A), based on previous reports that a region in the C-terminus is required for K_v2.1 clustering (Lim et al., 2000). These do not form clusters when expressed in HEK 293 cells (Fig. 13B, D; Fig. 15) and form substantially fewer clusters in INS 832/13 cells (Fig. 13C-F, Fig. 16). I found that the K_v2.1-ΔC318 constructs retained at least some ability to form clusters when in the INS 832/13 cells, which I attribute to an interaction with the endogenous full-length channel (Fig. 14). Nonetheless, as demonstrated previously (Lim et al., 2000), the truncated channel formed many fewer membrane-resident clusters than the full-length channel despite similar levels of expression (see 2-ME treated groups in Fig. 13B-C). Additionally, the density of membrane-resident secretory granules was reduced in INS 832/13 cells expressing mCherry-K_v2.1-ΔC318, compared with cells expressing mCherry-K_v2.1-WT (Fig. 13E-F), and co-localization was significantly reduced (from 29.1+/-2.4 to 18.3+/-1.8% of granules associated with an apparent K_v2.1 cluster; n=67, 69 cells, $p<0.001$), although this could result from reduced spot density which was not corrected for.

Importantly, the truncated constructs retain similar electrical function to the wild type channels in INS 832/13 (Fig. 14A-B) and HEK 293 (Fig. 15C) cells, and both the Myc-K_v2.1-WT and Myc-K_v2.1-ΔC318 interacted equally with Syntaxin 1A in INS 832/13 cells (Fig. 5C-D). However, while both the full length mCherry-K_v2.1-WT and Myc-K_v2.1-WT enhanced depolarization-induced exocytosis in INS 832/13 cells, the clustering-deficient mutants did not (Fig. 14E-F, Fig. 15D) suggesting that channel clustering per se, in addition to Syntaxin 1A binding (X. Q. Dai et al., 2012; Singer-Lahat et al., 2007), is required to facilitate exocytosis.

Figure 13. A clustering-deficient K_v2.1 reduces secretory granule recruitment to the plasma membrane

A) MCherry and Myc-tagged clustering-deficient K_v2.1 channels were generated by truncating the final 318 amino acids (mCherry/Myc-K_v2.1-ΔC318) of the rat sequence. B-D) When expressed in HEK 293 (B, n=6 experiments) or INS 832/13 cells (C, n=10 experiments) the Myc-K_v2.1-ΔC318 formed fewer high molecular weight clusters, which could be broken down to channel monomers by 2-mercaptoethanol. Although Myc-K_v2.1-ΔC318 retained some ability to form clusters in INS 832/13 cells, likely due to combination with native K_v2.1 (see Figure 12), quantification (D; n=6,10) revealed that the majority of signal remains tetrameric (i.e. single-channel rather than cluster). Additional assessment of the clustering of these constructs is presented in Fig 16. A-B) When expressed in INS 832/13 cells and visualized by TIRF microscopy, mCherry-K_v2.1-ΔC318 forms fewer clusters than mCherry-K_v2.1-WT and results in fewer membrane-resident secretory granules, marked by NPY-Venus (n=37, 62 cells from 5 experiments). Scale bars represent 10 μm. ***-$p<0.001$ compared with mCherry-K_v2.1-WT. (all panels by J Fu)

Figure 13

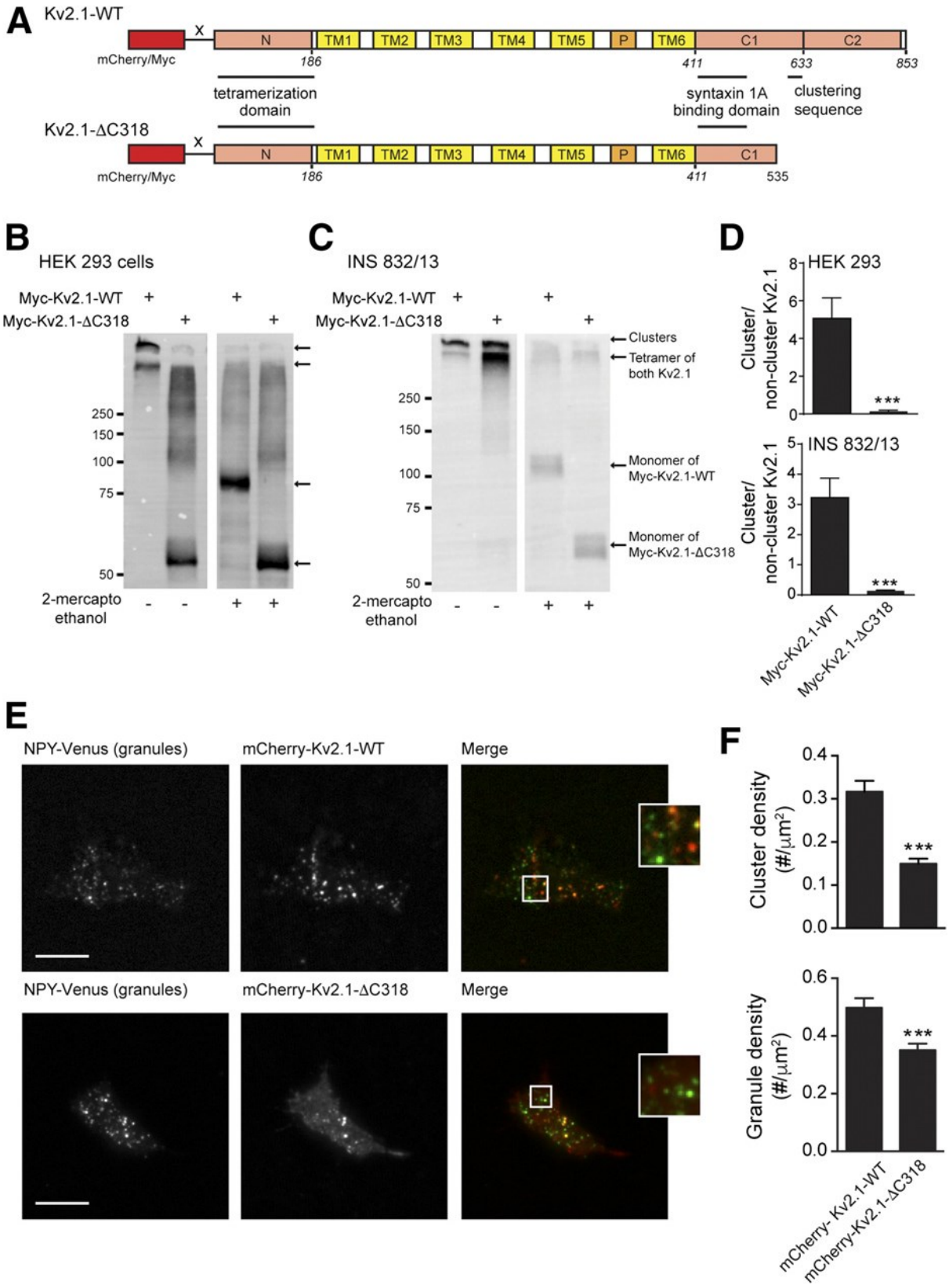
A
Kv2.1-WT
X
N
TM1
TM2
TM3
TM4
TM5
P
TM6
C1
C2
mCherry/Myc
186
411
633
853
tetramerization domain
syntaxin 1A binding domain
clustering sequence
Kv2.1-ΔC318
535
B
HEK 293 cells
Myc-Kv2.1-WT
Myc-Kv2.1-ΔC318
250
150
100
75
50
2-mercapto ethanol
C
INS 832/13
Clusters
Tetramer of both Kv2.1
Monomer of Myc-Kv2.1-WT
Monomer of Myc-Kv2.1-ΔC318
D
HEK 293
INS 832/13
Cluster/ non-cluster Kv2.1
***
Myc-Kv2.1-WT
Myc-Kv2.1-ΔC318
E
NPY-Venus (granules)
mCherry-Kv2.1-WT
Merge
mCherry-Kv2.1-ΔC318
F
Cluster density (#/μm²)
Granule density (#/μm²)
mCherry-Kv2.1-WT
mCherry-Kv2.1-ΔC318

Figure 14. Clustering-deficient K_v2.1 retains electrical activity and Syntaxin 1A binding, but does not facilitate exocytosis

A-B) Representative K_v currents (A) and quantified current-voltage relationships (B) from INS 832/13 cells expressing GFP alone, Myc-K_v2.1-WT, or Myc-K_v2.1-ΔC318. (n=17, 19, 18 cells). C-D) Co-immunoprecipitation of Syntaxin 1A (Syn1A) pulled-down both Myc-K_v2.1-WT and Myc-K_v2.1-ΔC318 equally well (n=7 experiments). E-F) Representative capacitance traces (E) and cumulative exocytotic responses (F) of INS 832/13 cells expressing GFP alone, Myc-K_v2.1-WT, or Myc-K_v2.1-ΔC318. (n=15, 22, 17 cells). *-$p<0.01$ as indicated, ***-$p<0.001$ versus GFP control. (All panels by J Fu).

Figure 14

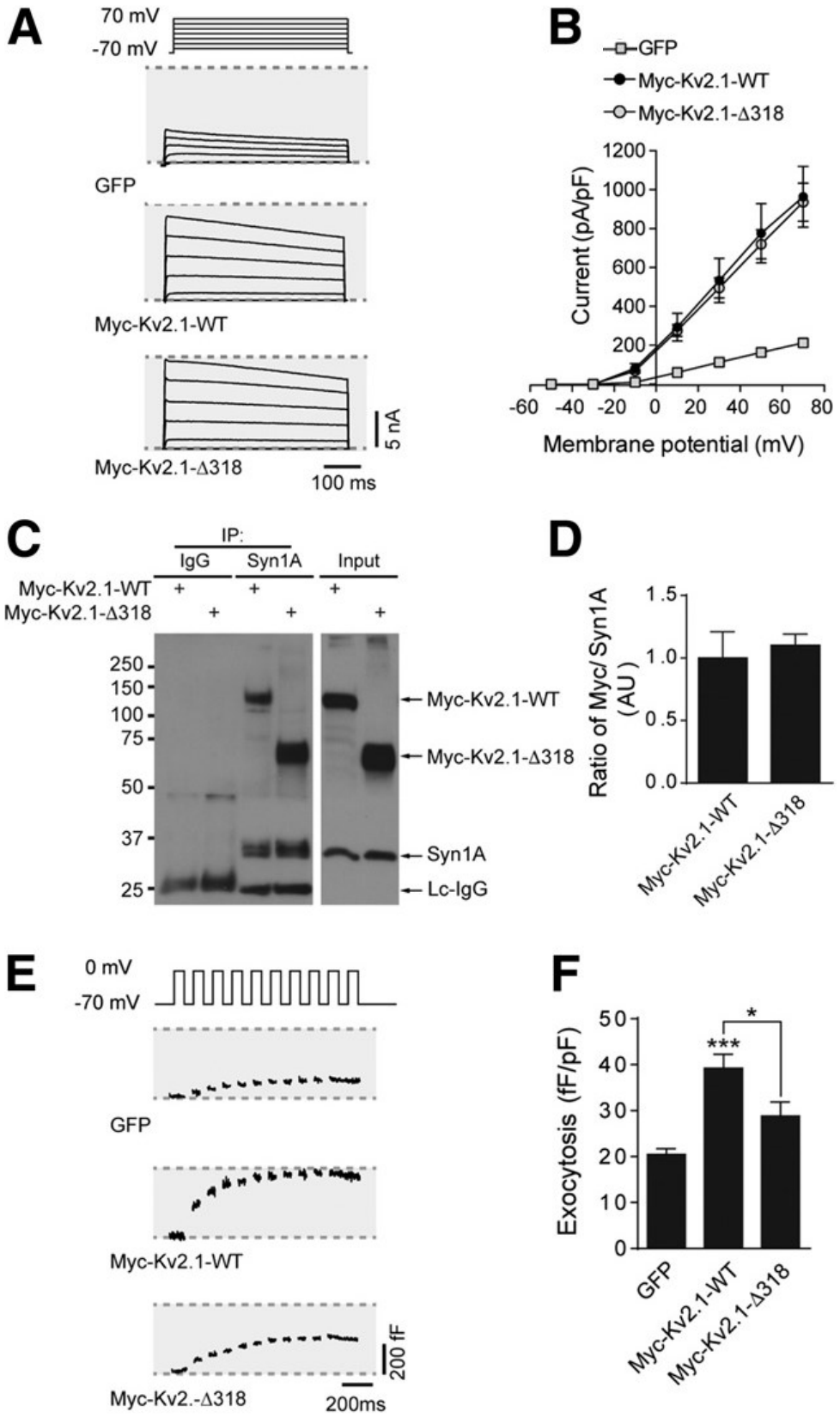
A
70 mV
-70 mV
GFP
Myc-Kv2.1-WT
Myc-Kv2.1-Δ318
5 nA
100 ms
B
GFP
Myc-Kv2.1-WT
Myc-Kv2.1-Δ318
Current (pA/pF)
Membrane potential (mV)
C
IP:
IgG
Syn1A
Input
Myc-Kv2.1-WT
Myc-Kv2.1-Δ318
250
150
100
75
50
37
25
Myc-Kv2.1-WT
Myc-Kv2.1-Δ318
Syn1A
Lc-IgG
D
Ratio of Myc/ Syn1A (AU)
Myc-Kv2.1-WT
Myc-Kv2.1-Δ318
E
0 mV
-70 mV
GFP
Myc-Kv2.1-WT
Myc-Kv2.-Δ318
200 fF
200ms
F
Exocytosis (fF/pF)
***
*
GFP
Myc-Kv2.1-WT
Myc-Kv2.1-Δ318

Figure 15. Wild-type (WT) and clustering-deficient (ΔC318) K_v2.1 tagged with mCherry mediate identical outward K^+ currents, but only the wild-type channel facilitates exocytosis

A) mCherry-K_v2.1-WT and mCherry-K_v2.1-ΔC318 visualized in HEK 293 and INS 832/13 cells by total internal reflection fluorescence (TIRF) microscopy.

B) The clustering-deficient mutant (ΔC318) forms fewer membrane-localized clusters in both HEK 293 (n=8, 9 cells) and INS 832/13 cells (n=20, 22 cells).

C) Current-voltage relationship of outward K^+ currents mediated by mCherry-K_v2.1-WT and mCherry-K_v2.1-ΔC318 expressed in HEK 293 cells. Representative traces (left) and averaged data (right) are shown. n=20, 20 cells.

D) Exocytosis was elicited by a series of 10 depolarizations from -70 to 0 mV in INS 832/13 cells transfected with control plasmid (mCherry), mCherry-K_v2.1-WT, or mCherry-K_v2.1-ΔC318. Representative capacitance traces (left) and averaged cumulative responses (right) are shown. n=29, 31, 32 cells.

*-$p<0.05$ and ***-$p<0.001$ compared with the wild-type or mCherry groups. (Panels A,B by G Plummer; panels C,D by J Fu).

Figure 15.

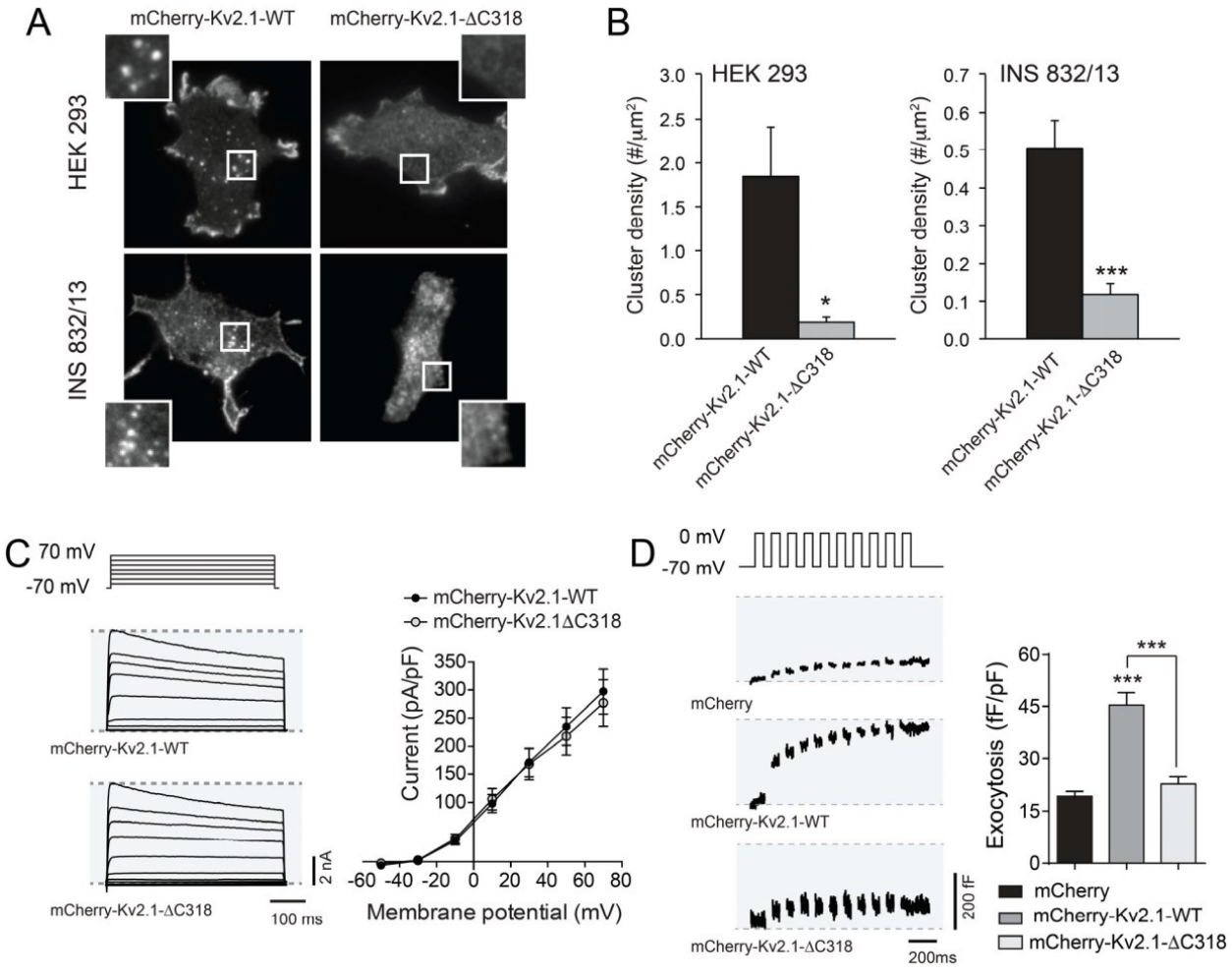
A
mCherry-Kv2.1-WT
mCherry-Kv2.1-ΔC318
HEK 293
INS 832/13
B
HEK 293
INS 832/13
Cluster density (#/μm²)
mCherry-Kv2.1-WT
mCherry-Kv2.1-ΔC318
*
***
C
70 mV
-70 mV
mCherry-Kv2.1-WT
mCherry-Kv2.1-ΔC318
2 nA
100 ms
mCherry-Kv2.1-WT
mCherry-Kv2.1ΔC318
Current (pA/pF)
Membrane potential (mV)
D
0 mV
-70 mV
mCherry
mCherry-Kv2.1-WT
mCherry-Kv2.1-ΔC318
200 fF
200ms
Exocytosis (fF/pF)
mCherry
mCherry-Kv2.1-WT
mCherry-Kv2.1-ΔC318

Figure 16. K_v2.1-ΔC318 combines retains some ability to cluster by combining with endogenous K_v2.1 in INS 832/13 cells

A) Although much of the Myc-K_v2.1-ΔC318 expressed in INS 832/13 cells can be observed as extracellular K_v2.1 channel monomers (i.e. tetrameric single channels) a portion can still form clusters that are evident even as the amount of loaded protein on the gel is reduced. Membrane is blotted with anti-Myc.

B) The anti-K_v2.1 antibody used here is known to recognize a C-terminus epitope that is lacking in the K_v2.1-ΔC318 constructs. I confirm that this antibody recognizes mCherry-K_v2.1-WT and Myc-K_v2.1-WT, but not the respective truncated (ΔC318) mutants. This blot also confirms the cell-surface expression of mCherry- K_v2.1-WT.

C) INS 832/13 cells expressing Myc-K_v2.1-WT, Myc-K_v2.1-ΔC318, or Myc alone were immune-stained with anti-Myc (red) and anti-K_v2.1 (green; which recognizes full-length and endogenous K_v2.1 but not the truncated mutant). A high degree of colocalization was observed between the truncated K_v2.1 and endogenous K_v2.1, suggesting the interaction of Myc-K_v2.1-ΔC318 with endogenous K_v2.1 channels. Scale bar is 10 μM.

D) Density of native K_v2.1 clusters, assessed by immunostaining with the anti-K_v2.1 antibody and imaged with TIRF microscopy, in INS 832/13 cells expressing Myc alone or Myc-K_v2.1-ΔC318 (n=21, 34 cells). **p<0.01 (all panels by J Fu).

Figure 16.

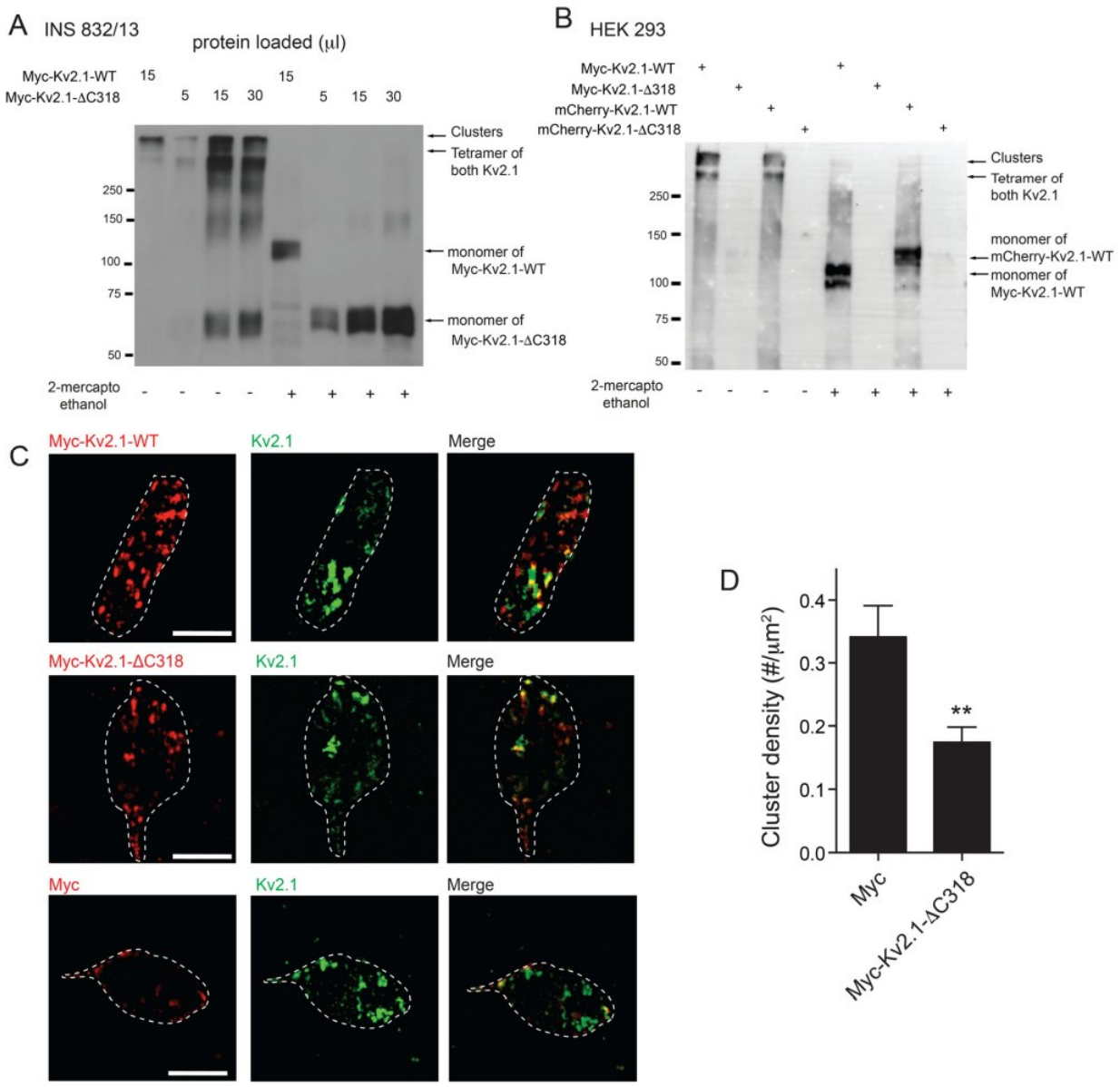
A
INS 832/13
protein loaded (µl)
Myc-Kv2.1-WT
Myc-Kv2.1-ΔC318
15
5
15
30
15
5
15
30
Clusters
Tetramer of both Kv2.1
monomer of Myc-Kv2.1-WT
monomer of Myc-Kv2.1-ΔC318
250
150
100
75
50
2-mercapto ethanol
- - - - + + + +
B
HEK 293
Myc-Kv2.1-WT
Myc-Kv2.1-Δ318
mCherry-Kv2.1-WT
mCherry-Kv2.1-ΔC318
Clusters
Tetramer of both Kv2.1
monomer of mCherry-Kv2.1-WT
monomer of Myc-Kv2.1-WT
250
150
100
75
50
2-mercapto ethanol
C
Myc-Kv2.1-WT
Kv2.1
Merge
Myc-Kv2.1-ΔC318
Kv2.1
Merge
Myc
Kv2.1
Merge
D
Cluster density (#/µm²)
0.4
0.3
0.2
0.1
0.0
**
Myc
Myc-Kv2.1-ΔC318

2.4.4 K_v2.1 clustering and granule recruitment to the plasma membrane

Knockdown of K_v2.1 (Fig. 17A) in INS 832/13 cells reduced the number of membrane-resident secretory granules at both low glucose (1 mM) and following 15 or 30 minute stimulation with 16.7 mM glucose (Fig. 17B-C). In cells expressing mCherry-K_v2.1-WT, glucose-stimulation increased the density of membrane resident secretory granules over 30 minutes, but this response was absent in cells expressing mCherry-K_v2.1-ΔC318 (Fig. 18A-C). Accordingly, expression of mCherry-K_v2.1-WT also enhanced the glucose-dependent facilitation of exocytosis in INS 832/13 cells (Fig. 19). While glucose stimulation tended to increase the total mCherry-K_v2.1-WT cluster density (Fig. 18C), this was not statistically significant. Of note, I do not observe a glucose-dependent increase in K_v current in human β-cells (Fig. 20).

Figure 17. K_v2.1 and a role for the channel in granule recruitment

A) Knockdown of K_v2.1 protein in Ad-shK_v2.1 infected INS 832/13 cells compared with controls (Ad-shScrambled; n=4 experiments). B-C) Knockdown of K_v2.1 in INS 832/13 cells resulted in a decreased density of membrane-resident secretory granules marked with NPY-Venus and visualized by TIRF microscopy at both 1 and 16.7 mM glucose. Representative images (B) and quantified data (C) are shown (n=30, 30, 27, 30, 28, 30 cells in 3 experiments) Scale bars represent 10 μm. **-$p<0.01$, and ***-$p<0.001$ compared with 1 mM glucose control or as indicated. (All panels by J Fu).

Figure 17

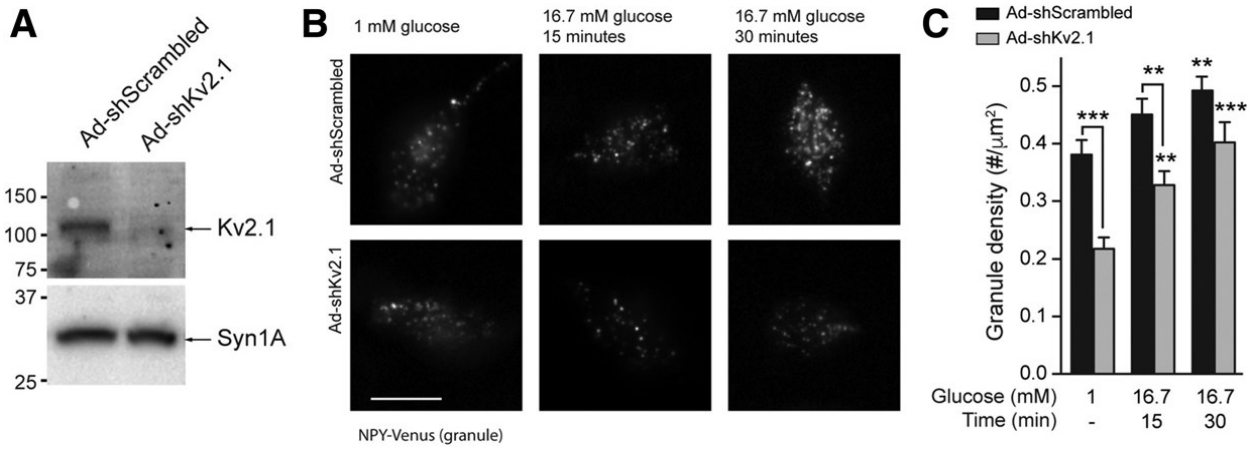
A
Ad-shScrambled
Ad-shKv2.1
150
100
75
37
25
Kv2.1
Syn1A
B
1 mM glucose
16.7 mM glucose
15 minutes
16.7 mM glucose
30 minutes
Ad-shScrambled
Ad-shKv2.1
NPY-Venus (granule)
C
Ad-shScrambled
Ad-shKv2.1
Granule density (#/μm²)
0.5
0.4
0.3
0.2
0.1
0.0
**
**
**
***
***
Glucose (mM) 1 16.7 16.7
Time (min) - 15 30

Figure 18. K_v2.1 clusters promote secretory granule recruitment

A-D) Representative images (A-B) and quantified data (C-D) of INS 832/13 cells expressing mCherry-K_v2.1-WT (red) or mCherry-K_v2.1-ΔC318 (red) and NPY-Venus (green) at 1 mM glucose and after 15 or 30 minutes of 16.7 mM glucose, visualized by TIRF microscopy. Glucose-stimulation increased the density of membrane-resident secretory granules (C) in the mCherry-K_v2.1-WT group (black bars), but not the mCherry-K_v2.1-ΔC318 group (grey bars), the latter of which had fewer channel clusters (D). *-$p<0.05$, **-$p<0.01$ compared with the 1 mM glucose condition, or as indicated. (All panels by J Fu).

Figure 18

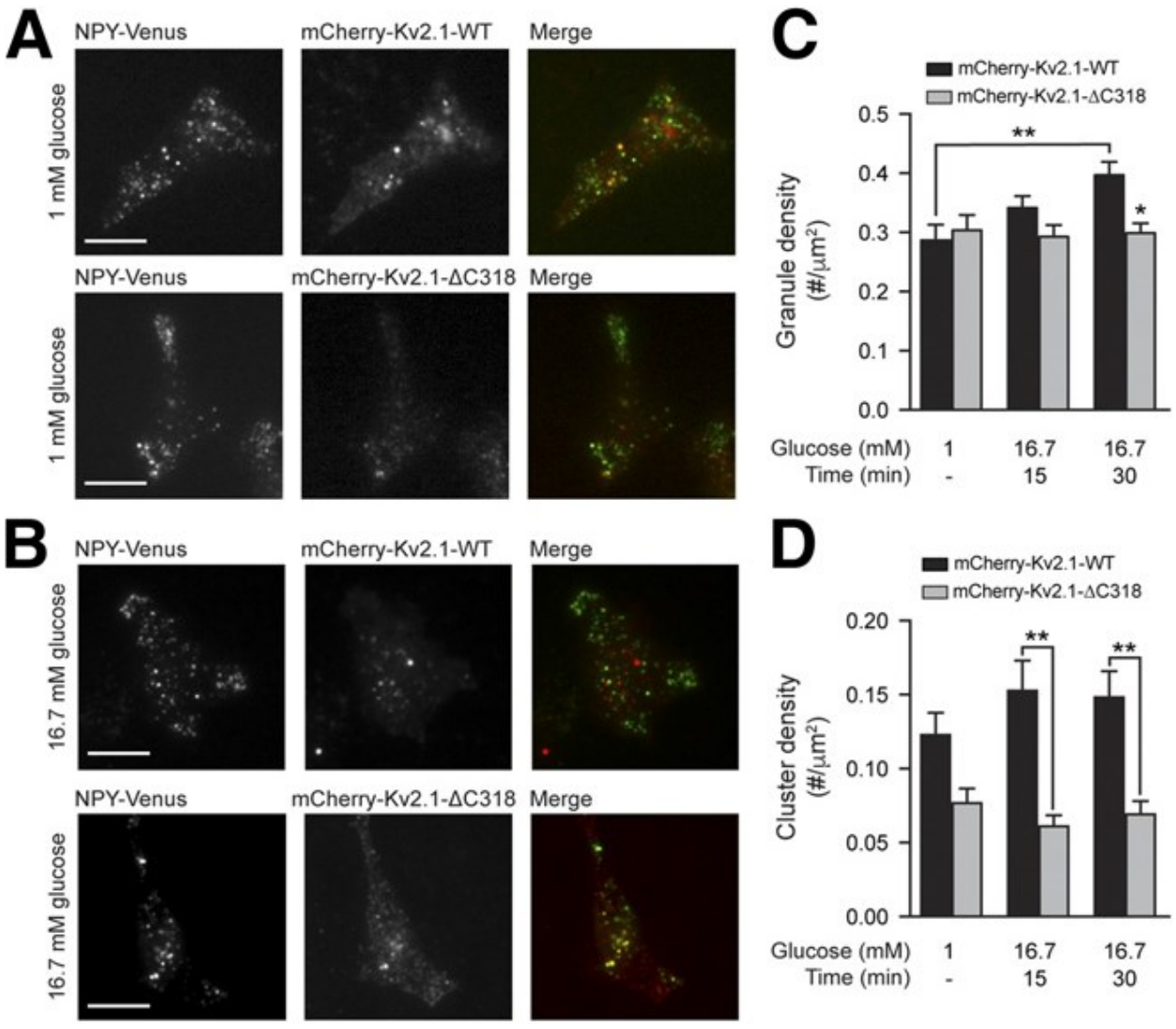
A
NPY-Venus
mCherry-Kv2.1-WT
Merge
1 mM glucose
NPY-Venus
mCherry-Kv2.1-ΔC318
Merge
1 mM glucose
B
NPY-Venus
mCherry-Kv2.1-WT
Merge
16.7 mM glucose
NPY-Venus
mCherry-Kv2.1-ΔC318
Merge
16.7 mM glucose
C
mCherry-Kv2.1-WT
mCherry-Kv2.1-ΔC318
Granule density (#/μm²)
0.5
0.4
0.3
0.2
0.1
0.0
**
*
Glucose (mM) 1 16.7 16.7
Time (min) - 15 30
D
mCherry-Kv2.1-WT
mCherry-Kv2.1-ΔC318
Cluster density (#/μm²)
0.20
0.15
0.10
0.05
0.00
**
**
Glucose (mM) 1 16.7 16.7
Time (min) - 15 30

Figure 19. Up-regulation of K_v2.1 enhances depolarization-induced exocytosis at low and high glucose in INS-1 832/13 cells

Exocytosis was elicited by a series of 10 depolarizations from -70 to 0 mV and measured as increases in cell capacitance in INS-1 832/13 cells following transfection with a control plasmid (mCherry) or the mCherry-tagged wild-type K_v2.1 (mCherry-K_v2.1-WT). Experiments were performed after a 1-hour pre-incubation at 1 mM glucose and subsequent exposure of cells to 1 or 16.7 mM glucose in the patch-clamp bath solution.

A-B) Representative membrane capacitance responses.

C) Cumulative exocytotic responses over the series of 10 membrane depolarizations. n=26, 36, 25, 17 cells.

***-$p<0.001$ compared with the mCherry groups. (All panels by J Fu).

Figure 19.

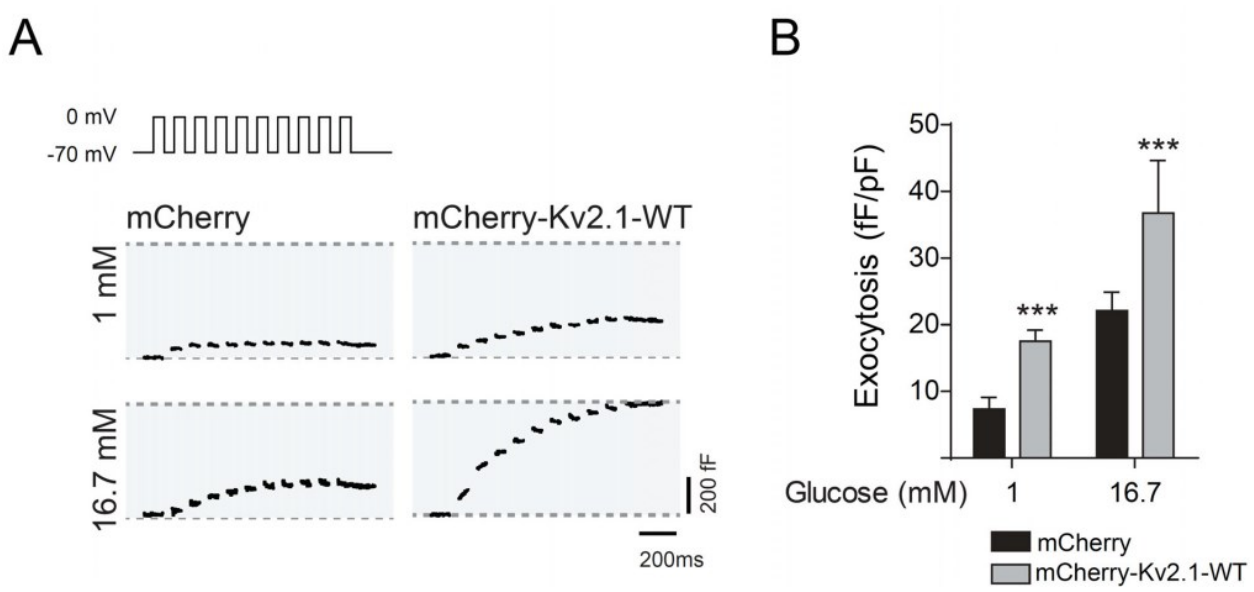
A
0 mV
-70 mV
mCherry
mCherry-Kv2.1-WT
1 mM
16.7 mM
200 fF
200ms
B
Exocytosis (fF/pF)
50
40
30
20
10
***
***
Glucose (mM)
1
16.7
mCherry
mCherry-Kv2.1-WT

Figure 20. No effect of prior glucose-stimulation on K_v currents recorded from human β-cells under the whole-cell patch-clamp condition

K_v currents were recorded from human β-cells, positively identified by insulin immunostaining, under glucose-stimulation conditions known to amplify the exocytotic response (Ferdaoussi et al, JCI, 2015).

A) Cells were pre-incubated at 1 mM glucose for 1 hour, and then exposed to 1 or 10 mM glucose in the bath solution for 15-30 minutes prior to making the whole-cell patch-clamp (at arrow) in order to test whether the resulting K_v currents were altered by glucose-treatment.

B) Current-voltage relationship of K_v currents elicited from a holding potential of -70 mV, measured from human β-cells (n=28 and 50 cells from 6 donors).

C) Voltage-dependence of steady-state inactivation of K_v currents from human β-cells from holding potentials ranging between -130 and 10 mV (n=35 and 40 cells from 6 donors). (All panels by L Senior)

Figure 20.

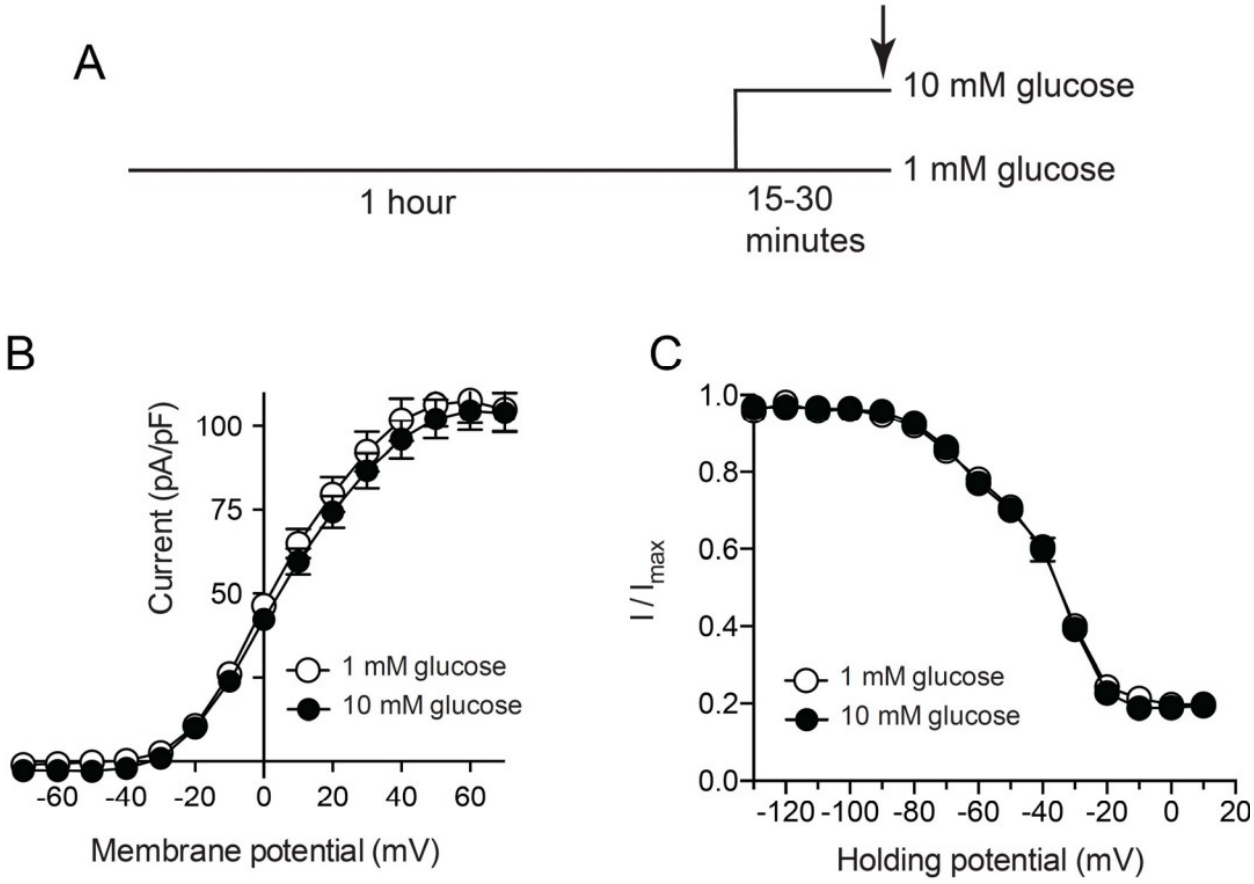
A
10 mM glucose
1 mM glucose
1 hour
15-30
minutes
B
Current (pA/pF)
100
75
50
1 mM glucose
10 mM glucose
-60 -40 -20 0 20 40 60
Membrane potential (mV)
C
I / I max
1.0
0.8
0.6
0.4
0.2
0.0
1 mM glucose
10 mM glucose
-120 -100 -80 -60 -40 -20 0 20
Holding potential (mV)

2.4.5 Up-regulation of $K_v2.1$ in T2D β-cells enhances exocytosis and insulin secretion

Insulin secretion is impaired in T2D due at least in part to a reduced exocytotic response (Ferdaoussi et al., 2015; Qin et al., 2017) A dissociation between secretory granules and sites of voltage-dependent Ca^{2+} entry has been reported in T2D models (Stephan C Collins et al., 2010; Michael B Hoppa et al., 2009). In β-cells from donors with T2D, I find that K_v currents are similar to those from ND donors (Fig. 21A-B), although knockdown of either KCNB1 (Fig. 21A) or KCNB2 (Fig. 21B) now fail to inhibit K_v currents. Indeed, compared with islets from ND donors, KCNB1 (Fig. 21C) and KCNB2 (not shown) is lower in islets of donors with T2D (to 38 and 24% of controls, respectively). Consistent with our recent reports (Ferdaoussi et al., 2015; Gooding et al., 2015) I find that the ability of glucose to amplify β-cell exocytosis is impaired in T2D β-cells (Fig. 21D, F). Up-regulation of $K_v2.1$-WT was sufficient to improve exocytotic function in β-cells from donors with T2D measured either by patch-clamp (Fig. 21E-F) or live cell TIRF microscopy (Fig. 21G-I). Notably, live-cell TIRF imaging demonstrates that while the full-length $K_v2.1$-WT increases exocytosis ND β-cells (Fig. 21H, I) and increases the exocytotic response in T2D β-cells to the level seen in control in ND cells (Fig. 21H, J), the truncated $K_v2.1$-ΔC318 construct is without effect. Finally, in islets from donors with T2D where the insulin secretory response is impaired compared with matched ND controls (Fig. 22), transduction with adenovirus expressing a full-length, but electrically inactive, $K_v2.1$ (Ad-$K_v2.1$W365C/Y380T) increased glucose-stimulated insulin secretion (Fig. 21J-L).

Figure 21. Up-regulation of K_v2.1 in human T2D β-cells improves exocytotic function

A-B) Knockdown of K_v2.1 (KCNB1; A; n=13, 13 cells from 2 donors) or K_v2.2 (KCNB2; B; n=19, 23 cells from 3 donors) expression failed to reduce voltage-dependent K+ currents in β-cells from donors with type 2 diabetes (T2D). C) Expression of K_v2.1 (KCNB1) mRNA in islets from donors with no diabetes (ND) or with T2D (n=11 and 5 donors). D-E) Representative capacitance responses at 10 mM glucose from un-transfected (D) β-cells of ND and T2D donors and of transfected β-cells (E) of T2D donors expressing GFP alone or together with K_v2.1-WT. F) The cumulative exocytotic responses from panels D and E (n=30, 30 cells from 3 ND and 3 T2D donors - left; n=32, 34 cells from 5 T2D donors - right). G) Images from live-cell TIRF of ND and T2D β-cells expressing mCherry, mCherry-K_v2.1-WT or mCherry-K_v2.1-ΔC318 and the granule marker NPY-EGFP (greyscale). Red dots indicate exocytotic events occurring over 2 minutes upon increasing glucose from 2.8 to 5 mM H, I) Average frequency of exocytotic events in ND (H; n=17, 20, 21 cells from 2 donors) and T2D (I; n=24, 34, 30 cells from 2 T2D donors) β-cells. J-K) Insulin secretory profiles of islets from a donor with T2D transduced with control adenovirus (Ad-GFP; circles) or an electrically silent full-length K_v2.1 (Ad-K_v2.1W365C/Y380T; squares). The first phase secretory response is shown on expanded time scale (K) (1 donor; experiment run in duplicate). L) Averaged and individual (circles) area under the curve (AUC) values for baseline, first phase, and second phase responses of islets from T2D donors transduced as in panels J-K (n=3 donors in duplicate). *-$p<0.05$ versus ND or as indicated; **-$p<0.01$ versus mCherry; ***-$p<0.001$ as indicated. (Panels A, C by JE Manning Fox; panels J-L by JE Manning Fox and A Spigelman; all other work by J Fu).

Figure 21

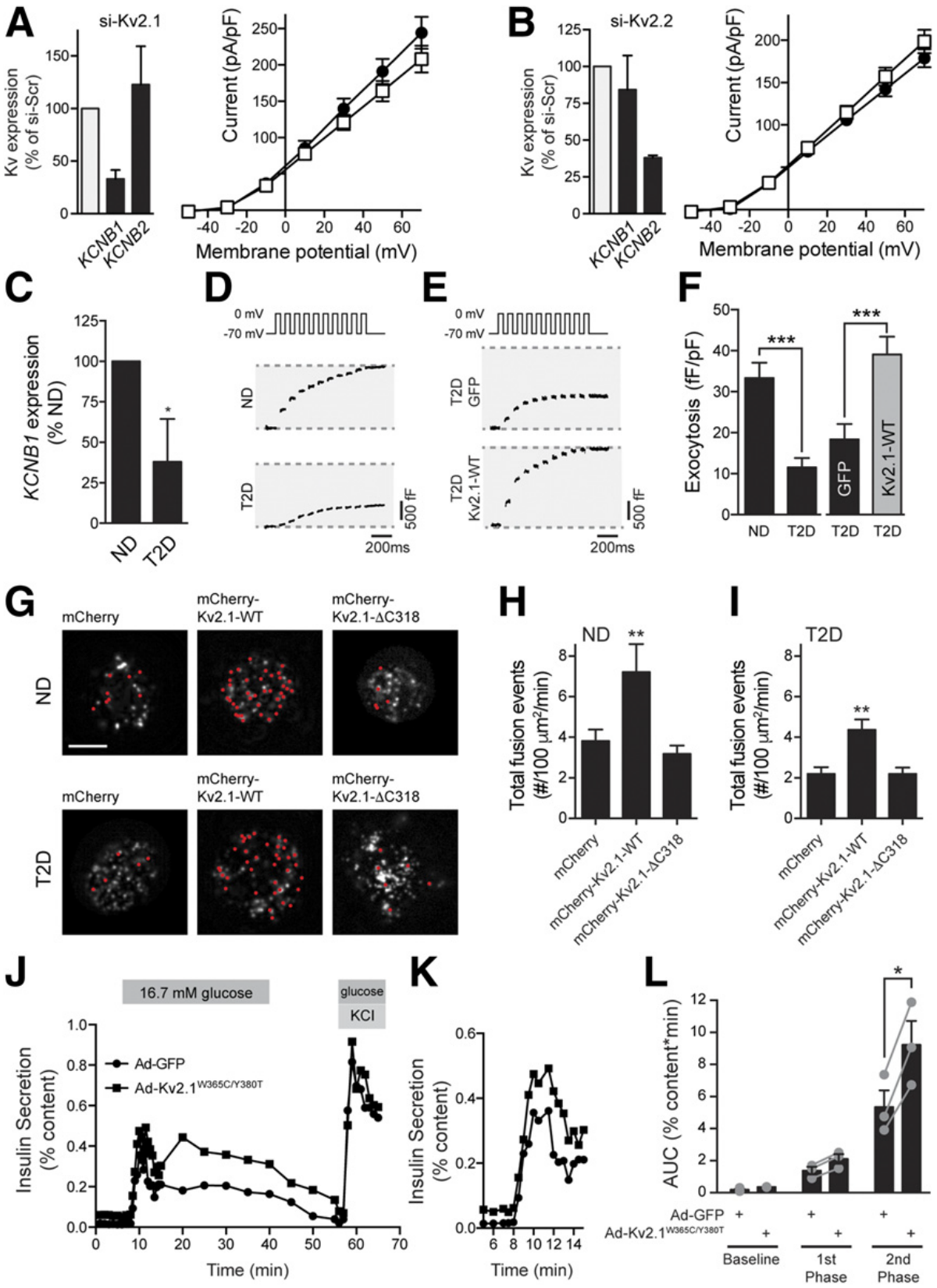
A
si-Kv2.1
Kv expression (% of si-Scr)
KCNB1
KCNB2
Current (pA/pF)
Membrane potential (mV)
B
si-Kv2.2
C
KCNB1 expression (% ND)
ND
T2D
D
0 mV
-70 mV
ND
T2D
500 fF
200ms
E
T2D GFP
T2D Kv2.1-WT
F
Exocytosis (fF/pF)
GFP
Kv2.1-WT
G
mCherry
mCherry-Kv2.1-WT
mCherry-Kv2.1-ΔC318
H
ND
Total fusion events (#/100 μm²/min)
I
T2D
J
16.7 mM glucose
glucose
KCl
Ad-GFP
Ad-Kv2.1W365C/Y380T
Insulin Secretion (% content)
Time (min)
K
L
AUC (% content*min)
Baseline
1st Phase
2nd Phase

Figure 22. Secretory dysfunction of islets from donors with T2D used in Figure 21 compared with matched controls

Impaired insulin secretion was confirmed in the T2D islets (n=3 donors) used for rescue experiments in Figure 8J compared with non-diabetic donors (n=3 donors) matched for age (53.7+/-3.3 versus 51.7+/-2.8), sex (2F and 1M in each group), and BMI (28.6+/-3.8 versus 28.4+/-1.2).

A) Insulin content was lower in islets from T2D donors, although this did not reach statistical significance.

B) Insulin secretion, as a percentage of insulin content, in response to 16.7 mM glucose in static incubation experiments was reduced in T2D islets.

C) The stimulation index (fold change in insulin secretion from 1 to 16.7 mM glucose) was reduced in the T2D islets).

*-$p<0.05$ as indicated; **-$p<0.01$ compared with ND; and ***-$p<0.001$ compared with the ND 1 mM glucose. (Data from baseline characterizations performed by the ADI IsletCore)

Figure 22.

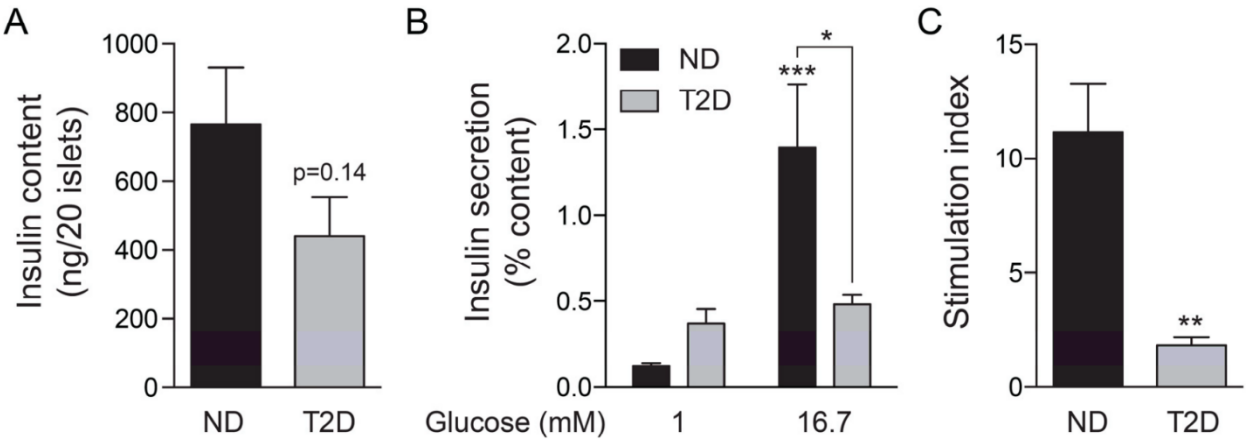
A
Insulin content (ng/20 islets)
1000
800
600
400
200
0
p=0.14
ND
T2D
B
Insulin secretion (% content)
2.0
1.5
1.0
0.5
0.0
ND
T2D
***
*
Glucose (mM)
1
16.7
C
Stimulation index
15
10
5
0
**
ND
T2D

2.5 DISCUSSION

The regulated exocytosis of insulin is disrupted in vitro, in animal models of T2D, and in β-cells from human donors with T2D (S C Collins, Salehi, Eliasson, Olofsson, & Rorsman, 2008; Ferdaoussi et al., 2015; Michael B Hoppa et al., 2009; Rosengren et al., 2012). The mechanisms underlying this are not entirely clear, although reduced SNARE expression (Andersson et al., 2012; Ostenson, Gaisano, Sheu, Tibell, & Bartfai, 2006), altered granule-Ca^{2+} channel coupling (S C Collins et al., 2008; Michael B Hoppa et al., 2009) and impaired metabolic signaling (Ferdaoussi et al., 2015) have all been suggested, and point to an important role for dysregulation of the distal secretory machinery. In the current work I present evidence suggesting that a reduction of $K_v2.1$ channels contributes to exocytotic dysfunction since these are required for efficient recruitment of secretory granules. Furthermore, clustering of the channels, in addition to Syntaxin 1A binding (X. Q. Dai et al., 2012; Singer-Lahat et al., 2007) is required for glucose-dependent granule recruitment and the facilitation of exocytosis.

$K_v2.1$ is long known to contribute a majority of the delayed K^+ current in rodent (David A Jacobson et al., 2007; Patrick E MacDonald, Sewing, et al., 2002) and human (Patrick E. MacDonald et al., 2001; Patrick E MacDonald, Sewing, et al., 2002) β-cells. Although immunolocalization studies suggest that $K_v2.2$ is expressed in human δ-cells and regulate somatostatin secretion (X. N. Li et al., 2013; Yan et al., 2004), these do not rule out expression in β-cells as transcriptomic analysis (Blodgett et al., 2015) and experimental studies (Jensen et al., 2013) suggest that $K_v2.2$ may be expressed at significant levels in these cells. Consistent with the latter reports, I observed higher expression of $K_v2.2$-encoding mRNA in human islets and INS 832/13 cells, and I find that this isoform mediates a substantial portion of the K_v current. However, $K_v2.2$ knockdown had no effect on β-cell exocytosis, consistent with its divergent C-

terminus homology from $K_v2.1$ and its inability to bind the Syntaxin 1A/SNAP-25 complex (Wolf-Goldberg et al., 2006). However, given that the expression of KCNB2 is reduced in T2D islets and upon metabolic perturbation in INS 832/13 cells (Jensen et al., 2013) a role in insulin secretion cannot be ruled out.

In neurons $K_v2.1$ channels localize to large plasma membrane clusters (Trimmer, 1991), the distribution of which is controlled by activity-(Cerda & Trimmer, 2011) and cell-cycle-(Cobb, Austin, Sack, & Trimmer, 2015) dependent phosphorylation. An exact physiological role for $K_v2.1$ clusters is unclear although they may be electrically silent (O'Connell et al., 2010), and act as 'platforms' for channel insertion (Deutsch et al., 2012) at sites where the cortical endoplasmic reticulum interacts with the plasma membrane (Du, Tao-Cheng, Zerfas, & McBain, 1998; Fox, Haberkorn, et al., 2013). Given the demonstration that $K_v2.1$ participates directly in exocytosis (X. Q. Dai et al., 2012; Singer-Lahat et al., 2007) I wondered whether this channel, like the L-type Ca^{2+} channel (BoK$_v$ist, Eliasson, Ammala, Renstrom, & Rorsman, 1995) with which it co-localizes (Fox et al., 2015), forms plasma membrane clusters in the β-cell. Indeed, native $K_v2.1$ in INS 832/13 cells and human β-cells form clusters at the plasma membrane as observed through both biochemical and imaging approaches. At least a sub-set of these clusters appear in close proximity to membrane-resident insulin granules and Syntaxin 1A clusters, however the exact relationship between granule docking/exocytosis sites and the $K_v2.1$ clusters remains to be resolved.

Consistent with previous reports (Baver & O'Connell, 2012; Lim et al., 2000) the C-terminus of the channel is required for clustering in HEK 293 cells. The ΔC318 C-terminus truncation did not, however, entirely abolish $K_v2.1$ clustering in INS 832/13 cells. This may result from hetero-tetramerization of the recombinant channel with native full-length $K_v2.1$ in

these cells, although a role for localization to lipid rafts known to occur in β-cells cannot be ruled out (F. Xia et al., 2004). Nonetheless, C-terminus-mediated clustering of $K_v2.1$ tetramers is required for effective facilitation of insulin exocytosis in β-cells since the $K_v2.1$-ΔC318 is unable to facilitate exocytosis in INS 832/13 cells or human β-cells despite efficient Syntaxin 1A binding, although altered interactions with other SNARE proteins cannot yet be ruled out. It should also be noted that the C-terminus truncation used here removes the distal C2 domain in addition to the clustering sequence (Lim et al., 2000). However, I have previously found no effect of the $K_v2.1$ C2 region on insulin exocytosis (Dai et al., 2012).

De-clustering of $K_v2.1$ occurs during brain ischemia, which suggests clustering may have an important physiological role in neurons (Rosengren et al., 2012). In human β-cells I show that KCNB1 expression and the contribution of $K_v2.1$-mediated current is decreased in T2D. Consistent with an impact of this on insulin exocytosis, knockdown of KCNB1 results in impaired secretory granule recruitment and exocytosis. Taken together, I hypothesize that a reduction of $K_v2.1$ expression contributes to the impairment of human β-cell exocytosis in T2D. The relationship of this to previous reports demonstrating reduced coupling between membrane-associated secretory granules, voltage-gated Ca^{2+} channels, and sites of localized Ca^{2+} entry (S C Collins et al., 2008; Michael B Hoppa et al., 2009) in models of T2D remains unclear. It is unlikely that reduced $K_v2.1$ expression is entirely responsible for impaired β-cell function in T2D, and indeed secretory granule fusion in T2D β-cells expressing the full-length $K_v2.1$ remained somewhat lower than ND β-cells over-expressing this construct. However, it seems possible that $K_v2.1$ channel clusters contribute to an excitosome complex thought to be important for coordinating signaling, excitability, and Ca^{2+} influx at the exocytotic site (Leung, Kwan, Ng, Kang, & Gaisano, 2007; Patrick E MacDonald, 2011). Disruption of $K_v2.1$ clustering likely

results in dysregulation of key interactions at these sites required for efficient secretory granule docking and exocytosis. It should also be considered that $K_v2.1$ clusters may play more than simply a structural role at the exocytotic site, since channels within clusters are capable of sensing membrane voltage and producing gating currents (O'Connell et al., 2010) and of interacting with the ER to potentially regulate intracellular Ca^{2+} stores (Fox, Haberkorn, et al., 2013).

Plasma membrane protein clustering is emerging as an important level of organization, primed to facilitate cellular functions (Garcia-Parajo, Cambi, Torreno-Pina, Thompson, & Jacobson, 2014), including insulin secretion (Gandasi & Barg, 2014). Our data provides evidence that $K_v2.1$ clusters play a key role in facilitating insulin exocytosis and implicate an important pathophysiological contribution of the loss of $K_v2.1$ in T2D. The regulation of $K_v2.1$ clusters in concert with many other protein-protein interactions at the plasma membrane, may be important for the efficient recruitment, docking, and priming of secretory granules.

2.6 CONCLUDING REMARKS

This present study in this chapter investigated the effect of K_v2 channels in delayed rectifier current and exocytosis from isolated β-cells and insulinoma cells. Quantitative PCR and electrophysiology confirmed that both $K_v2.1$ and $K_v2.2$ are expressed in in pancreatic β-cells. Although $K_v2.1$ and $K_v2.2$ contribute similar magnitude electrical currents, $K_v2.1$ plays a more important role in exocytosis compared to $K_v2.2$. However, this study does not provide any comparative western blot data due to lack of antibody which can specifically recognize $K_v2.2$. There are still other possibilities that $K_v2.2$ also contributes to insulin secretion and exocytosis. It is reported that $K_v2.1$ channels mediate insulin secretion in β-cells while $K_v2.2$ channels regulate somatostatin secretion from δ-cells (X. N. Li et al., 2013). In isolated β-cells, pyruvate-isocitrate cycling maintains $K_v2.2$ expression, allowing $K_v2.2$ to serve as a negative regulator of K_v channel activity. Moreover, considering the transcriptional level of Kv2.2 was found to be 8-9 times greater than $K_v2.1$, it was hard to explain the reason why there is an equivalent reduction in K_v current when silencing $K_v2.1$ or $K_v2.2$. Thus, I cannot entirely rule out the potential contribution of $K_v2.2$ in insulin secretion and exocytosis, considering the amount of $K_v2.2$ expression in isolated β-cells and islets.

I found that $K_v2.1$ is not randomly distributed on plasma membrane. Instead, $K_v2.1$ is highly compartmentalized as clusters in micro-domains in pancreatic β-cells and insulinoma cells. However, there are different types of compartmentalization. It is reported that $K_v2.1$, associated with Syntaxin1A , SNAP-25, VAMP-2 and $Ca_v1.2$, target to specialized cholesterol-rich lipid raft domains (F. Xia et al., 2004). Another possibility is $K_v2.1$ clusters represent endoplasmic reticulum/plasma membrane (ER/PM) junctions that function as membrane

trafficking hubs and that $K_v2.1$ plays a structural role in forming these membrane contact sites on plasma membrane (Johnson et al., 2018).

To confirm the importance to $K_v2.1$ clusters to exocytosis, the $K_v2.1$-Δ318 truncation was applied in these studies. However, as opposed to previous reports (Lim et al., 2000; Scannevin, Murakoshi, Rhodes, & Trimmer, 1996), I noticed that the $K_v2.1$-Δ318 still forms some clusters in insulin-secreting cells. Moreover, this seems to be due to $K_v2.1$-Δ318 associating with native endogenous $K_v2.1$ since this channel is expressed in insulinoma cells. It can explain why my results are different from the previous studies in HEK and neuronal cells. To exclude the interaction between SNARE proteins and $K_v2.1$, syntaxin1A was tested in my experiments (which still bound the truncated channel). However, there are also reports that syntaxin3 can bind with $K_v2.1$ C-terminus (Greitzer-Antes et al., 2018). Thus, this possibility should be investigated and tested.

Overexpression of $K_v2.1$ in T2D β-cells can enhance exocytosis and insulin secretion. Surprisingly, the second phase of insulin secretion was significantly increased. Considering that $K_v2.1$ clusters could provide a platform for docking granules, it is possible that $K_v2.1$ clusters or docking granules could contribute to the recruitment of new-coming insulin granules as well. Thus, in the following chapter, I investigate the possible role of $K_v2.1$ clusters and pre-docked granules in insulin secretion and exocytosis using live-cell imaging TIRFM technology.

CHAPTER 3

Spatial Patterning of Exocytosis in Human Pancreatic β-cells

This chapter, and portions of Chapter 4, are part of a paper being prepared for publication

Jianyang Fu, Xiaoqing Dai, Gregory Plummer, Kunimasa Suzuki, John M Githaka, Dafna Greitzer-Antes, Jocelyn E Manning Fox, Herbert Y. Gaisano, Patrick E MacDonald (2018).

3.1 ABSTRACT

Impaired insulin secretion in type 2 diabetes (T2D) has been linked to reduced insulin granule docking, disorganization of the exocytotic site, and an impaired glucose-dependent facilitation of insulin exocytosis. I analyze secretory granule fusion in human β-cells from 19 non-diabetic (ND) and 7 T2D donors using total internal reflected fluorescence (TIRF) microscopy. Exocytotic events in ND β-cells occur in a non-random fashion, at 'hot spots' across the surface of the plasma membrane. Mechanistically, docking granules, where sixty-five percent of exocytotic events in ND β-cells occurred around, are essential in regulating exocytosis "hot spots". In T2D β-cells, the proportion of exocytotic events that happen around sites where pre-docked granule are observed is reduced by 50% and the density of pre-docked granules is also reduced by 35.7%. Mechanistically, since $K_v2.1$ is associated with docked granules, I investigate the role of $K_v2.1$ clusters in compartmentalized exocytosis. I find that upregulation of $K_v2.1$-WT clusters, but not $K_v2.1$-Δ318, increases exocytosis hotspots. Moreover, spatial pattern of exocytosis is impaired in T2D β-cells, independent of the reduction in exocytotic events per se. Thus, this distinct spatial distribution of regulate exocytosis in human pancreatic β-cells may provide a novel insight into T2D.

3.2 INTRODUCTION

The regulated exocytosis of insulin from pancreatic β-cells, which is impaired in type 2 diabetes (T2D), plays a critical role in glucose homeostasis. Under glucose stimulation, an increased intracellular ATP/ADP ratio closes K_{ATP} channels, depolarizes β-cells, activates voltage-dependent Ca^{2+} channels (VDCCs) and increases intracellular Ca^{2+} concentration, which triggers exocytosis. Repolarization of pancreatic β-cells action potential is mediated by voltage-dependent K^+ (K_v) channels and Ca^{2+}-sensitive voltage K^+ (K_{Ca}) channels.

Interestingly, spatial analysis reveals that ion channels such as $K_v2.1$ form clusters at the plasma membrane and facilitates insulin exocytosis in pancreatic β-cells (Fu et al., 2017; Gandasi et al., 2017). This compartmentalization of ion channels suggests that the regulated exocytotic sites themselves may also compartmentalized, since clusters of ion channels may recruit SNARE proteins such as syntaxin1A, SNAP-25 and Munc18-1 (Toft-Bertelsen, Ziomkiewicz, Houy, Pinheiro, & Sørensen, 2016). Although it is reported that neurotransmitters are released by exocytosis at the "active zone" of a presynaptic nerve terminus (Südhof, 2012) and insulin granules undergo exocytosis at the "hotspots" in insulin-secreting INS-1 cells (Fu et al., 2017), whether this compartmentalized exocytosis also happens in human pancreatic β cells remains unclear.

In this study, I performed spatiotemporal analysis of exocytosis across the surface of human pancreatic β-cells. I find that exocytosis is highly compartmentalized at hotspots in non-diabetic donors (ND), while this spatial pattern is partially lost in type 2 diabetic (T2D) β-cells. Glucose, but not KCl, stimulation increases the proportion of exocytotic events that occur at hotspots, which happen around sites of pre-docked granules. Moreover, clustering of $K_v2.1$ clusters also contribute to compartmentalized exocytosis.

3.3 MATERIALS AND METHODS

3.3.1 Cells and cell culture

Human islets from the Clinical Islet Laboratory at the University of Alberta and the Alberta Diabetes Institute IsletCore were cultured in 5.5 mM glucose concentration DMEM with L-glutamine, 110 mg/l sodium pyruvate, 10% FBS, and 100 U/ml penicillin/streptomycin.

Islets from 19 donors without diabetes and 7 T2D donors contributed to this work. All human islet studies were approved by the Human Research Ethics Board (Pro00001754) at the University of Alberta and all families of organ donors provided written informed consent.

3.3.2 Adenoviruses, constructs, and treatments

Human pancreatic islets were dissociated using Cell Dissociation Buffer enzyme-free, Hanks' Balanced Salt Solution (ThermoFisher Scientific. Burlington, ON). Adenovirus NPY-eGFP virus was kindly donated by Herbert Y. Gaisano (University of Toronto). Isolated human pancreatic β-cells were infected with NPY-eGFP and further cultured for 24-36 h before imaging.

Knockdown of KCNB1 expression in human cells was carried out using a mixture of 4 siRNA duplexes (QIAGEN, Toronto, ON, Canada), in which each recognizes different regions of the target gene. Transfected cells were identified by co-transfection with an Alexa Fluor 488-tagged duplex (Cat. # 1027292, Qiagen). The cDNA encoding wild type rat $K_v2.1$ or the truncated $K_v2.1$-ΔC318 ($K_v2.1$ Glu536_Ile853 del) was amplified by PCR using a pCDNA3-$K_v2.1$ plasmid as a template, and inserted between BsrG-I and Xho-I site of Cherry-LacRep plasmid (Dundr et al., 2007) (from Mirek Dundr: Addgene plasmid#18985) by Gibson Assembly to make pmCherry-$K_v2.1$-WT and pmCherry-$K_v2.1$-ΔC318.

3.3.3 TIRFM Imaging

All TIRF imaging used a Cell-TIRF motorized system (IX83P2ZF, Olympus Canada) with a 100×/1.49 NA TIRFM objective, a Photometrics Evolve 512 camera (Photometrics), and Metamorph Imaging software (Molecular Devices). Stimulation was at 491 nm (LAS-491-50) and 561 nm (LAS-561-50, Olympus, Germany) with a quad filter passing through a major dichroic and band pass filter (405/488/561/640, Chroma Technology, Bellows Falls, VT). Penetration depth was set to 105 nm, calculated using existing angle of the laser and assuming a refractive index of 1.37. Emission was collected through bandpass filters of 525/25 nm and 605/26 nm for excitations of 488 and 561 nm, respectively. Images were acquired sequentially with single laser excitation to minimize potential bleed-through.

Live-cell acquisition was 5-Hz with a 200 ms exposure at 35°C. Before acquisition, cells were pre-incubated (30 mins) in bath containing (in mM) 138 NaCl, 5.6 KCl, 1.2 $MgCl_2$, 2.6 $CaCl_2$, 5 $NaHCO_3$, 1 glucose and 5 HEPES (pH 7.4 with NaOH) and then exposed to 5 mM glucose upon recording. For glucose stimulation experiments, the buffer instead contained 16.7mM glucose. For KCl stimulation, the buffer instead contained 75mM KCl. Fusion events, indicated by abrupt brightening (ratio of peak fluorescence to background >1.3) and then disappearance of NPY-EGFP fluorescence, were selected and analyzed with computer-assisted analysis software (Yuan et al., 2015) and normalized to membrane area. Docking granules were detected using “Find local maxima” function in Matlab. Exocytosis events occurring around docking granule were manually selected when the exocytotic sites are overlay with docking granules.

Spatial analysis is performed under Matlab, 2017r. Voronoi diagrams were used to separate each fusion event. Random simulation was with the same number of fusion events and

the same cell boundary. The ‘observation’ uniform index was calculated as the standard deviation of the fusion area divided by the mean of the fusion area. The ‘simulation’ uniform index was calculated similarly following a random distribution of events. Exocytotic hotspots, recognized by Matlab, was run with a center-to-center threshold value of 0.6 μm, which is < 4 or 5 pixels and represents the minimum resolvable distance to distinguish two granule fusion site in our system. The ’Hotspots Ratio (%)’ was calculated as the number of fusion events occurring at hotspots divided by the total fusion events multiplied by 100. The ‘Hotspots Density (#/100um^2)’ was calculated as the number of hotspots normalized to cell footprint area.

3.3.4 Statistical analysis

Data analysis was performed using Origin Lab (v7.0) and GraphPad Prism (v6.0c). All data are shown as the mean ± SEM. Statistical outliers were identified by an unbiased ROUT (robust regression followed by outlier identification) test. Comparison of multiple groups was by ANOVA and Bonferroni post-test. When comparing two means only, data were analyzed by the 2-tailed Student’s t test. A P-value less than 0.05 was considered significant.

3.4 RESULTS

3.4.1 Exocytosis occurs at hotspots in non-diabetic β-cells but this is decreased in T2D

Exocytosis is compartmentalized in soma and neurites of developing neurons (Urbina, Gomez, & Gupton, 2018) and endocrine cells (Yuan et al., 2015). However, the spatial pattern of exocytosis in human pancreatic β-cells remains unknown. To investigate when and where exocytosis occurs on the cell membrane, live time-lapse TIRF microscopy, which images fluorescence within 100nm above the coverslip, was applied in human β-cells from non-diabetic donors (3 donors, Fig 23A) and T2D donors (3 donors, Fig 23B). Single exocytotic events can be visualized as abrupt brightening of Neuropeptide Y (NPY)-eGFP fluorescence, which is barely detectable in intracellular granules due to low pH value. To identify sites of exocytosis and perform spatiotemporal analysis of vesicle fusion events, a MATLAB-based software was applied (Yuan et al., 2015) to live-cell imaging recorded with 5mM glucose in the bath solution for 2 mins. Temporal analysis reveals that accumulated fusion events are decreased 56.1% in T2D donors ($p<0.001$, $n=16$ for non-diabetic donors and $n=26$ for T2D donors) compared to non-diabetic donors (Fig 23C).

To determine whether exocytosis was randomly distributed or not, the spatial pattern was analyzed using a ‘uniform index’. Events were separated by Voronoi polygons which separates each exocytic site, and the ‘observed uniform index’ was calculated as the standard deviation of polygon area normalized to average area occupied by each exocytic site. In parallel, a ‘simulated uniform index’ is determined using the same exocytosis events and cell boundaries randomized under one hundred times of Monte Carlo stimulation. This is used to generate a standard deviation that would be reflective of truly random spatial organization of exocytotic events. A comparison between the observed and simulated ‘uniform index’ values can therefore assess

whether fusion events are spatially organized, independent of changes in the total number of events. In non-diabetic β-cells, the observed exocytosis spatial pattern exhibits a 29.5% higher uniform index compared to simulation while there is no significant difference in T2D β-cells ($p<0.05$, n=16 for non-diabetic donors and n=26 for T2D donors). This suggests that β-cells of non-diabetic donors exhibit significant spatial organization in the exocytosis of their fusion events, while events in T2D β-cells occur randomly.

Consistent with a previous report (Yuan et al., 2015), individual insulin granule exocytosis events are highly compartmentalized and clustered at hotspots. To further investigate the character of exocytotic hotspots in human pancreatic β-cells, 'hotspots ratio' and 'hotspot density' are calculated. Exocytotic hotspots are defined and recognized as multiple exocytotic events within the same defined neighborhood area (4*4 or 5*5-pixel area determined by average vesicle diameter). Each hotspot is further confirmed by manual fluorescent analysis (Fig 23A and B). Quantitative analysis reveals that, in non-diabetic donors, 41.6% of exocytosis happens within hotspots while only 18.3% of exocytosis occurs at hotspots in T2D donors. In addition to a decreased relative proportion of events occurring within hotspots in T2D, the density of hotspots themselves decreases by 33.3% in T2D donors compared to non-diabetic donors ($p<0.01$, n=16 for non-diabetic donors and n=26 for T2D donors).

One explanation for impaired compartmentalization of exocytosis in T2D β-cells is that there are less total exocytotic events. Indeed, I find that hotspots ratio is highly correlated with total exocytosis events (Figure 23D). Although the 'uniform index' analysis can take this into account and suggests a true impairment in exocytotic organization in T2D, I further examined the interaction between event frequency and hotspot ratio by examining a subset of β-cells that showed similar total exocytosis events (*dashed box in* Figure 23D). Interestingly, I find that the

pancreatic β-cells from non-diabetic donors still have spatial pattern ($p<0.05$, $n=9$) while there is no significant difference in T2D donors (Fig 23D). Besides, both hotspots ratio and hotspots density significantly decreased 28.6% and 34.8% respectively ($p<0.05$, $n=9$ for non-diabetic donors and $n=8$ for T2D donors). Thus, I conclude that exocytosis is compartmentalized at hotspots in non-diabetic pancreatic β-cells while this spatial pattern is impaired in T2D donors.

Figure 23. Exocytosis happens at hotspots in non-diabetic but are decreased in T2D β-cells

A) An example of a non-diabetic β cell with all fusion events (red circles), cell membrane (green lines) marked on the first frame with docking granules (bright dots), Scale bar, 5 μm. Voronoi diagram used to separate exocytosis sites with each calculated size labeled. Cluster of exocytosis sites is calculated as less than 4-pixel distance, calculated by the average diameter of insulin granules. Representative hotspots are labeled and analyzed with relative fluorescence time traces

B) An example of a T2D β cell with same analysis methods introduced above.

C) Accumulated fusion events are shown for temporal analysis. Average uniform index, hotpots ratio and hotspots density are shown for spatial analysis between non-diabetic and T2D β-cells. *P<0.05, **P<0.01, ***P<0.001.

D) Scatter plot with total fusion events (X- axis) and hotspots ratio (Y- axis) are shown. Only the events within the dash box are selected for spatial analysis to keep the total exocytosis events are the same. Average uniform index, hotpots ratio and hotspots density are shown for spatial analysis between non-diabetic and T2D β-cells. *P<0.05 (all panels by J Fu).

Figure 23

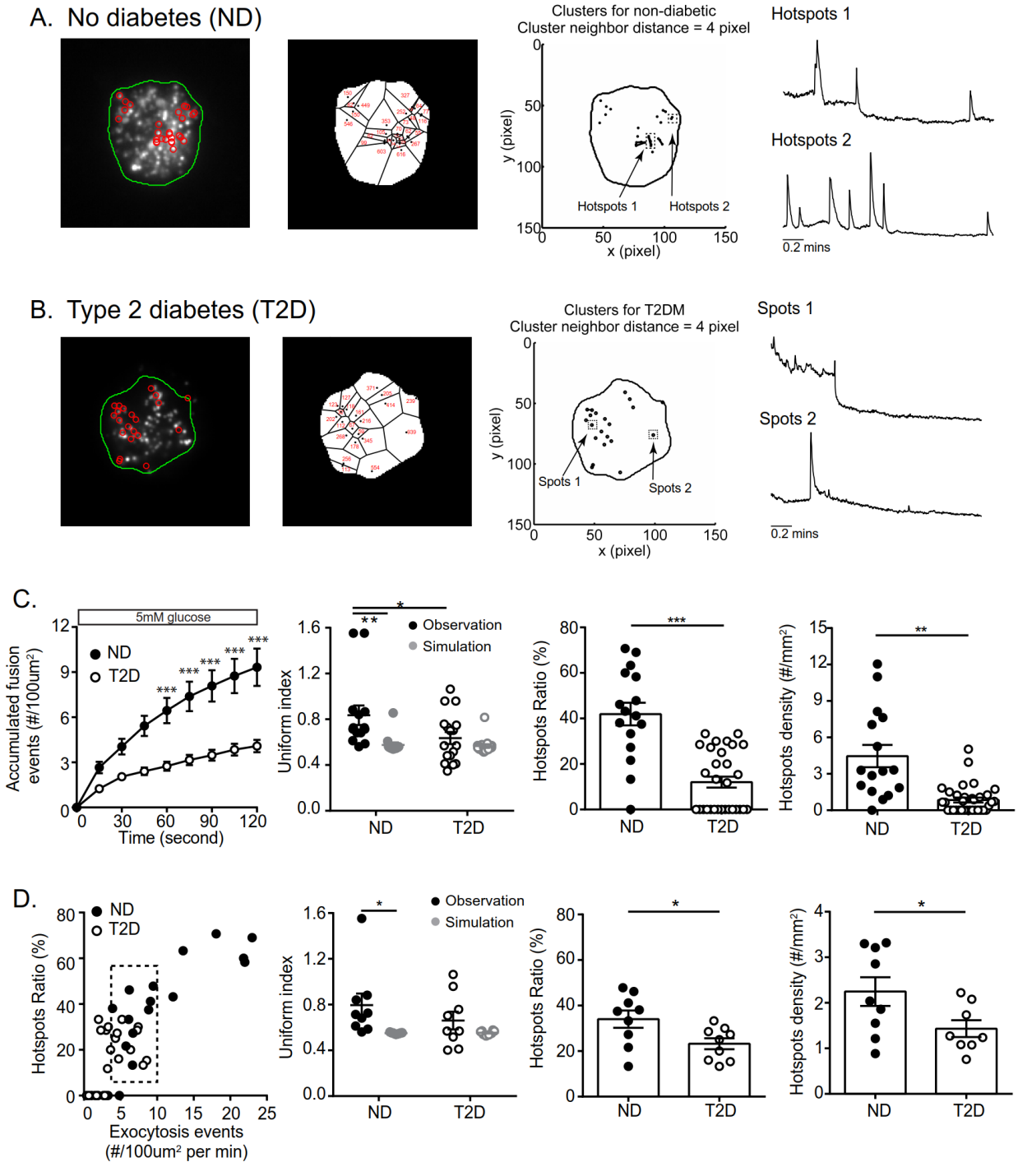
A. No diabetes (ND)
Clusters for non-diabetic
Cluster neighbor distance = 4 pixel
Hotspots 1
Hotspots 2
y (pixel)
x (pixel)
0.2 mins
B. Type 2 diabetes (T2D)
Clusters for T2DM
Cluster neighbor distance = 4 pixel
Spots 1
Spots 2
C.
5mM glucose
ND
T2D
Accumulated fusion events (#/100um²)
Time (second)
Observation
Simulation
Uniform index
Hotspots Ratio (%)
Hotspots density (#/mm²)
D.
Exocytosis events (#/100um² per min)

3.4.2 Exocytotic hotspots are up-regulated by glucose, but not KCl

KCl-induced exocytosis is considered analogous to the first phase of glucose-induced insulin secretion (D. Zhu et al., 2015), triggering the release of granules by directly depolarizing β-cells and increasing intracellular Ca^{2+}. Recently, it is reported that glucose and KCl stimulation have different effects on insulin granule behaviors in mouse β-cells (Bruning, Reckers, Drain, & Rustenbeck, 2017). To investigate the spatial pattern of exocytosis in human pancreatic β-cells with different stimulations, I perform spatiotemporal analysis under two different conditions, 30mM KCl stimulation with 1mM glucose and 30mM KCl stimulation associated with 5mM glucose. Temporal analysis (Fig 24A) reveals that exocytosis is impaired 58.9% and 68.2%, respectively, in T2D under these conditions ($p<0.001$, n=8 and 9 for non-diabetic donors and n=6, 8 for T2D donors). Spatial analysis indicates that while KCl stimulation has no effect on compartmentalization in both non-diabetic and T2D donors, glucose (5mM) can enhance the spatial organization of exocytosis to the subsequent KCl stimulus (Fig 24D-F).

In non-diabetic donors (Fig 24B), both hotspots ratio and hotspots density in KCl-induced group is 39.8% and 43.2% lower compared to the 5 mM glucose group. However, KCl with 5mM glucose can rescue hotspots ratio and density by 37.5% and 50.0% respectively ($p<0.05$, n=10, 8 and 9). In T2D donors (Fig 24C), KCl stimulation in low (1 mM) glucose will decrease 74.8% compared to KCl with 5mM glucose group ($p<0.01$, n=6 and 8) although there is no significant difference on the fraction of events occurring at hotspots (Fig 24D-F).

Figure 24. Exocytotic hotspots are up-regulated by glucose not KCl.

A-B) Temporal analysis of β cells from non-diabetic and T2D donors under the KCl only condition (A) and KCl with glucose conditions (B). C) Uniform index between different conditions are shown. D) Scatter plot with total fusion events (X-axis) and hotspots ratio (Y-axis) are shown. E-F) Both hotspots ratio and hotspots density within the selective box are presented. *P<0.05, **P<0.01, ***P<0.001 (all panels by J Fu).

Figure 24

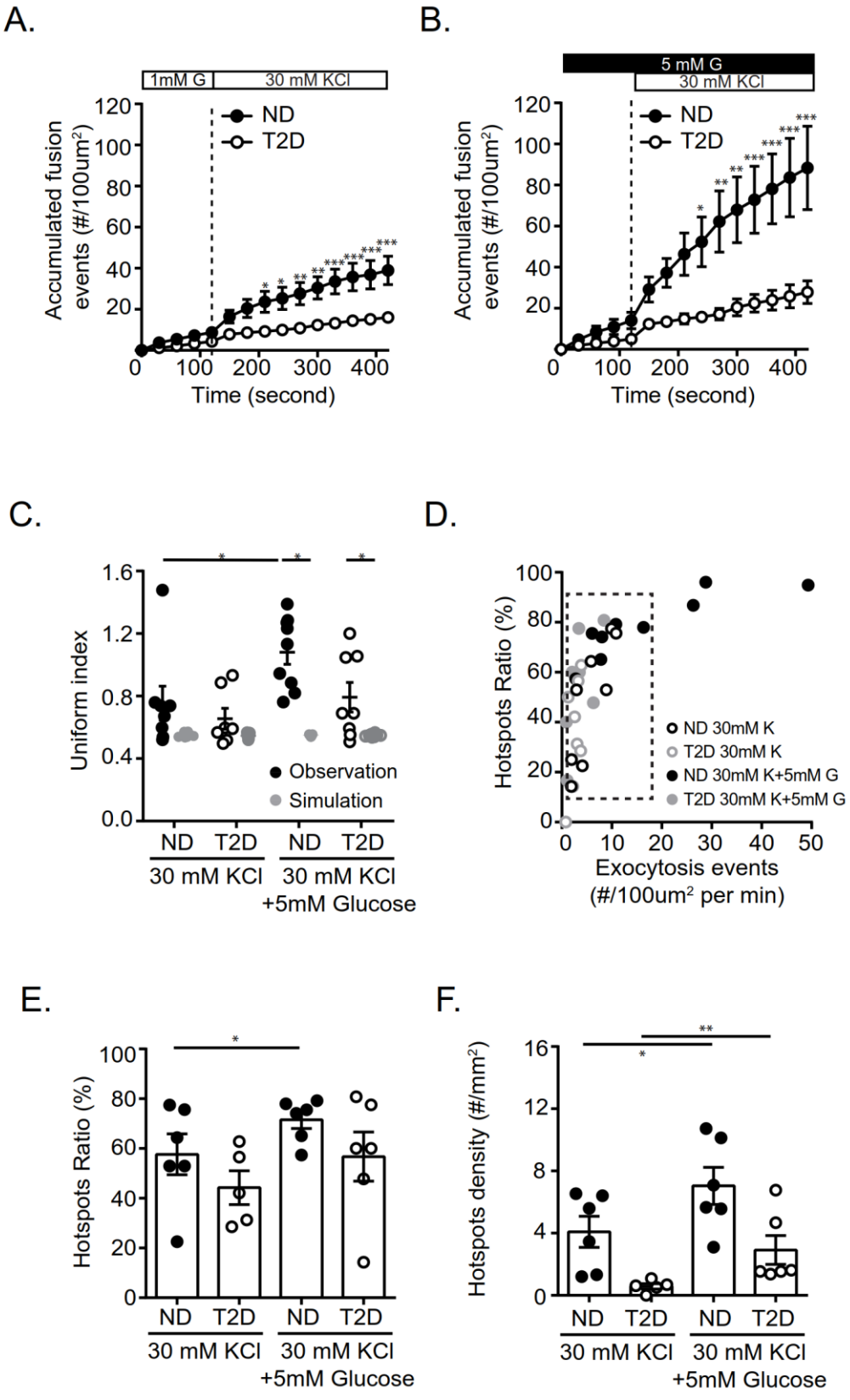
A.
1mM G
30 mM KCl
ND
T2D
Accumulated fusion events (#/100um²)
Time (second)
B.
5 mM G
30 mM KCl
ND
T2D
Accumulated fusion events (#/100um²)
Time (second)
C.
Uniform index
Observation
Simulation
ND T2D ND T2D
30 mM KCl 30 mM KCl
+5mM Glucose
D.
Hotspots Ratio (%)
ND 30mM K
T2D 30mM K
ND 30mM K+5mM G
T2D 30mM K+5mM G
Exocytosis events
(#/100um² per min)
E.
Hotspots Ratio (%)
ND T2D ND T2D
30 mM KCl 30 mM KCl
+5mM Glucose
F.
Hotspots density (#/mm²)
ND T2D ND T2D
30 mM KCl 30 mM KCl
+5mM Glucose

3.4.3 Exocytosis hotspots happen around docking granules

Insulin granule docking is a critical glucose-dependent step in insulin secretion, which is dysregulated in T2D (Gandasi et al., 2018). Considering that glucose stimulation recruits docking granules while KCl stimulation depletes docking granules (Mica Ohara-Imaizumi, Nakamichi, Tanaka, Ishida, & Nagamatsu, 2002), I hypothesized that docking granules serve as hotpots for exocytosis.

As illustrated in Fig 25A, exocytosis happens around a pre-docked granule on the same spot repeatedly; five times within 2mins. Notably, these events are not in the center of the pre-docked granule which maintains its relative fluoresce and indicates that these two events are not from the docked granule itself but from ones behind it. After 30 seconds, a third exocytosis happens in which the relative florescence decreased 41.3% to suggest that the original docked granule itself undergoes exocytosis. Sixteen seconds after this, another exocytotic event occurs at the same spot, which implies that this site still serves as a hotspot for new-coming granules.

One possibility is that single granules undergo “kiss-and-run exocytosis” several times. To exclude this possibly, one example of “kiss-and-run exocytosis” is shown in Fig 25B. The exocytosis site happens in the middle of the docking granule and the time latency between two events is only 1.2 second. To simplify spatial analysis, “kiss-and-run” exocytosis was not taken into count.

In T2D donors, hotspot exocytosis is less obvious (Fig 25C) and exocytosis events did not have similar spatial pattern to non-diabetic β-cells. To quantify the difference between non-diabetic donors and T2D donors, I calculated all exocytosis events in relation to pre-docked granules from the first 5 video frame. This reveals that 67.4% of exocytosis happens around docking granules in non-diabetic beta cells, this is only 55.2% of exocytosis T2D donors. More

importantly, the docking granule density is decreased 35.8% in T2D donors compared to non-diabetic donors, which is consistent with previous reports (Gandasi et al., 2018).

Figure 25. Exocytosis hotspots are marked by pre-docked granules

A) Cartoons illustrating compartmentalized exocytosis in non-diabetic β cells. Two exocytosis happens continuously behind the docking granules. After docking granule exocytosis, new comer granule exocytosis happens at the same hotspots. Imaging sequences of granule with insulin granule marked with NPY-eGFP. Relative fluorescence time traces are shown.

B) An example of "kiss-and-run" exocytosis is also shown.

C) An example of exocytosis in T2D donors is also shown.

D) Both exocytosis happens around docking granules and docking granule density significantly decreased in T2D pancreatic β-cells (n=28, 3 donors) compared to ND β-cells (N=16, 3 donors). **P<0.01, ***P<0.001 (all panels by J Fu).

Figure 25

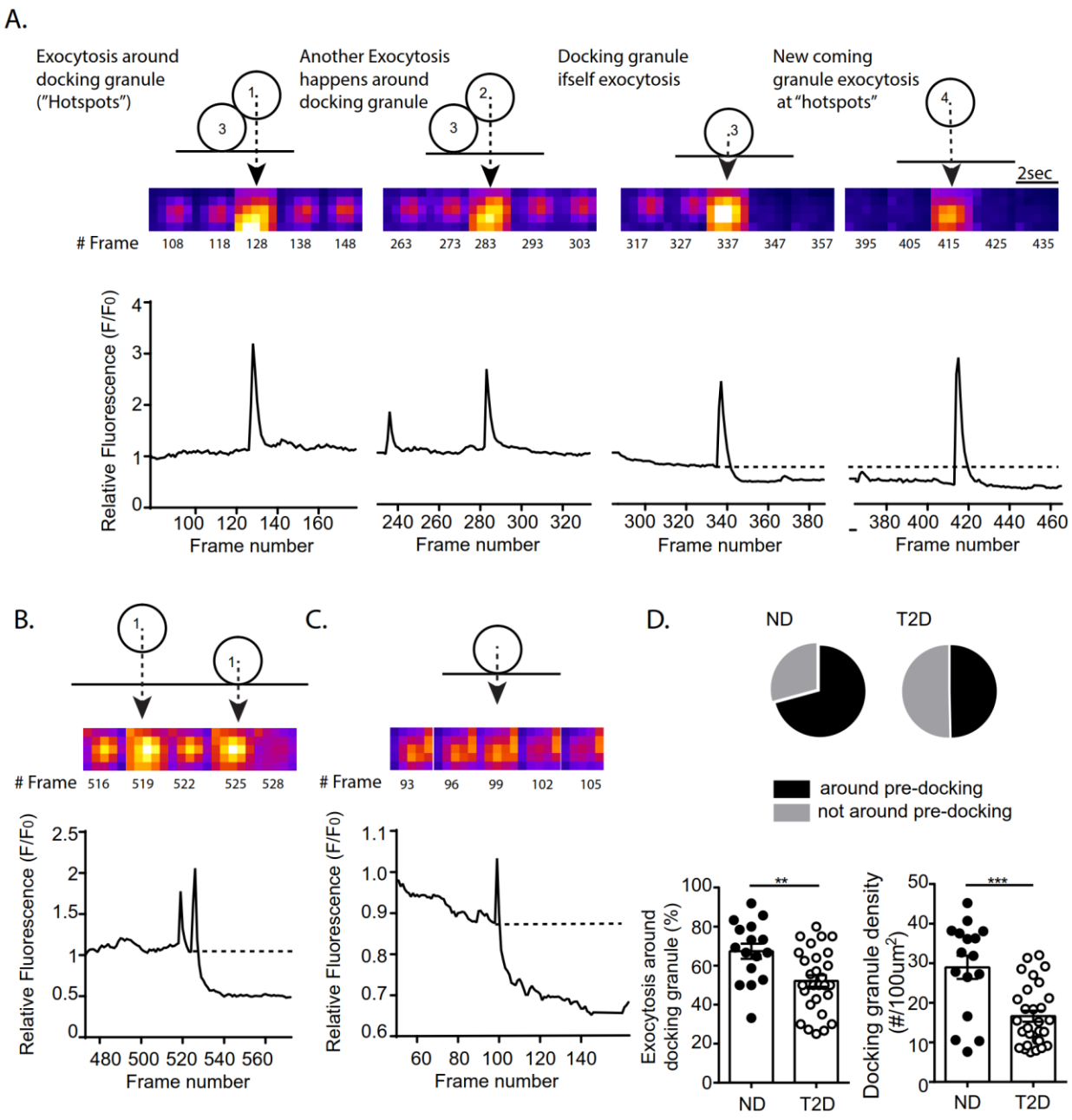
A.
Exocytosis around docking granule ("Hotspots")
Another Exocytosis happens around docking granule
Docking granule ifself exocytosis
New coming granule exocytosis at "hotspots"
2sec
Frame
Relative Fluorescence (F/F0)
Frame number
B.
C.
D.
ND
T2D
around pre-docking
not around pre-docking
Exocytosis around docking granule (%)
Docking granule density (#/100um2)

3.4.4 Exocytosis hotspots are regulated by $K_v2.1$

$K_v2.1$ is compartmentalized on the cell membrane, colocalized with docked granules and function as reservoir for newcomer secretory granules in β-cells (Fu et al., 2017; Greitzer-Antes et al., 2018). It is also reported that repetitive depolarization will trigger $K_v2.1$ clustering (Yalan Zhang, McKay, Bewley, & Kaczmarek, 2008). Thus, I assessed whether $K_v2.1$ clusters will regulate exocytosis hotspots. Consistent with our previous report (Fu et al., 2017), knockdown of $K_v2.1$ inhibits exocytosis, this time assessed as the accumulated fusion events visualized by TIRF microscopy (Figure 26A) (18.5 ± 1.5 compared to 8.3 ± 0.9, n=30, 30, $p<0.001$). Interestingly, the siRNA $K_v2.1$ group showed a 25% depression (Figure 26D) in the compartmentalization of exocytosis compared to control group (n=30, 30, $p<0.05$). Also, siRNA $K_v2.1$ will decreases hotspot density by around 50% (n=30, 30, $p<0.05$) (Figure 26H) without affecting the hotspots ratio (Figure 26G) in selected pancreatic β-cells.

Figure 26. Exocytosis hotspots are regulated by K_v2.1

A-C) Knockdown of K_v2.1 can significantly decrease docking granule density (A), decrease total exocytosis events (C), without changing the ratio of exocytosis that happens around docking granules (B).

D-H) Spatial analysis reveals that siRNA will significantly reduce compartmentalization compared to control group. In scatted spots graph, I select a window with similar exocytosis events (F), while the exocytosis hotspots density significant reduced (H) without affecting hotspots ratio (G). *P<0.05, **P<0.01, ***P<0.001 (all panels by J Fu).

Figure 26

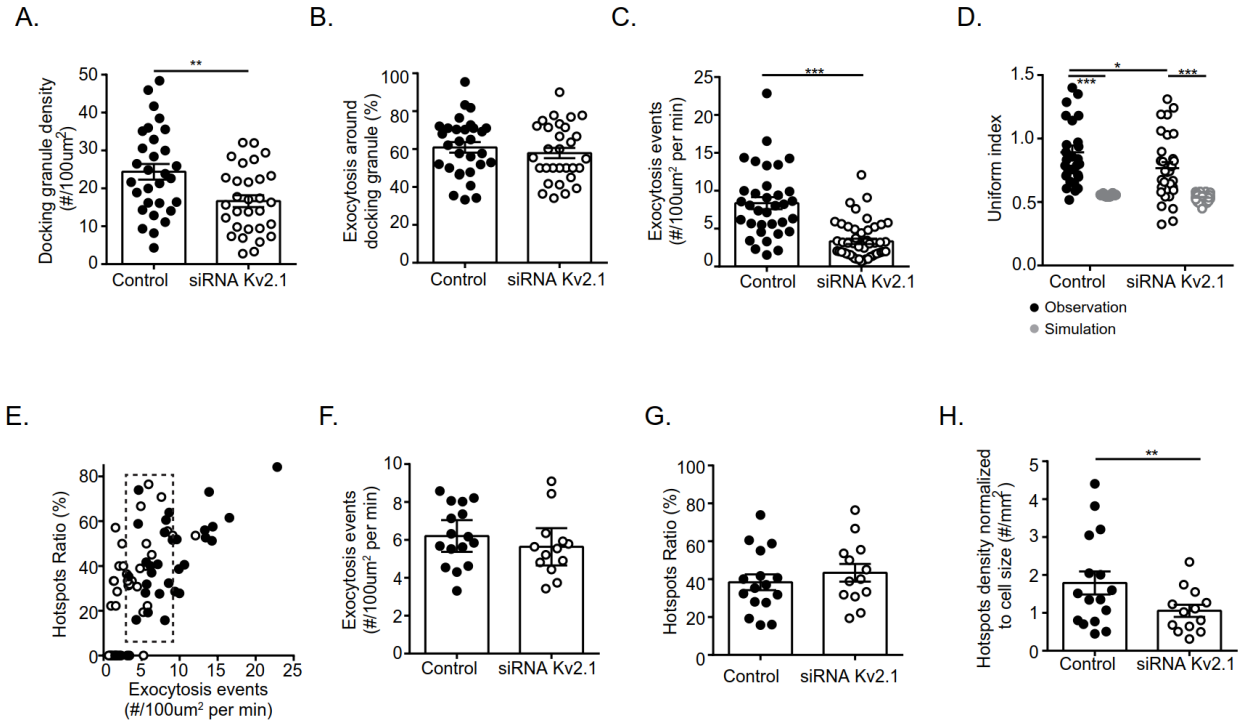
A.
B.
C.
D.
Docking granule density (#/100um²)
Exocytosis around docking granule (%)
Exocytosis events (#/100um² per min)
Uniform index
Control
siRNA Kv2.1
Observation
Simulation
E.
F.
G.
H.
Hotspots Ratio (%)
Exocytosis events (#/100um² per min)
Hotspots density normalized to cell size (#/mm²)

3.4.5 Upregulation of K_v2.1 increases exocytosis hotspots

Clustering of K_v2.1 promotes exocytosis and insulin secretion (Fu et al., 2017).To determine whether K_v2.1 clusters will facilitate exocytosis hotspots as well, I overexpress mCherry-K_v2.1-WT and mCherry-K_v2.1-Δ318 in human pancreatic β-cells. In non-diabetic donors, temporal analysis reveals that, while K_v2.1-Δ318 has less effect, only K_v2.1-WT can significantly increase exocytosis function by 50% ($p<0.001$, n=22 in mCherry, n=26 in mCherry-K_v2.1-WT and n=24 in mCherry-K_v2.1-Δ318) under 5mM glucose condition. Spatial analysis reveals that while K_v2.1-Δ318 has random exocytosis, K_v2.1-WT have the observation exocytosis spatial pattern exhibit 37.5% higher uniform index compared to simulation ($p<0.05$, n=26 in mCherry-K_v2.1-WT and n=24 in mCherry-K_v2.1-Δ318). Compared to K_v2.1-WT group, K_v2.1-Δ318 will significantly decrease both hotspots ratio and hotspots density 56.6% and 60% respectively. In T2D donors, overexpression of K_v2.1-WT can rescue fusion events and compartmentalization of exocytosis. Compared to the K_v2.1-WT group, K_v2.1-Δ318 will have a lower hotspots ratio and hotspots density 67.6% and 73.3% respectively (Figure 27A-B) ($p<0.001$, n=13 in mCherry, n=14 in mCherry-K_v2.1-WT and n=15 in mCherry-K_v2.1- Δ318).

To investigate the mechanisms of K_v2.1 clusters, I calculate docking granule density and exocytosis ratio around docking granule (Figure 27C-D). I find that, K_v2.1 clusters can recruit 30.0% more insulin granules and increase 42.4% exocytosis happens around docking granule compared to mCherry group in non-diabetic donors ($p<0.001$, n=30, 30, 30 in mCherry, mCherry-K_v2.1-WT and mCherry-K_v2.1-Δ318). Similarly, in T2D donors, K_v2.1 clusters can increase 37.5% docking granules and increase 50% for exocytosis happens around docking granules while cluster-deficiency mutation cannot have no effects on exocytosis spatial pattern. ($p<0.001$, n=13, 15, 15 in mCherry, mCherry-K_v2.1-WT and mCherry-K_v2.1-Δ318)

Figure 27. Upregulation of K_v2.1 clusters enhances exocytosis hotspots

A) Scatter spots graph of hotspots ratio and exocytosis events. Within selected window, exocytosis events were kept the same. Uniform index was significantly increased when overexpressed K_v2.1-WT but not K_v2.1-Δ318.

B) Similar results were found in pancreatic β-cells from T2D donors.

C-D) Both in non-diabetic donors (C) and T2D donors (D), mCherry-K_v2.1-WT, but not mCherry-K_v2.1-Δ318, can significantly increase docking granule density and the ratio happens around docking granules compared to the mCherry group. *P<0.05, **P<0.01, ***P<0.001 (all panels by J Fu).

Figure 27

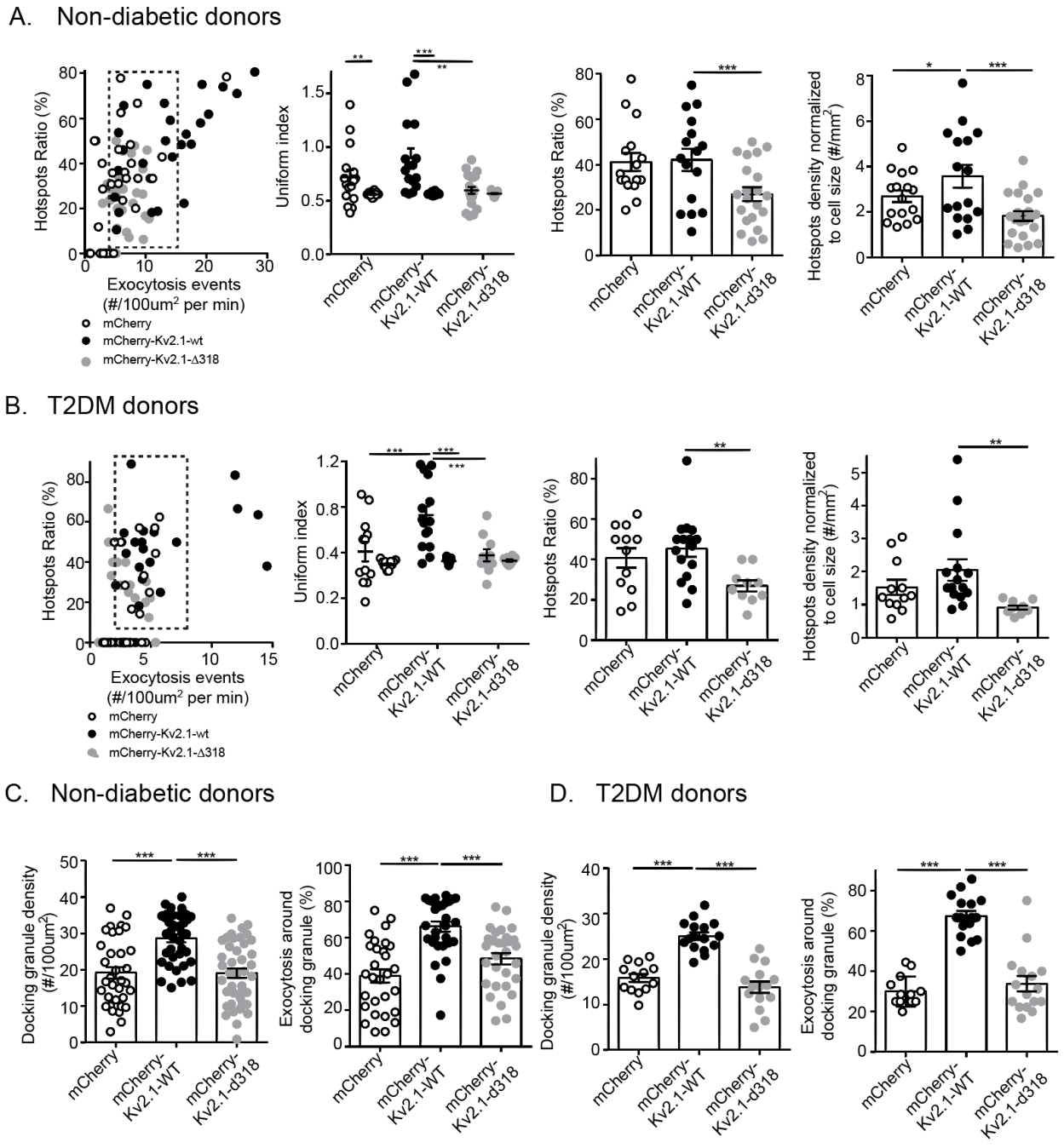
A. Non-diabetic donors
Hotspots Ratio (%)
Exocytosis events (#/100um² per min)
mCherry
mCherry-Kv2.1-wt
mCherry-Kv2.1-Δ318
Uniform index
Hotspots Ratio (%)
Hotspots density normalized to cell size (#/mm²)
B. T2DM donors
C. Non-diabetic donors
D. T2DM donors
Docking granule density (#/100um²)
Exocytosis around docking granule (%)
mCherry
mCherry-Kv2.1-WT
mCherry-Kv2.1-d318

3.5 DISCUSSION

Regulated exocytosis from human pancreatic β-cells is dysregulated in T2D patients. However, the spatial pattern of exocytosis is not fully studied. In this present work, I am the first to investigate the spatial pattern of exocytosis in human pancreatic β cells. I find that exocytosis is highly compartmentalized at hotspots in non-diabetic donors. In T2D, the spatial pattern is impaired. This spatial pattern can be regulated by glucose, and compartmentalized exocytosis prefers to happen around docked granules. Overexpression of clustering-sufficient $K_v2.1$ can increase docking granule density, thus rescue compartmentalized exocytosis in T2D donors.

The spatial pattern of exocytosis has been studied in neurons. It is reported that exocytosis happens compartmentalized in neurons at the "active zone". Similarly, the spatial patterning is drawing attentions in insulin-secreting cells. Previous study shows that exocytosis has hotspots in INS-1 insulinoma cells (Yuan et al., 2015). More than that, spatial and temporal analysis in insulin granule secretion in isolated intact human islets reveals that exocytosis localizes to preferential release sites (Almaca et al., 2015). Consistent with these studies, I find that exocytosis is compartmentalized in isolated single human β-cells from non-diabetic donors. Prolonged stimulation with high glucose increases compartmentalized exocytosis of granule secretion (Almaca et al., 2015). I also observe that glucose, but not KCl alone, will increase compartmentalized exocytosis. This phenomenon could be explained by the ability of glucose to recruit insulin granules to the cell membrane, while KCl will deplete docking granules. It is reported that glucose could recruit docking granules through K_{ATP} channels and Epac2A recruitments. In T2D donors, reduced granule docking density was found as a major upstream defect (Gandasi et al., 2018). Since I noticed spatial patterning was impaired in T2D, I hypothesize that docking granule provide a platform for exocytosis hotspots. Examination of one

hotspot illustrates exocytosis happening repeatedly around a docked granule. Even after that docking granule fused, the new-coming granule continuously exocytose at the same spot. Our results confirm that docking granules mark hotspots for exocytosis.

Not only does exocytosis have a spatial pattern, but also SNARE complexes and ion channels are compartmentalized on cell membrane. Both syntaxin1A (Gandasi & Barg, 2014; Murray & Tamm, 2009) and $Ca_v1.2$ (Gandasi et al., 2017) form clusters on cell membranes. In Chapter 2 I showed that $K_v2.1$ is compartmentalized in pancreatic β cells and co-localizes with docking granules. Here, I find that $K_v2.1$ clusters may serve as spatial regulators of exocytosis. While compartmentalized $K_v2.1$-WT can recruit more docking granules, $K_v2.1$-Δ318 does not have a similar function. Moreover, more exocytosis happens around docking granules in $K_v2.1$-WT groups compared to $K_v2.1$-Δ318 groups. Consistent with that, compared to $K_v2.1$-WT groups, $K_v2.1$-Δ318 groups have no effect on compartmentalized exocytosis.

To sum up, this present work has demonstrated that regulated exocytosis is compartmentalized at hotspots in non-diabetic β-cells but random in T2D donors. Moreover, docking insulin granules serve as hotspots for compartmentalized exocytosis. Mechanistically, I find that $K_v2.1$ clusters can recruit docking granules thus increasing exocytosis hotpots. Since both $K_v2.1$ expression and docking granule density are decreased in pancreatic β-cells from T2D donors, the spatial pattern of exocytosis is impaired as well. My study may prove a novel understanding for the pathophysiology of T2D.

3.6 CONCLUDING REMARKS

The studies in this chapter investigated the spatial and temporal pattern of exocytosis in isolated pancreatic β-cells. I demonstrate that exocytotic sites are not randomly distributed. Instead, exocytosis sites are compartmentalized at hotspots in pancreatic β-cells from non-diabetic patients. In contrast, this spatial pattern of compartmentalized exocytosis is impaired in β-cells from T2D donors. However, it is reported that in human islets, there are four distinct subtypes of β cells, which are distinguished by differential expression of ST8SIA1 and CD9. Importantly, the β cell subtype distribution is profoundly altered in type 2 diabetes (Dorrell et al., 2016). Since the β cells are not a single, homogenous cell population, my research needs to be further classified into different cell subtypes. Also, it is reported that intact pancreatic islets are controlled by 1%–10% of an islet's β-cell population (Johnston et al., 2016). These specialized pacemaker cells, termed "hubs", are defined by their high degree of connectivity to other β-cells and their rapid reaction to elevated glucose, which precedes the populous of "follower" β-cells (Kolic & Johnson, 2016). Currently, there is no available method to characterize "hub cells" and "follower beta cells" from isolated β-cells. Thus, this present study needs to take this into consideration as well.

Spatial and temporal analysis of insulin granule exocytosis in intact human pancreatic islets indicates that, secretory events are progressively localized to preferential release sites, coinciding with the transition to second phase insulin secretion (Almaca et al., 2015). Granule secretion was compartmentalized in neighboring beta cells, forming discrete regional clusters of activity. It is also reported that insulin secretion from β-cells in intact mouse islets is not randomly distributed. Instead, exocytosis sites targeted towards the vasculature (Low et al., 2014). Thus, this present study in isolated pancreatic β-cells is a step towards fully understanding

the cellular mechanisms of insulin secretion. Since the spatial pattern of insulin secretion is associated with vascular arrangements, it will be important to determine the spatial pattern using noninvasive *in vivo* imaging of pancreatic islet cell in live mouse model directly (Speier et al., 2008). Thus, β-cell stimulus-response coupling, which can be performed longitudinally under both physiological and pathological conditions, could be investigated.

I found that exocytosis sites are compartmentalized around docking granules. In T2D β-cells, since the docking granule density is downregulated, the compartmentalized exocytosis is impaired as well. Meanwhile, there could be other possibilities. Disruption of either the actin or the microtubule network could impair the spatial pattern (Yuan et al., 2015). Since the cytoskeleton is involved in insulin granule movement and trafficking (Heaslip et al., 2014) and microtubule is dysregulated in β cells of diabetic mice (X. Zhu et al., 2015), the interaction between compartmentalized exocytosis and cytoskeletal should be investigated.

$K_v2.1$ clusters are demonstrated to regulate the spatial pattern of exocytosis. Downregulated $K_v2.1$ expression could decrease the compartmentalized exocytosis while overexpression of $K_v2.1$ could increase the compartmentalization level of exocytosis sites. Other compartmentalized molecules should not be ruled out. $Ca_v1.2$ clusters is associated with insulin-containing granules in human pancreatic β-cells from ND donors and this spatial pattern is disturbed in T2D β-cells (Gandasi et al., 2017). It is reported that both syntaxin-1A and SNAP-25 clusters, associated with docked insulin granules on the plasma membrane, were reduced in β-cells from diabetic Goto–Kakizaki (GK) rat (M Ohara-Imaizumi et al., 2004). Thus, $Ca_v1.2$, syntaxin1A and SNAP-25 clusters may also regulate the spatial pattern of exocytosis. Another possibility is a close association of these molecules may form "excitosome" together. Thus, the mediator on "excitosome", specifically $K_v2.1$ clusters, is investigated in the following chapter.

CHAPTER 4

K_V2.1 SUMOylation Regulates Exocytosis Spatial Pattern In Human Pancreatic β-cells

The following chapter is to be submitted

Jianyang Fu, Kunimasa Suzuki, John M Githaka, Dafna Greitzer-Antes, Jocelyn E Manning Fox, Herbert Y. Gaisano, Patrick E MacDonald (2018).

4.1 ABSTRACT

Voltage-gated $K_v2.1$ potassium channels are important in pancreatic β-cells for determining electrical excitability, interacting with SNARE proteins and providing a platform for insulin granule docking. The covalent attachment of small ubiquitin-like modifier (SUMO) proteins regulates ion channels localization and function. It is shown that SUMO-1 exerts a strong inhibitory action on $K_v2.1$ channels and can regulate cellular excitability in native pancreatic β-cells. Considering $K_v2.1$ forms clusters and regulates compartmentalized exocytosis, I hypothesize that SUMO-1 could play a role in compartmentalized exocytosis through SUMOylation of $K_v2.1$ channels. In this study, I report that K145 (N-terminus) and K470 (C-terminus) in $K_v2.1$ channels are SUMOylated. SUMOylation at either K145 or K470 in $K_v2.1$ contributed to exocytosis while only K470 is related to electrical function of the channel. Moreover, co-transfection of SUMO-1 and $K_v2.1$-WT can impair compartmentalized exocytosis while SUMO-1 has no effect when $K_v2.1$ lacks its SUMOylation sites ($K_v2.1$ K145/K470R). My results indicate that both N- and C-termini of $K_v2.1$ may be SUMOylated. This SUMOylation on $K_v2.1$ channel can control the spatial pattern of exocytosis in human pancreatic β-cells.

4.2 INTRODUCTION

Post-translational attachment of a small ubiquitin-like modifier (SUMO) to the lysine (K) residue(s) of a target protein is defined as SUMOylation. This process modifies target protein localization and function to play an important role in signal transduction, gene transcription, maintenance of genome stability, tumourigenesis and glucose metabolism (Flotho & Melchior, 2013; Manyu Li et al., 2005; P. Yang et al., 2014). In human pancreatic β-cells, Homeostatic SUMOylation is reported as a key factor balancing β-cell survival vs secretory responsiveness (X. He et al., 2018; Patrick E MacDonald, 2018).

SUMOylation can regulate membrane proteins, including K^+ channels (X.-Q. Dai et al., 2009; Plant et al., 2010, 2011), Na^+ channels (Plant et al., 2016) and other ion channels (Chatelain et al., 2012). Specifically, SUMO can exert a strong inhibitory action on $K_v2.1$ and can regulate cellular excitability in β-cells. Although it is reported that C-terminus in $K_v2.1$ could be SUMOylated (Plant et al., 2011), the binding sites of SUMO-1 is still not well investigated.

SUMOylation can acutely mediate insulin secretion by the direct and reversible inhibition of β-cell exocytosis (Dai et al., 2011). Mechanistically, SUMO targets at the exocytotic sites. Several exocytotic and granule-trafficking proteins, including Synaptotagmin VII, syntaxin1A, synapsin 1A, RIM1α and tomosyn have been reported to be SUMOylated (Ferdaoussi & MacDonald, 2017).

In this chapter, I report that $K_v2.1$ can be SUMOylated at the N- and C-terminus. While SUMOylation on the C-terminus can inhibit delayed rectified currents, both sites regulate exocytosis function. $K_v2.1$ SUMOylation may inhibit exocytosis by impeding compartmentalized exocytosis. This present investigation indicates that SUMO dysfunction may contribute to impaired insulin secretion in human pancreatic β-cells from T2D donors.

4.3 MATERIALS AND METHODS

4.3.1 Cells and cell culture

Human islets from the Clinical Islet Laboratory at the University of Alberta and the Alberta Diabetes Institute IsletCore were cultured in DMEM with 5.5 mM glucose, L-glutamine, 110 mg/l sodium pyruvate, 10% FBS, and 100 U/ml penicillin/streptomycin. Islets from 19 donors without diabetes and 7 T2D donors contributed to this work (Supplementary Tables 1-3). All human islet studies were approved by the Human Research Ethics Board (Pro00001754) at the University of Alberta and all families of organ donors provided written informed consent. Human embryonic kidney (HEK) 293 cells were cultured in DMEM with 20 mM glucose, 10% FBS, 100 units/mL penicillin, and 100 mg/mL streptomycin at 37°C and 5% CO2. The glucose responsive INS 832/13 insulinoma cell line was cultured in RPMI-1640 with 11.1 mM glucose, 10% FBS, 10 mM HEPES, 0.29 mg/ml L-glutamine, 1 mM sodium pyruvate, 50 μM 2-mercaptoethanol, and 100 U/ ml penicillin/streptomycin.

4.3.2 Adenoviruses, constructs, and treatments

Human pancreatic islets were dissociated using Cell Dissociation Buffer enzyme-free, Hanks' Balanced Salt Solution (ThermoFisher Scientific. Burlington, ON). Adenovirus NPY-eGFP virus was kindly donated by Herbert Y. Gaisano (University of Toronto). Isolated human pancreatic β-cells were infected with NPY-eGFP and further cultured for 24-36 h before imaging. Recombinant adenoviruses producing green fluorescent protein (GFP) alone (Ad-GFP) or together with SUMO1 (Ad-SUMO1) were created using pAdtrackCMV and the AdEasy system (http://www.coloncancer.org/adeasy.htm) as described before (Dai et al., 2011; Vergari et al., 2012). NPY-eGFP infected human pancreatic β-cells were transfected for 36-48 h with the

human SUMO1-GFP in the pEGFP-C1 vector (a gift from Dr. Steven Ogg, University of Alberta) and the pIRES-EGFP control vector (Clontech, Palo Alto, CA) using lipofectamine 2000 (Life Technologies, Burlington, ON, Canada).

To generate $K_v2.1$ SUMO mutations, site-directed mutagenesis is performed on a $K_v2.1$ expression vector to introduce the mutation from lysine to arginine at position 145, 470 or 145/470. The mutations are confirmed by Sanger DNA sequencing.

4.3.3 TIRFM Imaging

See the same to the "MATERIALS AND METHODS" part in Chapter 3.

4.3.4 SUMOylation sites prediction and protein structure visualization

$K_v2.1$ Protein sequences of human (Q14721), rabbit (Q9MZ19), rat (P15387), mouse (Q03717) and pig (O18868) were obtained from Uniprot (http://www.uniprot.org/). The SUMOplot™ Analysis Program (http://www.abgent.com/sumoplot.html) and GPS-SUMO 2.0 Online Service (http://sumosp.biocuckoo.org/online.php) were used to predict and identify possible SUMOylation sites. Protein structures were visualized using the PyMOL. Protein structure alignment is performed by UCSF Chimera (Lvov et al., 2009).

4.3.5 Electrophysiology

Patch-clamp measurement of K_v currents and exocytosis in single human β-cells or INS 832/13, identified by positive insulin immunostaining following the experiment, were performed at 32-35^{o}C as described in Chapter 2.

4.3.5 Statistical analysis

Data analysis was performed using Fit Master (HEKA Electronik), Origin Lab (v7.0) and GraphPad Prism (v6.0c). All data are shown as the mean ± SEM. Statistical outliers were identified by an unbiased ROUT (robust regression followed by outlier identification) test. Comparison of multiple groups was by ANOVA and Bonferroni post-test. When comparing two means only, data were analyzed by the 2-tailed Student's t test. A P-value less than 0.05 was considered significant.

4.4 RESULTS

4.4.1 K_v2.1 harbors conserved SUMOylation motifs

Since SUMO-1 increases docked granules (Xiao Qing Dai et al., 2011) but impedes hotspots formation, I hypothesize that SUMO-1 may regulate spatial pattern of exostosis through K_v2.1 SUMOylation. SUMOylation consists of the covalent binding of the SUMO moiety to a lysine residue of the consensus sequence on the substrate protein (ΨKxD/E, where Ψ is a large hydrophobic residue, K is the target lysine, x can be any residue, and D/E are aspartate or glutamate). Previously, a lysine in the C-terminus of K_v2.1 (K470) is reported to be SUMOylated with SUMO-1 in hippocampal neurons (Plant et al., 2011). To identify other lysine residues in K_v2.1 potentially targeted by SUMO, I used online prediction software (GPS-SUMO 2.0 and SUMOplot™) to analyze the primary sequence of K_v2.1 and then alignment tools to assess whether these potential sites are evolutionary conserved across species, including human, rabbit, rat, mouse and pig. As illustrated in Fig 28, I find that K_v2.1 is more conserved at a putative N-

terminus SUMOylation site (K145, shown as K149 in figure 28) than at the C-terminus site (K470, shown as K474 in figure 28).

To confirm K145 can be SUMOylated, I compared sequence difference in N-terminus between K_v2 and other K_v1 channels. As opposed to $K_v2.2$, K145 in $K_v2.1$ is similar to reported SUMOylated site in the N-terminus of K_v1 channels (Fig 29A) (K138 in $K_v1.1$, K134 in $K_v1.2$ and K211 in $K_v1.5$). To further compare the structure, I assigned $K_v1.5$ and $K_v2.1$ together using UCSF Chimera. I found that both K211 in $K_v1.5$ and K145 in $K_v2.1$ lie between the T1 tetramerization domain of K_v channel, which indicates that SUMO-1 may bind at this site (Fig 29B). Protein-protein docking was also simulated using ClusPro server (Kozakov et al., 2017). Both van der Waals (VDW) energies and electrostatic (ELEC) per mole of solute have been taken into consideration. As illustrate in Fig 30, SUMO-1 can directly binds at T1 tetramerization domain in $K_v2.1$. However, it is important to note that this does not consider the direct covalent attachment that would be mediated by a SUMO-ligase.

Figure 28. Potential SUMOylation sites in K_v2.1 channels

A. A schematic representation of three different potential SUMOylation sites in K_v2.1 channel K145 in N-terminus, K470 in C-terminus and K255 in the 3rd transmembrane domains.

B. Two different SUMOylation prediction software are applied in different species including human, rat, mouse, rabbit and pig. K145 and K470 are predicted as potential SUMOylation targets, while K255 is not a potential SUMOylation site in K_v2.1 channel (all panels by J Fu).

Figure 28

A.

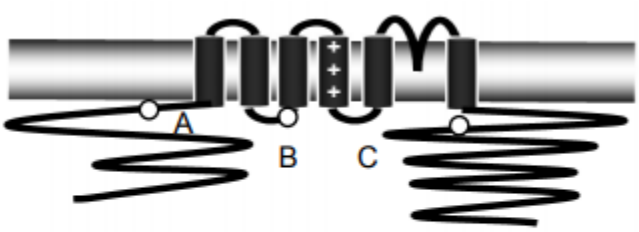

N-terminal SUMOylation sites A: K149
C-terminal SUMOylation sites C: K474
Probability SUMOylation sites B: K259

B.

Species	Position	Protein sequences	GPS-SUMO 2.0			SUMOplot™
			Score	Cut-off	P-Value	Score
Human	K149	EQMNEE LKRE AETLR	12.009	2.13	0.006**	0.91
Rabbit	K149	EQMNEE LKRE AETLR	12.009	2.13	0.006**	0.91
Rat	K149	EQMNEE LKRE AETLR	12.009	2.13	0.006**	0.91
Mouse	K149	EQMNEE LKRE AETLR	12.009	2.13	0.006**	0.91
Pig	K149	EQMNEE LKRE AETLR	12.009	2.13	0.006**	0.91

Species	Position	Protein sequences	GPS-SUMO 2.0			SUMOplot™
			Score	Cut-off	P-Value	Score
Human	K474	KNGENM GKKD KVQDN	2.131	0	0.637	0.67
Rabbit	K474	KNGENL AKKE KVQDN	5.904	0	0.024*	0.79
Rat	K474	KNGESI AKKD KVQDN	2.277	2.13	0.046*	0.79
Mouse	K474	KNGEGV AKKD KVQDN	2.277	2.13	0.046*	0.79
Pig	K475	KNVENM GQKD KVQDN	0.37	0	0.342	0

Species	Position	Protein sequences	GPS-SUMO 2.0			SUMOplot™
			Score	Cut-off	P-Value	Score
Human	K259	PKKWKF FKGP LNAID	1.573	0	0.831	0.74
Rabbit	K259	PKKWKF FKGP LNAID	1.573	0	0.831	0.74
Rat	K259	PKKWKF FKGP LNAID	1.573	0	0.831	0.74
Mouse	K259	PKKWKF FKGP LNAID	1.573	0	0.831	0.74
Pig	K259	PKKWKF FKGP LNAID	1.573	0	0.831	0.74

Figure 29. K_v2.1 harbors conserved SUMOylation motif

A) A schematic representation of K_v2.1. T1, tetramerization domain, TM1-TM6, transmembrane domain. Different species were compared.

B) Structural alignment of K_v2.1 (red) and K_v1.5 (yellow). SUMOylation site on N-terminus in K_v2.1 (green) is structurally close to N- terminus in K_v1.5 (blue) (all panels by J Fu).

Figure 29

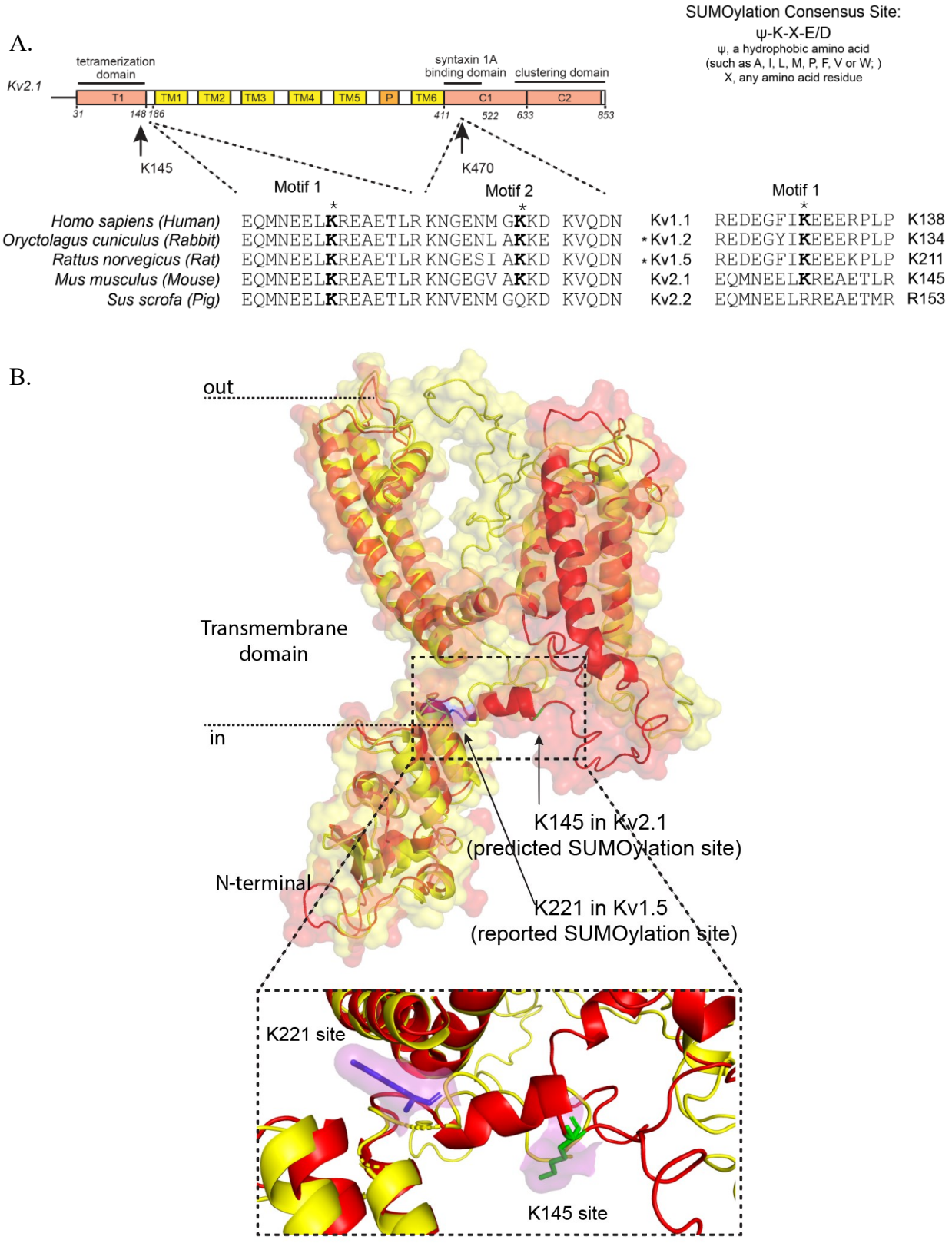
A.
SUMOylation Consensus Site:
ψ-K-X-E/D
ψ, a hydrophobic amino acid
(such as A, I, L, M, P, F, V or W;)
X, any amino acid residue
tetramerization domain
syntaxin 1A binding domain
clustering domain
Kv2.1
T1
TM1
TM2
TM3
TM4
TM5
P
TM6
C1
C2
31
148
186
411
522
633
853
K145
K470
Motif 1
Motif 2
Motif 1
Homo sapiens (Human) EQMNEELKREAETLR KNGENM GKKD KVQDN Kv1.1 REDEGFIKEEERPLP K138
Oryctolagus cuniculus (Rabbit) EQMNEELKREAETLR KNGENL AKKE KVQDN *Kv1.2 REDEGYIKEEERPLP K134
Rattus norvegicus (Rat) EQMNEELKREAETLR KNGESI AKKD KVQDN *Kv1.5 REDEGFIKEEEKPLP K211
Mus musculus (Mouse) EQMNEELKREAETLR KNGEGV AKKD KVQDN Kv2.1 EQMNEELKREAETLR K145
Sus scrofa (Pig) EQMNEELKREAETLR KNVENM GQKD KVQDN Kv2.2 EQMNEELRREAETMR R153
B.
out
Transmembrane domain
in
N-terminal
K145 in Kv2.1
(predicted SUMOylation site)
K221 in Kv1.5
(reported SUMOylation site)
K221 site
K145 site

Figure 30 K_v2.1 monomer binds with SUMO-1

A. A schematic representation of K_v2.1 monomer could bind with SUMO-1 using protein docking simulation.

B. A schematic representation the interaction between K145 in K_v2.1 (label as green) and the tail of SUMO-1 (label as yellow). (All panels by J Fu).

Figure 30

A.

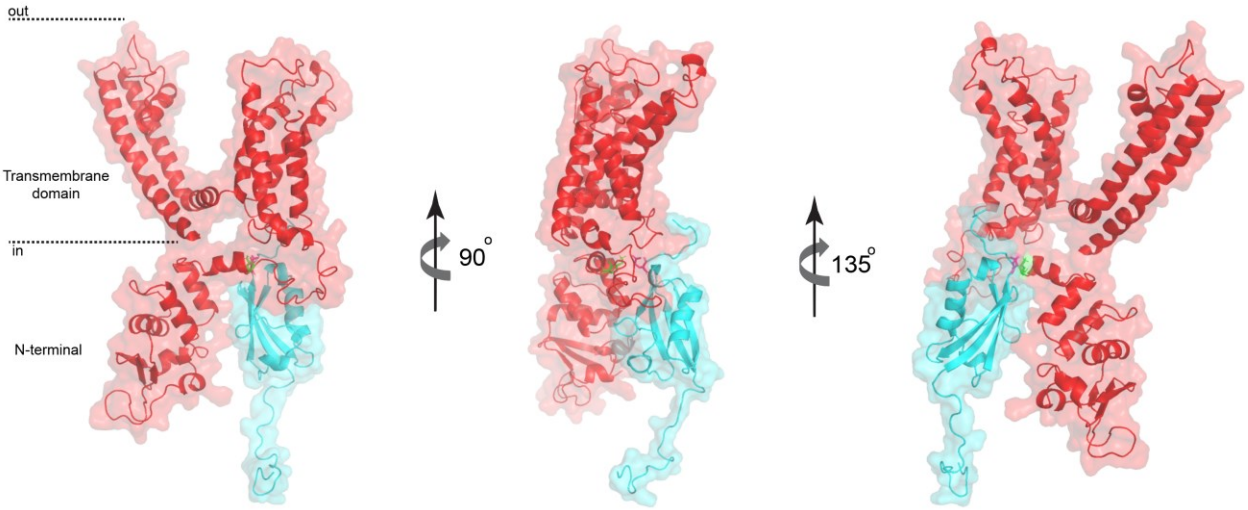
out
Transmembrane domain
in
N-terminal
90°
135°

B.

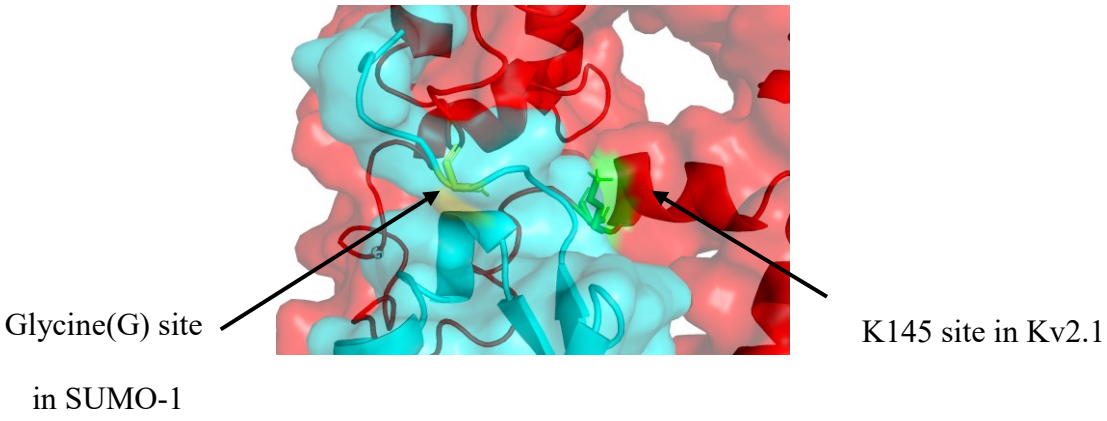
Glycine(G) site in SUMO-1
K145 site in Kv2.1

4.4.2 Only SUMOylation on C-terminus of K_v2.1 contributes to electrical function

To examine the impacts of K_v2.1 SUMOylation, mutants with lysine substitution at K145R or K470R alone or in combination were generated. Since the K_v2.1 SUMO-mutation groups did not affect protein expression, it indicates that the change of electrical function is not due to the expression difference between SUMO-mutation groups.

SUMO-1-GFP and K_v2.1 SUMO-mutation were co-transfected into INS-cells and HEK cells respectively. Only the cells will green fluorescent are recorded. Consistent with a previous report (Plant et al., 2011), only K_v2.1-K470R (similar to K_v2.1-K145/470R), but not K_v2.1-K145R will have enhanced by 53.2% the K^+ current compared with K_v2.1-WT in INS-1 cells (Fig 31A) ($p<0.01$, n=43 in K_v2.1-WT and n=31 in K_v2.1-K470R).

Similarly, K_v2.1-K470R, which has similar electrical function as K_v2.1-K145/470R, will significantly increase 55.2% current in HEK cells (Fig 31B) ($p<0.05$, n=17 in K_v2.1-WT and n=16 in K_v2.1-K470R), which indicates that only SUMOylation on the C-terminus of K_v2.1 accounts for repolarization currents.

Figure 31 SUMOylation on K470, not K145 of K_v2.1 regulates the repolarization currents

A. In INS-1 cells, representative band was shown to prove the expression of K_v2.1-WT, K_v2.1-K145R, K_v2.1-K470R and K_v2.1-K145R/470R are similar. While the electrical current is the same between K_v2.1-WT and K_v2.1-K145R, both K_v2.1-K470R and K_v2.1-K145R/470R has significant higher currents ($p<0.01$, $n=43$ in K_v2.1-WT and $n=31$ in K_v2.1-K470R).
B. Similar results performed in HEK cells confirmed the importance of SUMOylation of K470 in K_v2.1 on electrical function ($p<0.05$, $n=17$ in K_v2.1-WT and $n=16$ in K_v2.1-K470R) (all panels by J Fu).

Figure 31

A.

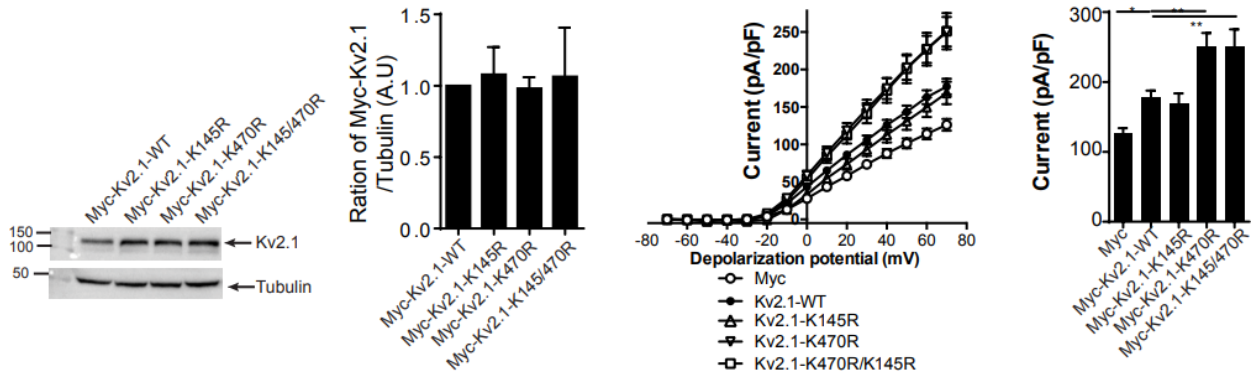
Myc-Kv2.1-WT
Myc-Kv2.1-K145R
Myc-Kv2.1-K470R
Myc-Kv2.1-K145/470R
150
100
50
Kv2.1
Tubulin
Ration of Myc-Kv2.1 /Tubulin (A.U)
1.5
1.0
0.5
0.0
Current (pA/pF)
Depolarization potential (mV)
Myc
Kv2.1-WT
Kv2.1-K145R
Kv2.1-K470R
Kv2.1-K470R/K145R

B.

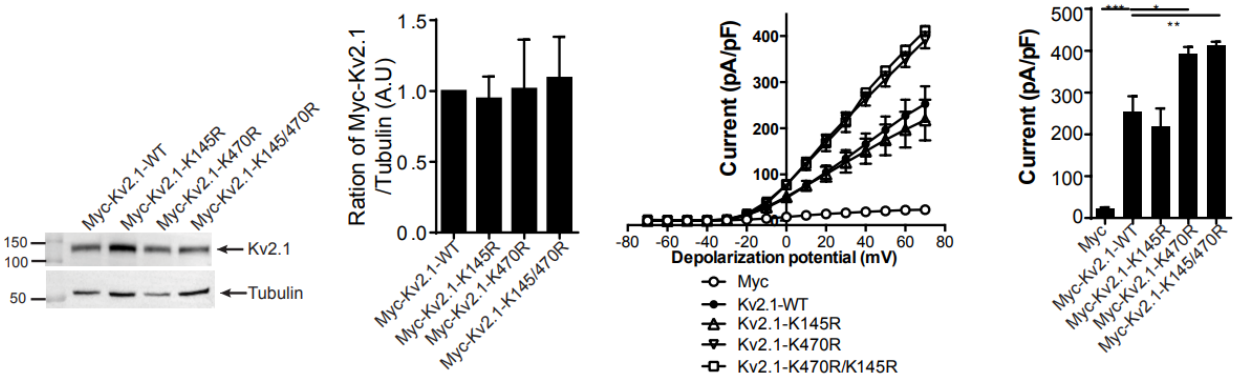
Myc-Kv2.1-WT
Myc-Kv2.1-K145R
Myc-Kv2.1-K470R
Myc-Kv2.1-K145/470R
150
100
50
Kv2.1
Tubulin
Ration of Myc-Kv2.1 /Tubulin (A.U)
1.5
1.0
0.5
0.0
Current (pA/pF)
Depolarization potential (mV)
Myc
Kv2.1-WT
Kv2.1-K145R
Kv2.1-K470R
Kv2.1-K470R/K145R

4.4.3 SUMOylation on both the N- and C-terminus of K_v2.1 regulates exocytosis

As opposed to the effect on electrical function, SUMO-1 can significantly impair exocytosis in both K_v2.1-K145R (36.1%, $p<0.05$, n=19 with GFP and n=20 with GFP-SUMO-1) and K_v2.1-K470R (21.4%, $p<0.01$, n=27 with GFP and n=31 with GFP-SUMO-1) while SUMO-1 has no effect in K_v2.1-K145/470R group in INS-1 cells (shown as Figure 32). Since SUMO-1 could inhibit exocytosis in either mutation while this effect is totally lost in K_v2.1-K145/470R mutation, I conclude that K_v2.1 is a SUMO substrate in vivo and that SUMOylation can occur at both N-terminus (K145) and C-terminus (K470) residues.

Figure 32 Both K145 and K470 SUMOylation sites in K_v2.1 are essential for exocytosis

A. SUMO-1 could impair the function of exocytosis when co-transfected with K_v2.1-WT.

B. SUMO-1 could impair exocytosis when co-transfected with K_v2.1-K145.

   ($p<0.05$, n=19 with GFP and n=20 with GFP-SUMO-1)

C. SUMO-1 could impair exocytosis when co-transfected with K_v2.1-K470R.

   ($p<0.01$, n=27 with GFP and n=31 with GFP-SUMO-1)

D. SUMO-1 cannot impair exocytosis function when co-transfected with K_v2.1-K145/470R (all panels by J Fu).

Figure 32

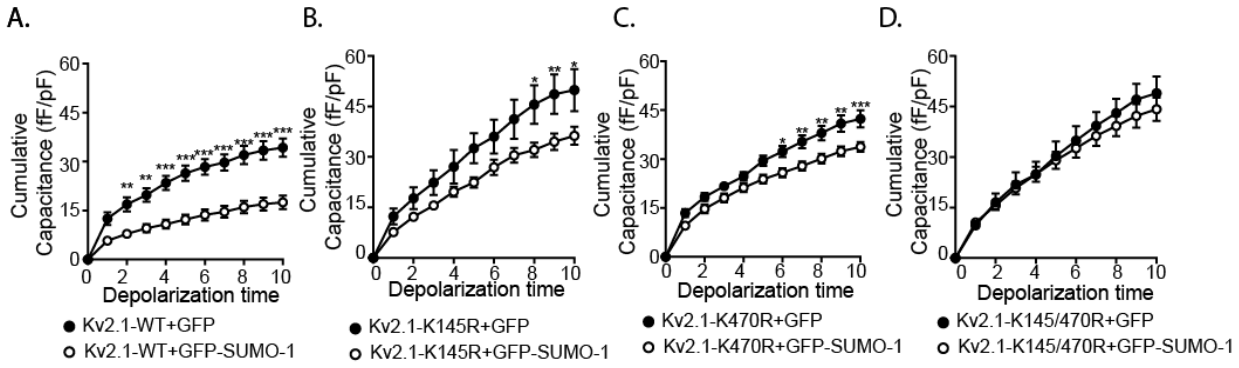
A.
B.
C.
D.
Cumulative Capacitance (fF/pF)
Depolarization time
Kv2.1-WT+GFP
Kv2.1-WT+GFP-SUMO-1
Kv2.1-K145R+GFP
Kv2.1-K145R+GFP-SUMO-1
Kv2.1-K470R+GFP
Kv2.1-K470R+GFP-SUMO-1
Kv2.1-K145/470R+GFP
Kv2.1-K145/470R+GFP-SUMO-1

4.4.4 SUMOylation of K_v2.1 impairs compartmentalized exocytosis

To assess the effects of K_v2.1 SUMOylation on exocytosis hotspots under 16.7 mM glucose stimulation for 5 mins, I overexpressed K_v2.1-WT with and without SUMO-1. Total exocytotic events significantly decreased 55.5% under SUMO-1 group ($p<0.001$, n=9, 9 with and without SUMO-1). Although the SUMO-1 expressing group still shows compartmentalization of fusion events, the uniform index decreased 38.5% compared to control group ($p<0.05$, n=9, 9 with and without SUMO-1). Also, SUMO-1 can decrease hotspots ratio from 67.6 ± 6.6 to 39.3± 5.3 ($p<0.05$, n=9, 9) without affecting hotspot density.

SUMO-1 cannot decrease exocytotic function with both N- and C-terminus mutation of K_v2.1 (K_v2.1-K145/470R). Besides, uniform index, hotspots ratio and hotspots density remains the same under SUMO-1 co-expression for the K_v2.1-K145/470R mutation group, which suggests that SUMO-1 affects exocytosis hotspots through K_v2.1 SUMOylation (Fig 33).

To further assess the effect of SUMO under high glucose stimulation I examined the spatial patterning of fusion events for first 5 mins, second 5 mins and third 5 mins following glucose stimulation. Both the hotspots ratio and hotspots density keep increasing under glucose stimulation in K_v2.1-WT group without SUMO-1. However, this spatial pattern will be impaired in the SUMO-1 co-expressing group. Surprisingly, SUMO-1 will not affect spatial pattern in K_v2.1-K145/470R group (Fig 34).

Figure 33. SUMOylation of K_v2.1 impairs exocytosis hotspots

A. Temporal analysis reveals that SUMO-1 will significantly reduce accumulated fusion events. SUMO-1 will significantly reduce uniform index. Moreover, SUMO-1 can significantly reduce hotspots ratio without affecting hotspots density.

B. SUMO-1 will have no effect on K_v2.1 SUMOylated mutation (K_v2.1-K145/470R) groups both under temporal analysis and spatial analysis. *P<0.05, **P<0.01, ***P<0.001 (all panels by J Fu).

Figure 33

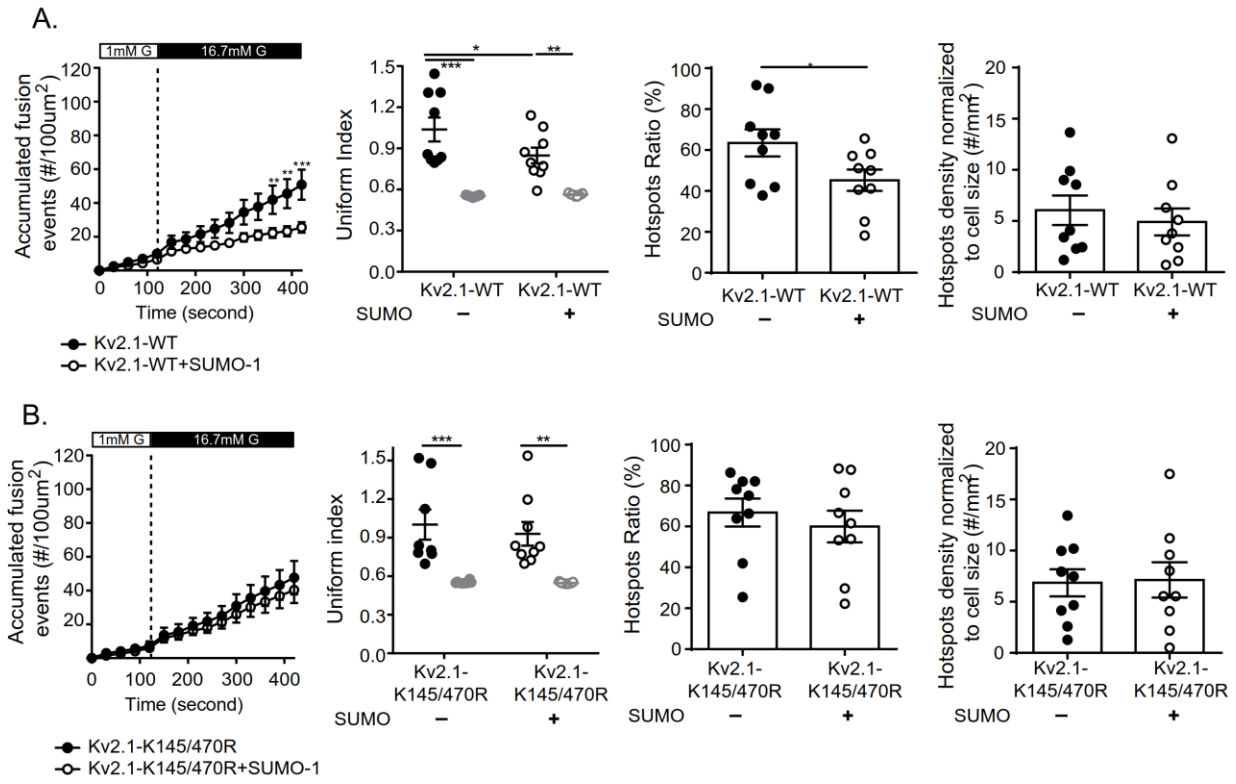
A.
1mM G
16.7mM G
Accumulated fusion events (#/100um2)
Time (second)
Kv2.1-WT
Kv2.1-WT+SUMO-1
Uniform Index
Kv2.1-WT
SUMO
Hotspots Ratio (%)
Hotspots density normalized to cell size (#/mm2)
B.
Kv2.1-K145/470R
Kv2.1-K145/470R+SUMO-1
Uniform index

Figure 34 Compartmentalized exocytosis process is impaired by SUMOylation

A. Exocytosis is become more compartmentalized in K_v2.1-WT groups under 16.7mM glucose stimulation while this process is impaired in K_v2.1-WT and SUMO-1 co-transfected groups.

B. SUMO-1 has no effects on K_v2.1-K145/470R mutation groups under 16.7mM glucose stimulation (all panels by J Fu).

Figure 34

A. Kv2.1-WT

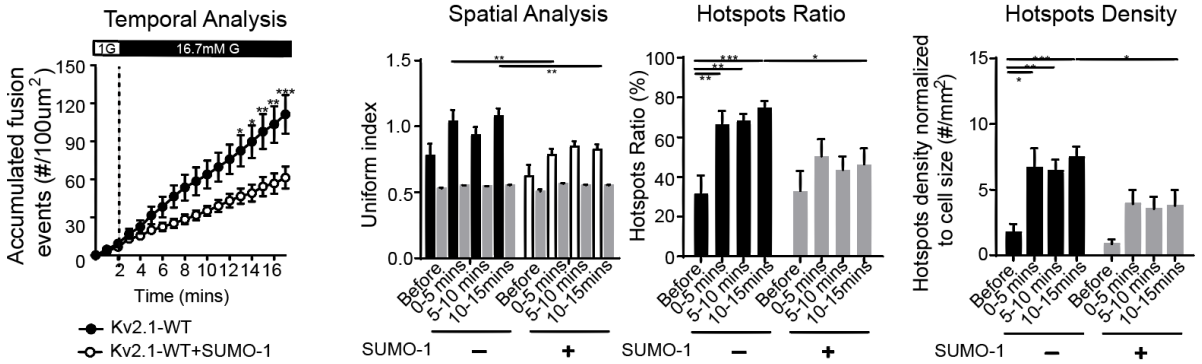

B. Kv2.1-K145/470R

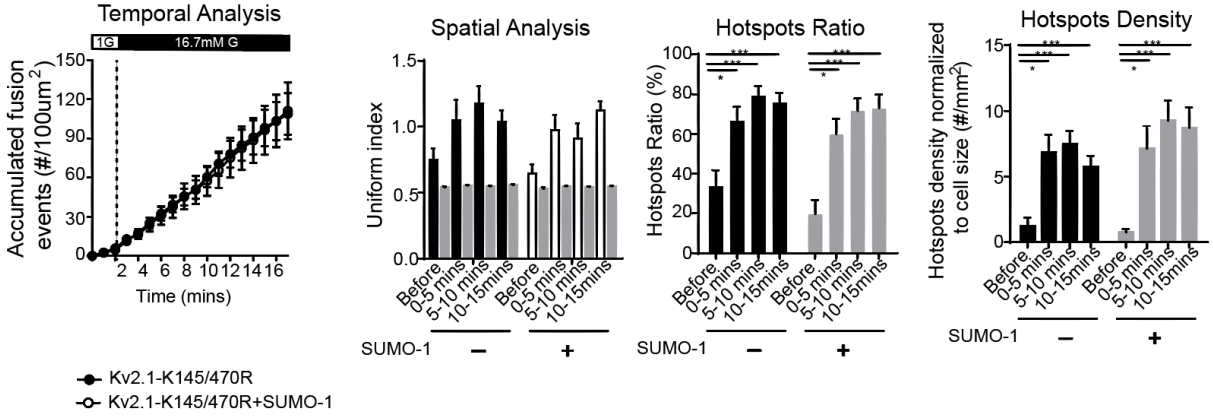

4.5 DISCUSSION

SUMOylation is an important regulatory mechanism for proteins. In pancreatic β-cells, SUMOylation regulates transcription factors targeting in the nucleus, including MafA (Shao & Cobb, 2009) and pancreatic duo-denal homeobox-1 (Pdx1) (Kishi, Nakamura, Nishio, Maegawa, & Kashiwagi, 2003). Moreover, it is reported that SUMO plays a role in mitochondrial (Braschi, Zunino, & McBride, 2009; Kruse et al., 2009) and ion channel regulation, including K2P1 (Rajan et al., 2005), K_v1.5 (M. D. Benson et al., 2007), TRPM4 (Kruse et al., 2009) and K_v2.1 (Dai et al., 2009; Plant et al., 2011). The present study identifies that K_v2.1 may be SUMOylated by SUMO-1 on both N-terminus (K145) and C-terminus (K470). While SUMOylation on both sites controls insulinoma exocytotic function, only K470 is related to electrical function of K_v2.1. My results from time-elapse TIRF microscopy suggests that, SUMOylation of K_v2.1 on both K145 and K470 sites, could regulate the spatial pattern of exocytosis in human pancreatic β-cells.

SUMOylation is an important regulatory mechanism for membrane proteins. There are 4 confirmed SUMO isoforms in humans, SUMO-1, SUMO-2, SUMO-3 and SUMO-4. As SUMO-4 cannot produce protein capable of SUMOylation in vivo (Bohren, Nadkarni, Song, Gabbay, & Owerbach, 2004), only three SUMO isoforms are functional. SUMO-2 and -3 differ by 3 amino acids, which are thought to have overlapping function. Thus, they are often regarded as SUMO-2/3, which share approximately 50% amino acid identity with SUMO-1 (Saitoh & Hinchey, 2000). Since it was reported that K_v2.1 could be SUMOylated by SUMO-1 (X.-Q. Dai et al., 2009; Plant et al., 2011), I only investigate the interaction between SUMO-1 and K_v2.1, though I cannot rule out the possible role of SUMO-2/3. Consistent with previous studies, my results

indicated that SUMO-1 could inhibit K_v2.1 current, specifically through SUMOylation on C-terminus (K470) of K_v2.1.

My work confirmed that K_v2.1 can also be SUMOylated at the channel N-terminus. Using SUMOylation prediction software, K_v2.1 channel contains a more conserved consensus SUMOylation motif at K145. Protein-protein docking simulation results indicate that K145 could bind with the tail of SUMO-1 when taking both Van der Waals forces and electric force into consideration. This result is consistent with SUMOylation on other K_v channels. It is reported that K_v1 channel α-subunits in N-terminus, including K_v1.1, K_v1.2 and K_v1.5 contain similarly located consensus SUMOylation motifs (M. D. Benson et al., 2007). SUMO-1 interact with Na_v1.2 on the N-terminus as well (Plant et al., 2016). Thus, structure alignment of K_v1.5 and K_v2.1 was performed. My results indicate that both K221 in K_v1.5 and K145 in K_v2.1 lie between the T1 tetramerization domain and the first transmembrane segment. Thus, it indicates that the N-terminus of K_v2.1 could be SUMOylated as well. It is further confirmed by exocytotic capacitance responses.

Considering K_v2.1 clusters could regulate compartmentalized exocytosis and SUMO could impair exocytosis in pancreatic β-cells, SUMO-1 may impair compartmentalized exocytosis through its interaction with K_v2.1, thus change the spatial pattern of exocytosis. My results confirmed that K_v2.1 SUMOylation could impair the spatial pattern of exocytosis. Since SUMO-1 will impede exocytosis hotspots without affecting the percentage of hotspots density, it suggests that other protein clusters, such as Ca_v1.2, syntaxin1A or SNAP-25 may also contributed to compartmentalized exocytosis as well.

To sum up, my studies confirmed that both the N- and C-terminus of K_v2.1 could associated with SUMO-1. K_v2.1 SUMOylation could impair compartmentalized exocytosis.

4.6 CONCLUDING REMARKS

This study in this chapter confirms that SUMOylation on $K_v2.1$ plays an important role in the spatial pattern of exocytosis. Specifically, SUMO-1 could interact with both K145 and K470 sites. While K470 controls the electrical function of $K_v2.1$, both these sites contribute to the exocytotic function of the channel. However, there are some limitations. It is reported that SUMO-1 could impede $K_v2.1$ current through acceleration of channel inactivation and an inhibition of recovery from inactivation (Dai et al., 2009). Moreover, SUMO modification is also reported to regulate $K_v1.5$ inactivation. Thus, the effect of K470 SUMOylation on $K_v2.1$ inactivation should also be tested. Although protein-protein docking simulation results indicates that SUMO-1 could bind with $K_v2.1$ on T1 domains, to increase physiologic relevance this simulation should be performed using the tetramer of $K_v2.1$channels, rather than the $K_v2.1$ monomer. Moreover, deSUMOylation could be taken into consideration as well. SUMO-specific protease 1 could de-SUMOylated Kv2.1 and related to glucose stimulation, SENP1 may play a role in compartmentalized exocytosis as well. $K_v2.1$ phosphorylation is reported to be involved in the spatial distribution of this channel (Cobb et al., 2015; Mandikian et al., 2014). Thus, cross talk between SUMOylation and phosphorylation should be discussed. K470 on C-terminus could be SUMOylated, while S480 can be phosphorylated (Mandikian, Cerda, Sack, & Trimmer, 2011). Whether SUMO tagging of K470 lysine residues could affect phosphorylation or dephosphorization from neighboring sites (S480) has not been determined.

The spatial pattern of exocytosis changes during neuronal development (Urbina et al., 2018). Spatial distribution was not uniform in immature cells while spatial distribution of exocytosis in neurons would change over developmental time. Thus, cell cycle and development of β-cells should be taken into consideration for compartmentalized exocytosis.

CHAPTER 5

Summary, General Discussion and Future directions

5.1 SUMMARY

Insulin secretion is precisely regulated by repetitive action potential firing, mediated by ion channels which depolarize the membrane potential in response to glucose metabolism. While the electrical role of ion channels ($K_v2.1$) is well-studied, the non-electrical role and its spatial pattern, are not well investigated. Similarly, the spatial pattern of insulin secretion from isolated single β-cells, is still not fully assessed. Moreover, the modification of $K_v2.1$, SUMOylation is less investigated.

In attempt to provide a novel insight on the pancreatic β-cells and gain better understanding of delayed rectified K^+ channels, the present dissertation focuses on the compartmentalization of $K_v2.1$ and exocytosis. The major findings in this thesis are summarized as follows (Figure 35):

- Both $K_v2.1$ and $K_v2.2$ can mediate repolarization through delayed rectified K^+ currents in human pancreatic β-cells. However, only $K_v2.1$, not $K_v2.2$ control exocytosis directly in β-cells.
- Similar to reports in neurons and HEK cells, $K_v2.1$ compartmentalize as clusters in human pancreatic β-cells and INS-1 832/13 cells. Specifically, around 6~12 $K_v2.1$ ion channels form one cluster.
- Spatially, $K_v2.1$ clusters are co-localized with docking insulin granules. A clustering-deficient $K_v2.1$ reduces secretory granule density on the plasma membrane.
- Clustering of $K_v2.1$ can promote exocytosis independently from its repolarization ability and interaction with Syntaxin1A .
- $K_v2.1$ clusters play an essential role in granule recruitment under glucose stimulation.

- In human T2D β-cells, consistent with the impaired exocytosis function, the expression level of $K_v2.1$ decreased. Overexpression $K_v2.1$ can increase the exocytosis function both in non-diabetes donors and T2D donors. Moreover, transduction with electrically inactive $K_v2.1$ could increase glucose-stimulated insulin secretion directly.
- Exocytosis from human non-diabetic β-cells is highly compartmentalized. Exocytosis sites form clusters at "hotspots" while exocytosis sites in T2D β-cells are randomly distributed on plasma membrane.
- Compartmentalized exocytosis is regulated by glucose stimulation but not KCl stimulation.
- Exocytosis events are compartmentalized around pre-docking granules in non-diabetic β-cells. In β-cells from T2D donors, both compartmentalized exocytosis and pre-docking insulin granule density decreased compared to β-cells from non-diabetic donors.
- Down regulated $K_v2.1$ expression will decrease compartmentalized exocytosis.
- I demonstrated that $K_v2.1$ clusters are important for compartmentalized exocytosis in both non-diabetic donors and T2D donors.
- Similar to other K_v channels, $K_v2.1$ has two SUMOylation sites, including K145 on N-terminus and K470 on C-terminus. Both SUMOylated sites contribute to exocytosis while only K470 on C-terminus regulates the electrical function of repolarization.
- I found that SUMOylation of $K_v2.1$ on both K145 and K470 sites will impede compartmentalized exocytosis in pancreatic β-cells.

Figure 35

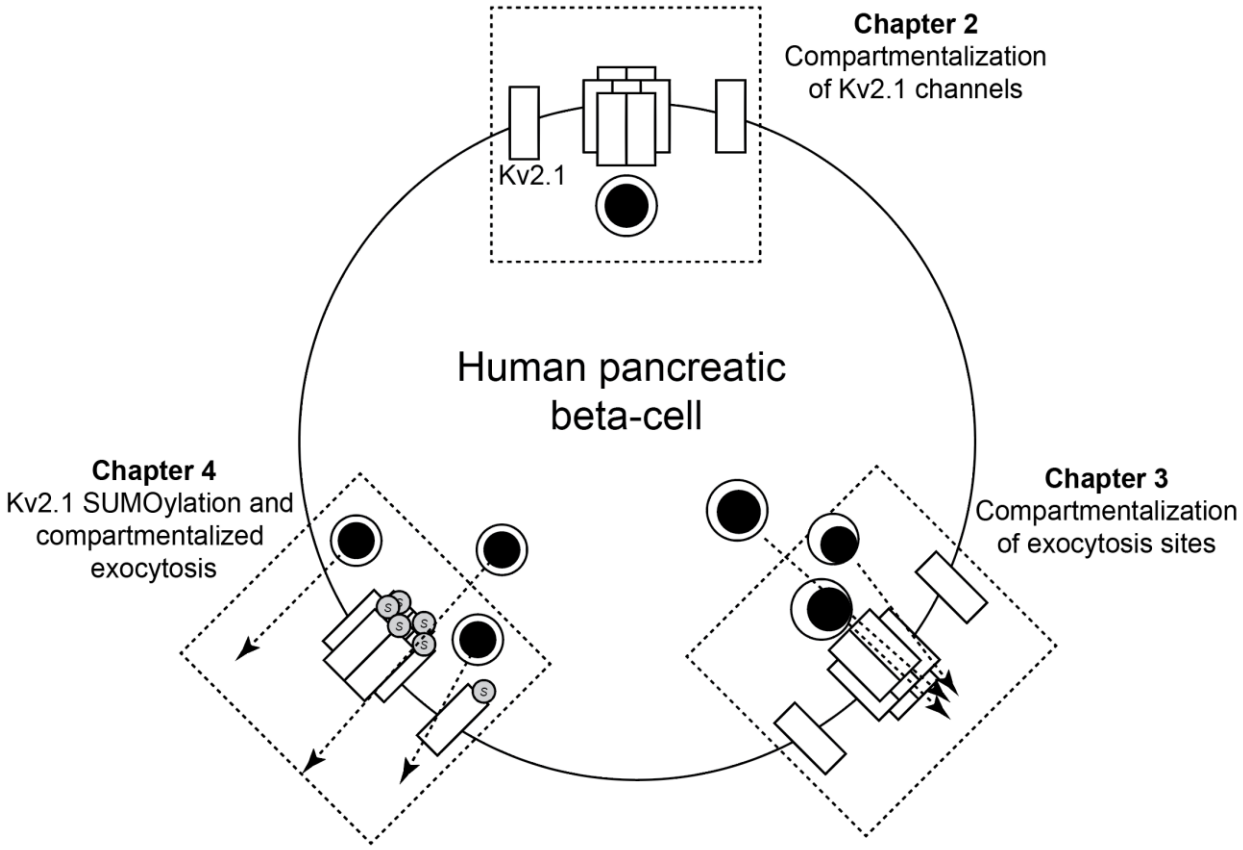

Figure 35. A general schematic diagram to summarize the main finding of the current thesis.

5.2 GENERAL DISCUSSION

Compartmentalization of the cell membrane is considered as playing an import role in receptor signal transduction (K. Jacobson, Mouritsen, & Anderson, 2007), membrane protein trafficking (Bavari et al., 2002; Ionescu-Tirgoviste et al., 2015) and cell membrane organization (Bavari et al., 2002). In this present thesis, compartmentalization of ion channels, $K_v2.1$ and exocytosis sites have been the focus of investigation. Moreover, SUMOylation sites of $K_v2.1$ and its contribution to compartmentalized exocytosis have been studied as well.

5.2.1 The role and spatial pattern of $K_v2.1$ in pancreatic β-cells

5.2.1.1 Evidence that K_v2 is important for pancreatic β-cells

The first evidence that repolarization plays an essential role in exocytosis was from intracellular microelectrode measurement of electrical activity in islets of Langerhans (DEAN & MATTHEWS, 1968). Since the development of Hodgkin–Huxley model in 1952 (Hodgkin & Huxley, 1952), it is hypothesized that the repolarizing K^+ current may be important for regulating exocytosis in isolated pancreatic β-cells. This hypothesis is further confirmed by tetraethylammonium (TEA), a K_v channel antagonist, the prolongs action potentials (Atwater, Ribalet, & Rojas, 1979) and increases insulin secretion (Henquin, 1977; Henquin, Meissner, & Preissler, 1979) directly. Mechanistically, electrical activity (Patrick E MacDonald, Sewing, et al., 2002) and intracellular Ca^{2+} concentration (Rosario et al., 1993) enhanced by TEA has been investigated and reported. Experiments performed on HIT-T15 cells and rat islets confirmed that TEA could enhance insulin secretion in a glucose-dependent manner. Consistently, 4-aminopyridine (4-AP) and tetrapentylammonium (TPeA), K_v channel antagonists, could enhance tolbutamide-stimulated insulin secretion (Su, Yu, Lenka, Hescheler, & Ullrich, 2001).

Moreover, $K_v2.1$ null mice have reduced fastinsg blood glucose level and elevated serum insulin level. Both glucose tolerance and insulin secretion are enhanced compared to $K_v2.1^{-/-}$ mouse (David A Jacobson et al., 2007). Thus, blocking K_v channels may enhance insulin secretion in presence of glucose and $K_v2.1$ antagonists are regarded as potential drugs for T2D.

However, some other experiments suggested that K_v channels may have multiple roles in regulating insulin secretion. Different from rodent cells, in human islets, the K_v2 channel blocker stromatoxin had no effect on insulin secretion and electrical activity (Braun et al., 2008). Moreover, one group reported that no clear difference between $K_v2.1$ knockout mice and controls in plasma glucose and insulin levels during an IPGTT (X. N. Li et al., 2013). Deletion of $K_v2.1$ mouse models is reported to be strikingly hyperactive, this may contribute to alteration in eating behavior and metabolism (Speca et al., 2014). Thus, it makes the previous $K_v2.1^{-/-}$ mouse results (David A Jacobson et al., 2007) less convincing.

One of the possible explanations is, K_v2 channels are also expressed in non-β cells within the islets. It is reported that $K_v2.1$ regulates insulin secretion in β-cells while $K_v2.2$ modulates somatostatin release in δ-cells (X. N. Li et al., 2013). Thus, $K_v2.1$ selective inhibitors should become a novel avenues to promote insulin secretion for the treatment of T2D. Our lab also reported that K_v2 channels are also expressed in pancreatic α-cells, which are sensitive to stromatoxin, a K_v2 channels antagonist. Thus, K_v currents in pancreatic in α-cells are positive regulators of glucagon secretion induced by low glucose in mouse and human islets. In this present thesis, I focus on human pancreatic β-cells only. I find that both $K_v2.1$ and $K_v2.2$ are expressed in β-cells and contribute to the delayed outward K^+ current, however only $K_v2.1$ facilitates insulin exocytosis. In islets from donors with T2D, expression of KCNB1 ($K_v2.1$) and KCNB2 ($K_v2.2$) and the contribution of these channels to outward K^+ currents are reduced.

Besides from the classic electricsal role of K_v2.1, non-electrical function of the ion channels could be another explanation. It is reported that other K_v channels could regulate independently of their electrical functions. K_v10.1 channels could regulate the mitogen-active protein (MAP) kinase signaling. K_v11.1 and K_v1.3 is involved in cell proliferation (Lori et al., 2009). Similarly, K_v2.1, could facilitate the insulin granule exocytosis directly. Earlier works show that K_v2.1 could physically and dynamically interact with SNAP-25 and Syntaxin1A in PC12 cells, oocytes, β-cells and *in vitro* (Leung et al., 2003; Patrick E MacDonald, Wang, et al., 2002; Michaelevski et al., 2003). However, there is no report on K_v2.2 and SNARE proteins interaction. Considering 60% of their C-terminus is differently, it may explain why only K_v2.1, not K_v2.2 is essential for the facilitation of insulin granule exocytosis.

5.2.1.2 Evidence that spatial pattern of membrane proteins is essential for exocytosis

K_v2 can form clusters at micro-domains in developing hippocampal neurons (Antonucci et al., 2001) and spinal motoneurons (Muennich and Fyffe, 2004). K_v2.1 channels in particular are localized distinctly to soma and proximal dendrites of mammalian central neurons, most pyramidal cells of the cortex and hippocampal neurons (Sarmiere, Weigle, & Tamkun, 2008). It can also giving a platform for new income K_v2.1 granules (Deutsch et al., 2012). Thus, I hypothesize that, similar to neurons, K_v2.1 could also compartmentalize into clusters in an insulin-producing β-cell line and human β-cells. My work demonstrate the existence of K_v2.1 clusters in INS 832/13 cells and isolated non-diabetic human pancreatic β-cells through both biochemical and imaging approaches. More importantly, I noticed that compartmentalization of K_v2.1 will be impaired in pancreatic β-cells from T2D donors. This phenomenon is consistent with de-clustering of K_v2.1 during brain ischemia (Misonou, Mohapatra, Menegola, & Trimmer,

2005). It suggests that compartmentalization of ion channels may have an essential pathophysiological role in both neurons and β-cells.

Similar to K_v channels, instead of being distributed randomly on the plasma membrane, $Ca_v1.2$ channels are also clustered on plasma membrane (Franzini-Armstrong, Protasi, & Tijskens, 2005; Simon & Llinas, 1985). In non-diabetic β-cells, this compartmentalized structure form Ca^{2+} micro-domains as hot spots to ensure high Ca^{2+} concentration which efficiently trigger insulin granule exocytosis. However, under long-term free fatty acids (FFA) exposure, this $Ca_v1.2$ compartmentalization is disrupted and Ca^{2+} influx through the dispersed channels becomes less efficiency in triggering exocytosis (Frances M Ashcroft & Rorsman, 2012). Moreover, insulin granules that is docked at the plasma membrane and associated with clusters of Ca^{2+} channels and Munc13. Upon depolarization, these granules are exposed to micro-domains of high [Ca^{2+}], which strongly increases their release probability and decreases their latency. Thus, exocytosis and insulin release are efficiently coupled to cellular electrical activity in micro-domains only rather than the bulk cytosolic Ca^{2+} concentration that accumulates as a consequence of channel opening (Gandasi et al., 2017).

Similar to ion channels clusters, SNARE (soluble N- ethylmaleimide -sensitive factor attachment protein receptor) proteins also compartmentalized all over the neuronal (Ullrich et al., 2015) and pancreatic β-cell (Barg, Knowles, Chen, Midorikawa, & Almers, 2010b) plasma membrane. It is reported that Syntaxin1A form clusters at the presynaptic active zone and assemble reversibly at sits of secretor granule in live cells. Syntaxin1A clusters can facilitate the docking of insulin granules via interaction with Munc18 clusters (Borisovska, 2018). Super-resolution imaging confirm that Syntaxin1A clusters co-localized with $Ca_v1.2$ clusters as well (Sajman, Trus, Atlas, & Sherman, 2017). Total internal reflection fluorescence microscopy find

that there was a strong correlation between Syntaxin1A clusters, SNAP-25 clusters and insulin granules fusions (M Ohara-Imaizumi et al., 2004). In this present thesis, I find that Syntaxin1A clusters interact with K_v2.1 clusters. Mechanistically, Syntaxin1A binds with C1-terminus of K_v2.1 and it is independent from proximal restriction and clustering (PRC) domains on C2-terminus in K_v2.1.

5.2.2 The spatial characters of exocytosis and related proteins

As mentioned above, while the SNARE complex mediates the molecular events of exocytosis in association with ion channel, such as K_v2.1 and Ca_v1.2, it is actually coupled to "excitosome" on plasma membrane. Since both SNARE proteins and ion channels are compartmentalized, I hypothesis that the exocytosis sites should be compartmentalized at or around "excitosome" as well. It is reported that exocytosis is not random distributed on plasma membrane. Instead, neurotransmitters are compartmentalized exocytosis at the active zone of a presynaptic nerve terminus (Südhof, 2012). The presynaptic active zone provides sites for vesicle docking and release at central nervous synapses and is essential for compartmentalized exocytosis (Wong et al., 2018). Thus, the cytomatrix at the activate zone is drawing attentions and maybe involved in the development of T2D.

CAZ (cytomatrix assembled at the active zone) is defined as a group of specialized cytoskeletal matrix that are assembled at the active zone. It is reported that CAZ, including bassoon, RIMs, α-liprin, ELKs as well as Bassoon and Piccolo (Mica Ohara-Imaizumi et al., 2005), have been identified and are thought to have a function in synaptic vesicle exocytosis and in the spatial organization of transmitter release. More importantly, as Piccolo and Bassoon are

unique marker proteins of these vesicles they are called Piccolo-Bassoon transport vesicles (PTVs) (Dresbach, Fejtová, & Gundelfinger, 2006).

SNARE ("soluble NSF-attachment protein receptor") and SM ("Sec1/Munc18-like") proteins, including Syntaxin1A, SNAP-25, Munc 13 and Munc 18, are also important for active zone. At the active zone, there are two principle functions for SNARE protein. First, to prime SNARE/SM protein fusion machinery for exocytosis, thus rendering synaptic vesicles fusion competent. Second, to mediate short-term plasticity by regulating priming activity. It is reported that RIMs proteins can mediate vesicles priming by directly activating Munc13. Thus, the interaction between CAZ and SNARE/SM proteins are essential for exocytosis at active zone.

Despite different debates and opinions on active zones, voltage-gated Ca^{2+} channels (Ca_v), localized around all neuronal active zones and ribbon synapses, is regarded as having a central role. Ca^{2+} itself is thought to control two main processes in the functioning of synaptic vesicles. First, Ca^{2+} is involved in vesicles recruitment to the presynaptic membrane in preparation for release. This activity involves the association of the vesicles with the SNARE complex. The recruitment is dependent upon Ca^{2+} in the 0–500 nM range, where the recruitment rate will be greater than the release rate since Ca^{2+} dependence of release is minimal in this range. The second Ca^{2+}-dependent process, release itself, predominates at Ca^{2+} concentrations greater than 5 μM. In the latter range, Ca^{2+}-dependent release obeys a high-power exponential function of Ca^{2+} concentration (Ramakrishnan, Drescher, & Drescher, 2012). For the ion channels, Ca_v can open in response to membrane depolarization and give rise to an influx of Ca^{2+}. Active zone proteins RIM and Munc 13 is also reported to bind at the synprint site via their C2 domain and orchestrate the clustering of Ca^{2+} channels in neuronal synapses (Bohme et al.,

2016; Calloway, Gouzer, Xue, & Ryan, 2015). Thus, compartmentalized Ca^{2+} concentration and Ca_v channels are essential for granule exocytosis.

Although there are no 'active zones' identified in pancreatic β-cells there are a number of active zone-related proteins (Munc 13, RIM and $Ca_v1.2$ channels) which may direct exocytosis to certain domains on cell membrane and facilitate organizing the individual exocytosis sites. It is reported that rapid insulin secretion requires Munc13-mediated recruitment of L-type Ca^{2+} channels, $Ca_v1.2$ clustering close proximity to insulin granules. Loss of this organization underlies disturbed insulin secretion kinetics in T2D (Gandasi et al., 2017). Similarly, I find that $K_v2.1$ is compartmentalized in micro-domains in pancreatic cells and this spatial organization is impaired in T2D. Exocytosis sites also compartmentalized. Overexpress $K_v2.1$ clusters can also improve exocytosis through increasing docking granule density on the cell membrane.

5.2.3 Regulation of SUMOylation on $K_v2.1$ and compartmentalization exocytosis

Previously, posttranslational modification by SUMO has been reported to mediate the target proteins from the nucleus, to regulate protein-DNA and protein-protein interactions, and to protect against ubiquitin-mediated degradation (Melchior, Schergaut, & Pichler, 2003). However, the role of SUMOylation outside the nucleus, especially modification of ion channel has merged recently (M. Benson, Iniguez-Lluhi, & Martens, 2017).

Several ion channels, including K^+ leak channel K2P1 (Rajan et al., 2005), the ionotropic kainate receptor subunit GluR6 (Feligioni, Nishimune, & Henley, 2009), the GluR7a/b subunits (Wilkinson, Nishimune, & Henley, 2008), cardiac I_{Ks} channels (KCNQ1) (Xiong et al., 2017), $K_v1.5$ (KCNA5) (M. D. Benson et al., 2007), and $K_v2.1$ (KCNB1) (X.-Q. Dai et al., 2009; Plant et al., 2011) have been shown to be SUMO-modified. SUMOylation of these channels, except

GluR7a/b, has been shown to have important regulatory consequences on the currents mediated by these channels. Consistent with previous reports, I find that $K_v2.1$ can be SUMOylated. Protein docking results indicate that, it can be SUMOylated at both N- and C-terminus. While SUMOylation on N-terminus have no effect on the current, I find the SUMOylation on C-terminus could inhibit $K_v2.1$ current.

Besides its effect on electrical function, SUMOylation of SNARE proteins at the exocytotic site is a key regulator of secretory function in different cell types. In pancreatic β-cells this is controlled by cytosolic redox signals downstream of NADPH (nicotinamide adenine dinucleotide phosphate) (Ferdaoussi & MacDonald, 2017). SUMO acts as a "brake" to prevent the Ca^{2+}-induced exocytotic release of insulin downstream of insulin granule priming. Glucose-dependent deSUMOylation and MAG-dependent signaling may work together to increase the pool of releasable insulin granules. A deSUMOylation-dependent release of syntaxin-1A from tomosyn (Ferdaoussi et al., 2017) could provide substrate on which MAG (Myelin-associated glycoprotein)-activated Munc13-1 can act to enhance granule priming. Many other SNARE proteins, such as deSUMOylation of Synaptotagmin VII and Munc18-1 (Shen et al., 2015), may also occur to facilitate exocytosis.

In the present studies, I investigate another mechanism by which SUMOylation may affect the spatial pattern of exocytosis in pancreatic β-cells. I find that SUMOylation of $K_v2.1$ may decrease the percentage of exocytosis that happens at hotspots without affecting the density of these hotspots.

5.3 FUTURE DIRECTIONS

In this present thesis, I investigate in the compartmentalization of ion channels ($K_v2.1$) and regulated exocytosis. Although I provide the spatial and temporal information of insulin granules and ion channels, many questions remain to be answered:

5.3.1 Better understanding of $K_v2.1$

- Although C-terminus of $K_v2.1$ is most investigated in this thesis, it is unclear whether N-terminus also contribute to the formation of $K_v2.1$ clusters.
- The interaction and crosstalk between $K_v2.1$ clusters and other molecular clusters remains to be investigated. It is reported that $K_v2.1$ clusters are colocalized with $Ca_v1.2$ clusters in HEK cells (Fox et al., 2015), but how about in pancreatic β-cells? Moreover, since $K_v2.1$ can bind with syntaxin1A while syntaxin1A form clusters, does $K_v2.1$ form clusters with syntaxin1A? Considering $Ca_v1.2$ clusters can interact with syntaxin1A clusters (Sajman et al., 2017), $Ca_v1.2$/$K_v2.1$/Syntaxin1A may assemble into larger nano-clusters together on the plasma membrane.
- It is reported that the "excitosome" contains Munc18a/syntaxin-1A/SNAP25/VAMP-2/synaptotagmin-7 complex. Since the N-terminus of $K_v2.1$ binds with SNAP-25 and the C-terminus of $K_v2.1$ interacts with Syntaxin1A, could $K_v2.1$ bind with Munc 18a and VAMP-2 as well?
- I find that both N- and C- terminus of $K_v2.1$ can be SUMOylated. How does it bind with SUMO-1? Is it possible that SUMO-1 binds with both N- and C-terminus of $K_v2.1$ to regulate the inactivation of $K_v2.1$?

- SUMOylation of $K_v2.1$ could be (de)SUMOylated from SUMO-Specific Protease 1 (SENP1). Considering SENP1 is related to glucose stimulation as well, is it possible that SENP-1 could contribute to compartmentalized exocytosis?

5.3.1 To further investigate the contribution of $K_v2.2$.

- Can $K_v2.2$ form micro-domains? If so, would these $K_v2.2$ clusters contain $K_v2.1$ or interact with $K_v2.1$ clusters?
- If $K_v2.2$ cannot form micros-domains, why not? Since the "proximal restriction and clustering" (PRC) domain in C-terminus of $K_v2.1$ is considered essential or the clustering of $K_v2.1$, does insertion of PRC sequence into $K_v2.2$ cause them to form $K_v2.2$ clusters?
- Different from $K_v2.1$, $K_v2.2$ cannot interact with SNARE proteins and SUMO. Does $K_v2.2$ respond to glucose stimulation and metabolism and regulate exocytosis?

5.3.2 Clearer imaging of regulated exocytosis

- With the development of super-resolution imaging microscopy, time-lapse live cell could be imaged in other methodologies, such as stimulated emission depletion microscopy (STED) or photo-activated localization microscopy (PALM). Moreover, Non-invasive 3D live cell imaging, such as lattice light-sheet microscopy, could be used to build a high-resolution 3D movie of subcellular dynamics.
- I reported exocytosis sites are compartmentalized at "hotspots" in pancreatic β-cells. However, is that possible that insulin granules have been recycled on the "hotspots"? Thus, endocytosis-exocytosis coupling should be taken into consideration as well.
- Does compartmentalization of exocytosis investigated in this thesis include "compound exocytosis" and "kiss-and-run exocytosis"?

5.4 CONCLUSIONS

This thesis provides strong evidence for the importance of organization at the plasma membrane in pancreatic β-cells. Besides the classic electrical function of $K_v2.1$ in repolarization, and its non-electrical role in binding with syntaxin1A and SNAP-25, I reported that $K_v2.1$ is highly compartmentalized and co-localized with docking insulin granules. However, this spatial pattern is impaired in β-cells from T2D donors. Overexpression to reform clustered $K_v2.1$ can recruit more docking granules to the plasma membrane and rescue exocytosis in T2D β-cells.

Another part of this thesis focuses on secretory granules and exocytosis itself in pancreatic β-cells. I find that exocytosis events also cluster together, with a majority of exocytosis happening around pre-docking granules. In T2D β-cells, consistent with a decreased pre-docking granule density, the spatial pattern of exocytosis was also impaired. Overexpression of $K_v2.1$ may rescue compartmentalized exocytosis in T2D β-cells by recruiting more docking granules. Finally, SUMOylation of $K_v2.1$ on both N- and C- terminus could regulate the spatial pattern of exocytosis directly.

Thus, compartmentalization of ion channels and related insulin granule exocytosis may present a novel target for the treatment of T2D and next research hotspots for better understanding of endocytosis and exocytosis.

REFERENCE LIST

Aguilar-Bryan, L., & Bryan, J. (1999). Molecular biology of adenosine triphosphate-sensitive potassium channels. *Endocrine Reviews*, *20*(2), 101–135. https://doi.org/10.1210/edrv.20.2.0361

Aguiree, F., Brown, A., Cho, N. H., Dahlquist, G., Dodd, S., Dunning, T., … Patterson, C. (2017). IDF diabetes atlas.

Almaca, J., Liang, T., Gaisano, H. Y., Nam, H. G., Berggren, P.-O., & Caicedo, A. (2015). Spatial and temporal coordination of insulin granule exocytosis in intact human pancreatic islets. *Diabetologia*, *58*(12), 2810–2818. https://doi.org/10.1007/s00125-015-3747-9

Andersson, S. A., Olsson, A. H., Esguerra, J. L. S., Heimann, E., Ladenvall, C., Edlund, A., … Eliasson, L. (2012). Reduced insulin secretion correlates with decreased expression of exocytotic genes in pancreatic islets from patients with type 2 diabetes. *Molecular and Cellular Endocrinology*, *364*(1–2), 36–45. https://doi.org/10.1016/j.mce.2012.08.009

Anja, B., & Laura, R. (2017). The cost of diabetes in Canada over 10 years: applying attributable health care costs to a diabetes incidence prediction model. *Health Promotion and Chronic Disease Prevention in Canada: Research, Policy and Practice*, *37*(2), 49.

Aoyagi, K., Sugaya, T., Umeda, M., Yamamoto, S., Terakawa, S., & Takahashi, M. (2005). The activation of exocytotic sites by the formation of phosphatidylinositol 4,5-bisphosphate microdomains at syntaxin clusters. *The Journal of Biological Chemistry*, *280*(17), 17346–17352. https://doi.org/10.1074/jbc.M413307200

Arikkath, J., & Campbell, K. P. (2003). Auxiliary subunits: essential components of the voltage-gated calcium channel complex. *Current Opinion in Neurobiology*, *13*(3), 298–307.

Ashcroft, F. M., & Gribble, F. M. (2000). New windows on the mechanism of action of K(ATP) channel openers. *Trends in Pharmacological Sciences*, *21*(11), 439–445.

Ashcroft, F. M., Harrison, D. E., & Ashcroft, S. J. H. (1984). Glucose induces closure of single potassium channels in isolated rat pancreatic β-cells. *Nature*, *312*, 446. Retrieved from http://dx.doi.org/10.1038/312446a0

Ashcroft, F. M., & Rorsman, P. (1989). Electrophysiology of the pancreatic beta-cell. *Progress in Biophysics and Molecular Biology*, *54*(2), 87–143.

Ashcroft, F. M., & Rorsman, P. (2012). Diabetes mellitus and the beta cell: the last ten years. *Cell*, *148*(6), 1160–1171. https://doi.org/10.1016/j.cell.2012.02.010

Aslamy, A., & Thurmond, D. C. (2017). Exocytosis proteins as novel targets for diabetes prevention and/or remediation? *American Journal of Physiology. Regulatory, Integrative and Comparative Physiology*, *312*(5), R739–R752. https://doi.org/10.1152/ajpregu.00002.2017

Atwater, I., Ribalet, B., & Rojas, E. (1979, March). Mouse pancreatic beta-cells: tetraethylammonium blockage of the potassium permeability increase induced by depolarization. *The Journal of Physiology*.

Barg, S., Knowles, M. K., Chen, X., Midorikawa, M., & Almers, W. (2010a). Syntaxin clusters assemble reversibly at sites of secretory granules in live cells. *Proceedings of the National Academy of Sciences*, *107*(48), 20804–20809. https://doi.org/10.1073/pnas.1014823107

Barg, S., Knowles, M. K., Chen, X., Midorikawa, M., & Almers, W. (2010b, November). Syntaxin clusters assemble reversibly at sites of secretory granules in live cells.

Proceedings of the National Academy of Sciences of the United States of America. https://doi.org/10.1073/pnas.1014823107

Baum, J., Simons Jr, B. E., Unger, R. H., & Madison, L. L. (1962). Localization of glucagon in the alpha cells in the pancreatic islet by immunofluorescent technics. *Diabetes*, *11*, 371.

Bavari, S., Bosio, C. M., Wiegand, E., Ruthel, G., Will, A. B., Geisbert, T. W., … Aman, M. J. (2002). Lipid raft microdomains: a gateway for compartmentalized trafficking of Ebola and Marburg viruses. *Journal of Experimental Medicine*, *195*(5), 593–602.

Baver, S. B., & O'Connell, K. M. S. (2012). The C-terminus of neuronal Kv2.1 channels is required for channel localization and targeting but not for NMDA-receptor-mediated regulation of channel function. *Neuroscience*, *217*, 56–66. https://doi.org/10.1016/j.neuroscience.2012.04.054

Bell, G. I., Santerre, R. F., & Mullenbach, G. T. (1983). Hamster preproglucagon contains the sequence of glucagon and two related peptides. *Nature*, *302*(5910), 716–718.

Benson, M. D., Li, Q.-J., Kieckhafer, K., Dudek, D., Whorton, M. R., Sunahara, R. K., … Martens, J. R. (2007). SUMO modification regulates inactivation of the voltage-gated potassium channel Kv1.5. *Proceedings of the National Academy of Sciences of the United States of America*, *104*(6), 1805–1810. https://doi.org/10.1073/pnas.0606702104

Benson, M., Iniguez-Lluhi, J. A., & Martens, J. (2017). Sumo Modification of Ion Channels. *Advances in Experimental Medicine and Biology*, *963*, 127–141. https://doi.org/10.1007/978-3-319-50044-7_8

Best, L. (2005). Glucose-induced electrical activity in rat pancreatic β-cells: dependence on intracellular chloride concentration. *The Journal of Physiology*, *568*(1), 137–144.

Betzig, E., Patterson, G. H., Sougrat, R., Lindwasser, O. W., Olenych, S., Bonifacino, J. S., … Hess, H. F. (2006). Imaging intracellular fluorescent proteins at nanometer resolution. *Science (New York, N.Y.)*, *313*(5793), 1642–1645. https://doi.org/10.1126/science.1127344

Black, J. A., Frezel, N., Dib-Hajj, S. D., & Waxman, S. G. (2012). Expression of Nav1.7 in DRG neurons extends from peripheral terminals in the skin to central preterminal branches and terminals in the dorsal horn. *Molecular Pain*, *8*, 82. https://doi.org/10.1186/1744-8069-8-82

Blodgett, D. M., Nowosielska, A., Afik, S., Pechhold, S., Cura, A. J., Kennedy, N. J., … diIorio, P. (2015). Novel Observations From Next-Generation RNA Sequencing of Highly Purified Human Adult and Fetal Islet Cell Subsets. *Diabetes*, *64*(9), 3172–3181. https://doi.org/10.2337/db15-0039

Bohme, M. A., Beis, C., Reddy-Alla, S., Reynolds, E., Mampell, M. M., Grasskamp, A. T., … Sigrist, S. J. (2016). Active zone scaffolds differentially accumulate Unc13 isoforms to tune Ca(2+) channel-vesicle coupling. *Nature Neuroscience*, *19*(10), 1311–1320. https://doi.org/10.1038/nn.4364

Bohren, K. M., Nadkarni, V., Song, J. H., Gabbay, K. H., & Owerbach, D. (2004). A M55V polymorphism in a novel SUMO gene (SUMO-4) differentially activates heat shock transcription factors and is associated with susceptibility to type I diabetes mellitus. *The Journal of Biological Chemistry*, *279*(26), 27233–27238. https://doi.org/10.1074/jbc.M402273200

Bokvist, K., Eliasson, L., Ammala, C., Renstrom, E., & Rorsman, P. (1995). Co-localization of L-type Ca2+ channels and insulin-containing secretory granules and its significance for the initiation of exocytosis in mouse pancreatic B-cells. *The EMBO Journal*, *14*(1), 50–57.

Borisovska, M. (2018). Syntaxins on granules promote docking of granules via interactions with munc18. *Scientific Reports*, *8*(1), 193. https://doi.org/10.1038/s41598-017-18597-z

Braschi, E., Zunino, R., & McBride, H. M. (2009). MAPL is a new mitochondrial SUMO E3 ligase that regulates mitochondrial fission. *EMBO Reports*, *10*(7), 748–754. https://doi.org/10.1038/embor.2009.86

Braun, M., Ramracheya, R., Bengtsson, M., Zhang, Q., Karanauskaite, J., Partridge, C., … Rorsman, P. (2008). Voltage-gated ion channels in human pancreatic beta-cells: electrophysiological characterization and role in insulin secretion. *Diabetes*, *57*(6), 1618–1628. https://doi.org/10.2337/db07-0991

Bruning, D., Reckers, K., Drain, P., & Rustenbeck, I. (2017). Glucose but not KCl diminishes submembrane granule turnover in mouse beta-cells. *Journal of Molecular Endocrinology*, *59*(3), 311–324. https://doi.org/10.1530/JME-17-0063

Brunton, T. L. (1874). Lectures on the Pathology and Treatment of Diabetes Mellitus. *British Medical Journal*, *1*(680), 39–41.

Calloway, N., Gouzer, G., Xue, M., & Ryan, T. A. (2015). The active-zone protein Munc13 controls the use-dependence of presynaptic voltage-gated calcium channels. *ELife*, *4*. https://doi.org/10.7554/eLife.07728

Casas, S., Novials, A., Reimann, F., Gomis, R., & Gribble, F. M. (2008). Calcium elevation in mouse pancreatic beta cells evoked by extracellular human islet amyloid polypeptide involves activation of the mechanosensitive ion channel TRPV4. *Diabetologia*, *51*(12), 2252–2262.

Catterall, W. A. (1986). Molecular Properties of Voltage-Sensitive Sodium Channels. *Annual Review of Biochemistry*, *55*(1), 953–985. https://doi.org/10.1146/annurev.bi.55.070186.004513

Cerda, O., & Trimmer, J. S. (2011). Activity-dependent phosphorylation of neuronal Kv2.1 potassium channels by CDK5. *The Journal of Biological Chemistry*, *286*(33), 28738–28748. https://doi.org/10.1074/jbc.M111.251942

Chang, K.-J., & Rasband, M. N. (2013). Excitable domains of myelinated nerves: axon initial segments and nodes of Ranvier. *Current Topics in Membranes*, *72*, 159–192. https://doi.org/10.1016/B978-0-12-417027-8.00005-2

Chatelain, F. C., Bichet, D., Douguet, D., Feliciangeli, S., Bendahhou, S., Reichold, M., … Lesage, F. (2012). TWIK1, a unique background channel with variable ion selectivity. *Proceedings of the National Academy of Sciences of the United States of America*, *109*(14), 5499–5504. https://doi.org/10.1073/pnas.1201132109

Cheng, K., Andrikopoulos, S., & E Gunton, J. (2013). First phase insulin secretion and type 2 diabetes. *Current Molecular Medicine*, *13*(1), 126–139.

Cho, N. H., Shaw, J. E., Karuranga, S., Huang, Y., da Rocha Fernandes, J. D., Ohlrogge, A. W., & Malanda, B. (2018). IDF Diabetes Atlas: Global estimates of diabetes prevalence for 2017 and projections for 2045. *Diabetes Research and Clinical Practice*, *138*, 271–281. https://doi.org/10.1016/j.diabres.2018.02.023

Christie, M. J., Adelman, J. P., Douglass, J., & North, R. A. (1989). Expression of a cloned rat brain potassium channel in Xenopus oocytes. *Science (New York, N.Y.)*, *244*(4901), 221–224.

Cobb, M. M., Austin, D. C., Sack, J. T., & Trimmer, J. S. (2015). Cell Cycle-dependent Changes in Localization and Phosphorylation of the Plasma Membrane Kv2.1 K+ Channel Impact Endoplasmic Reticulum Membrane Contact Sites in COS-1 Cells. *The Journal of Biological Chemistry*, *290*(49), 29189–29201. https://doi.org/10.1074/jbc.M115.690198

Collins, S. C., Hoppa, M. B., Walker, J. N., Amisten, S., Abdulkader, F., Bengtsson, M., …

Rorsman, P. (2010). Progression of diet-induced diabetes in C57BL6J mice involves functional dissociation of Ca2(+) channels from secretory vesicles. *Diabetes*, *59*(5), 1192–1201. https://doi.org/10.2337/db09-0791

Collins, S. C., Salehi, A., Eliasson, L., Olofsson, C. S., & Rorsman, P. (2008). Long-term exposure of mouse pancreatic islets to oleate or palmitate results in reduced glucose-induced somatostatin and oversecretion of glucagon. *Diabetologia*, *51*(9), 1689–1693. https://doi.org/10.1007/s00125-008-1082-0

Cook, D. L., & Hales, C. N. (1984). Intracellular ATP directly blocks K+ channels in pancreatic B-cells. *Nature*, *311*(5983), 271–273.

Cox, J. J., Reimann, F., Nicholas, A. K., Thornton, G., Roberts, E., Springell, K., … Raashid, Y. (2006). An SCN9A channelopathy causes congenital inability to experience pain. *Nature*, *444*(7121), 894.

Craig, T. J., Anderson, D., Evans, A. J., Girach, F., & Henley, J. M. (2015). SUMOylation of Syntaxin1A regulates presynaptic endocytosis. *Scientific Reports*, *5*, 17669.

Dadi, P. K., Vierra, N. C., & Jacobson, D. A. (2014). Pancreatic beta-cell-specific ablation of TASK-1 channels augments glucose-stimulated calcium entry and insulin secretion, improving glucose tolerance. *Endocrinology*, *155*(10), 3757–3768. https://doi.org/10.1210/en.2013-2051

Dai, X.-Q., Kolic, J., Marchi, P., Sipione, S., & MacDonald, P. E. (2009). SUMOylation regulates Kv2.1 and modulates pancreatic -cell excitability. *Journal of Cell Science*, *122*(6), 775–779. https://doi.org/10.1242/jcs.036632

Dai, X. Q., Manning Fox, J. E., Chikvashvili, D., Casimir, M., Plummer, G., Hajmrle, C., … MacDonald, P. E. (2012). The voltage-dependent potassium channel subunit Kv2.1 regulates insulin secretion from rodent and human islets independently of its electrical function. *Diabetologia*, *55*(6), 1709–1720. https://doi.org/10.1007/s00125-012-2512-6

Dai, X. Q., Plummer, G., Casimir, M., Kang, Y., Hajmrle, C., Gaisano, H. Y., … MacDonald, P. E. (2011). SUMOylation regulates insulin exocytosis downstream of secretory granule docking in rodents and humans. *Diabetes*, *60*(3), 838–847. https://doi.org/10.2337/db10-0440

Davies, A., Hendrich, J., Van Minh, A. T., Wratten, J., Douglas, L., & Dolphin, A. C. (2007). Functional biology of the alpha(2)delta subunits of voltage-gated calcium channels. *Trends in Pharmacological Sciences*, *28*(5), 220–228. https://doi.org/10.1016/j.tips.2007.03.005

De Vos, A., Heimberg, H., Quartier, E., Huypens, P., Bouwens, L., Pipeleers, D., & Schuit, F. (1995, November). Human and rat beta cells differ in glucose transporter but not in glucokinase gene expression. *Journal of Clinical Investigation*.

Dean, P. M., & Matthews, E. K. (1970). Glucose-induced electrical activity in pancreatic islet cells. *The Journal of Physiology*, *210*(2), 255–264.

DEAN, P. M., & MATTHEWS, E. K. (1968). Electrical Activity in Pancreatic Islet Cells. *Nature*, *219*, 389. Retrieved from http://dx.doi.org/10.1038/219389a0

Delgado-Ramirez, M., De Jesus-Perez, J. J., Arechiga-Figueroa, I. A., Arreola, J., Adney, S. K., Villalba-Galea, C. A., … Rodriguez-Menchaca, A. A. (2018). Regulation of Kv2.1 channel inactivation by phosphatidylinositol 4,5-bisphosphate. *Scientific Reports*, *8*(1), 1769. https://doi.org/10.1038/s41598-018-20280-w

Deutsch, E., Weigel, A. V, Akin, E. J., Fox, P., Hansen, G., Haberkorn, C. J., … Tamkun, M. M. (2012). Kv2.1 cell surface clusters are insertion platforms for ion channel delivery to the plasma membrane. *Molecular Biology of the Cell*, *23*(15), 2917–2929.

https://doi.org/10.1091/mbc.E12-01-0047
Dorrell, C., Schug, J., Canaday, P. S., Russ, H. A., Tarlow, B. D., Grompe, M. T., … Grompe, M. (2016). Human islets contain four distinct subtypes of beta cells. *Nature Communications*, *7*, 11756. https://doi.org/10.1038/ncomms11756
Dresbach, T., Fejtová, A., & Gundelfinger, E. D. (2006). Assembly of Presynaptic Active Zones. In A. Dityatev & A. El-Husseini (Eds.), *Molecular Mechanisms of Synaptogenesis* (pp. 235–245). Boston, MA: Springer US. https://doi.org/10.1007/978-0-387-32562-0_17
Drews, G., Krippeit-Drews, P., & Dufer, M. (2010). Electrophysiology of islet cells. *Advances in Experimental Medicine and Biology*, *654*, 115–163. https://doi.org/10.1007/978-90-481-3271-3_7
Drucker, D. J. (2007). The role of gut hormones in glucose homeostasis. *The Journal of Clinical Investigation*, *117*(1), 24–32. https://doi.org/10.1172/JCI30076
Du, J., Tao-Cheng, J. H., Zerfas, P., & McBain, C. J. (1998). The K+ channel, Kv2.1, is apposed to astrocytic processes and is associated with inhibitory postsynaptic membranes in hippocampal and cortical principal neurons and inhibitory interneurons. *Neuroscience*, *84*(1), 37–48.
Dufer, M., Gier, B., Wolpers, D., Krippeit-Drews, P., Ruth, P., & Drews, G. (2009). Enhanced glucose tolerance by SK4 channel inhibition in pancreatic beta-cells. *Diabetes*, *58*(8), 1835–1843. https://doi.org/10.2337/db08-1324
Dufer, M., Neye, Y., Horth, K., Krippeit-Drews, P., Hennige, A., Widmer, H., … Drews, G. (2011). BK channels affect glucose homeostasis and cell viability of murine pancreatic beta cells. *Diabetologia*, *54*(2), 423–432. https://doi.org/10.1007/s00125-010-1936-0
Duman, J. G., & Forte, J. G. (2003). What is the role of SNARE proteins in membrane fusion? *American Journal of Physiology. Cell Physiology*, *285*(2), C237-49. https://doi.org/10.1152/ajpcell.00091.2003
Dundr, M., Ospina, J. K., Sung, M.-H., John, S., Upender, M., Ried, T., … Matera, A. G. (2007). Actin-dependent intranuclear repositioning of an active gene locus in vivo. *The Journal of Cell Biology*, *179*(6), 1095–1103. https://doi.org/10.1083/jcb.200710058
Feligioni, M., Nishimune, A., & Henley, J. M. (2009, April). Protein SUMOylation modulates calcium influx and glutamate release from presynaptic terminals. *The European Journal of Neuroscience*. https://doi.org/10.1111/j.1460-9568.2009.06692.x
Ferdaoussi, M., Dai, X., Jensen, M. V, Wang, R., Peterson, B. S., Huang, C., … MacDonald, P. E. (2015). Isocitrate-to-SENP1 signaling amplifies insulin secretion and rescues dysfunctional beta cells. *The Journal of Clinical Investigation*, *125*(10), 3847–3860. https://doi.org/10.1172/JCI82498
Ferdaoussi, M., Fu, J., Dai, X., Manning Fox, J. E., Suzuki, K., Smith, N., … MacDonald, P. E. (2017). SUMOylation and calcium control syntaxin-1A and secretagogin sequestration by tomosyn to regulate insulin exocytosis in human ß cells. *Scientific Reports*, *7*(1), 1–9. https://doi.org/10.1038/s41598-017-00344-z
Ferdaoussi, M., & MacDonald, P. E. (2017). Toward Connecting Metabolism to the Exocytotic Site. *Trends in Cell Biology*, *27*(3), 163–171. https://doi.org/10.1016/j.tcb.2016.10.003
Ferrer, J., Wasson, J., Salkoff, L., & Permutt, M. A. (1996). Cloning of human pancreatic islet large conductance Ca(2+)-activated K+ channel (hSlo) cDNAs: evidence for high levels of expression in pancreatic islets and identification of a flanking genetic marker. *Diabetologia*, *39*(8), 891–898.
Festa, A., D'Agostino, R., Hanley, A. J. G., Karter, A. J., Saad, M. F., & Haffner, S. M. (2004).

Differences in insulin resistance in nondiabetic subjects with isolated impaired glucose tolerance or isolated impaired fasting glucose. *Diabetes*, *53*(6), 1549–1555.
Flotho, A., & Melchior, F. (2013). Sumoylation: a regulatory protein modification in health and disease. *Annual Review of Biochemistry*, *82*, 357–385.
Fox, P. D., Haberkorn, C. J., Akin, E. J., Seel, P. J., Krapf, D., & Tamkun, M. M. (2015). Induction of stable ER-plasma-membrane junctions by Kv2.1 potassium channels. *Journal of Cell Science*, *128*(11), 2096–2105. https://doi.org/10.1242/jcs.166009
Fox, P. D., Haberkorn, C. J., Weigel, A. V, Higgins, J. L., Akin, E. J., Kennedy, M. J., … Tamkun, M. M. (2013). Plasma membrane domains enriched in cortical endoplasmic reticulum function as membrane protein trafficking hubs. *Molecular Biology of the Cell*, *24*(17), 2703–2713. https://doi.org/10.1091/mbc.E12-12-0895
Fox, P. D., Loftus, R. J., & Tamkun, M. M. (2013). Regulation of Kv2.1 K(+) conductance by cell surface channel density. *The Journal of Neuroscience : The Official Journal of the Society for Neuroscience*, *33*(3), 1259–1270. https://doi.org/10.1523/JNEUROSCI.3008-12.2013
Franzini-Armstrong, C., Protasi, F., & Tijskens, P. (2005). The assembly of calcium release units in cardiac muscle. *Annals of the New York Academy of Sciences*, *1047*, 76–85. https://doi.org/10.1196/annals.1341.007
Freeman, S. A., Desmazieres, A., Fricker, D., Lubetzki, C., & Sol-Foulon, N. (2016). Mechanisms of sodium channel clustering and its influence on axonal impulse conduction. *Cellular and Molecular Life Sciences : CMLS*, *73*(4), 723–735. https://doi.org/10.1007/s00018-015-2081-1
Fu, J., Dai, X., Plummer, G., Suzuki, K., Bautista, A., Githaka, J. M., … MacDonald, P. E. (2017). Kv2.1 Clustering Contributes to Insulin Exocytosis and Rescues Human beta-Cell Dysfunction. *Diabetes*, *66*(7), 1890–1900. https://doi.org/10.2337/db16-1170
Fukumoto, H., Seino, S., Imura, H., Seino, Y., Eddy, R. L., Fukushima, Y., … Bell, G. I. (1988, August). Sequence, tissue distribution, and chromosomal localization of mRNA encoding a human glucose transporter-like protein. *Proceedings of the National Academy of Sciences of the United States of America*.
Gaisano, H. Y. (2014). Here come the newcomer granules, better late than never. *Trends in Endocrinology and Metabolism: TEM*, *25*(8), 381–388. https://doi.org/10.1016/j.tem.2014.03.005
Gaisano, H. Y. (2017). Recent new insights into the role of SNARE and associated proteins in insulin granule exocytosis. *Diabetes, Obesity & Metabolism*, *19 Suppl 1*, 115–123. https://doi.org/10.1111/dom.13001
Gandasi, N. R., & Barg, S. (2014). Contact-induced clustering of syntaxin and munc18 docks secretory granules at the exocytosis site. *Nature Communications*, *5*(May), 1–14. https://doi.org/10.1038/ncomms4914
Gandasi, N. R., Yin, P., Omar-Hmeadi, M., Ottosson Laakso, E., Vikman, P., & Barg, S. (2018). Glucose-Dependent Granule Docking Limits Insulin Secretion and Is Decreased in Human Type 2 Diabetes. *Cell Metabolism*, *27*(2), 470–478.e4. https://doi.org/10.1016/j.cmet.2017.12.017
Gandasi, N. R., Yin, P., Riz, M., Chibalina, M. V, Cortese, G., Lund, P.-E., … Barg, S. (2017, June). Ca(2+) channel clustering with insulin-containing granules is disturbed in type 2 diabetes. *The Journal of Clinical Investigation*. https://doi.org/10.1172/JCI88491
Garcia-Parajo, M. F., Cambi, A., Torreno-Pina, J. A., Thompson, N., & Jacobson, K. (2014).

Nanoclustering as a dominant feature of plasma membrane organization. *Journal of Cell Science*, *127*(Pt 23), 4995–5005. https://doi.org/10.1242/jcs.146340
Gerich, J. E. (2002). Is Reduced First-Phase Insulin Release the Earliest Detectable Abnormality in Individuals Destined to Develop Type 2 Diabetes? *Diabetes*, *51*(suppl 1), S117 LP-S121. Retrieved from http://diabetes.diabetesjournals.org/content/51/suppl_1/S117.abstract
Githaka, J. M., Vega, A. R., Baird, M. A., Davidson, M. W., Jaqaman, K., & Touret, N. (2016). Ligand-induced growth and compaction of CD36 nanoclusters enriched in Fyn induces Fyn signaling. *Journal of Cell Science*, *129*(22), 4175–4189. https://doi.org/10.1242/jcs.188946
Godazgar, M., Zhang, Q., Chibalina, M. V, & Rorsman, P. (2018, May). Biphasic voltage-dependent inactivation of human Na(V)1.3, 1.6 and 1.7 Na(+) channels expressed in rodent insulin-secreting cells. *The Journal of Physiology*. https://doi.org/10.1113/JP275587
Gong, L., & Yeh, E. T. H. (2006). Characterization of a family of nucleolar SUMO-specific proteases with preference for SUMO-2 or SUMO-3. *The Journal of Biological Chemistry*, *281*(23), 15869–15877. https://doi.org/10.1074/jbc.M511658200
Gooding, J. R., Jensen, M. V, Dai, X., Wenner, B. R., Lu, D., Arumugam, R., … Newgard, C. B. (2015). Adenylosuccinate Is an Insulin Secretagogue Derived from Glucose-Induced Purine Metabolism. *Cell Reports*, *13*(1), 157–167. https://doi.org/10.1016/j.celrep.2015.08.072
Greitzer-Antes, D., Xie, L., Qin, T., Xie, H., Zhu, D., Dolai, S., … He, Y. (2018). Kv2. 1 clusters on β-cell plasma membrane act as reservoirs that replenish pools of newcomer insulin granule through their interaction with syntaxin-3. *Journal of Biological Chemistry*, jbc-RA118.
Gromada, J., Hoy, M., Renstrom, E., Bokvist, K., Eliasson, L., Gopel, S., & Rorsman, P. (1999). CaM kinase II-dependent mobilization of secretory granules underlies acetylcholine-induced stimulation of exocytosis in mouse pancreatic B-cells. *The Journal of Physiology*, *518 (Pt 3*, 745–759.
Gutman, G. A., Chandy, K. G., Grissmer, S., Lazdunski, M., Mckinnon, D., Pardo, L. A., … Wang, X. (2005). International Union of Pharmacology. LIII. Nomenclature and Molecular Relationships of Voltage-Gated Potassium Channels. *Pharmacological Reviews*, *57*(4), 473 LP-508. Retrieved from http://pharmrev.aspetjournals.org/content/57/4/473.abstract
Hanefeld, M., Koehler, C., Fuecker, K., Henkel, E., Schaper, F., & Temelkova-Kurktschiev, T. (2003). Insulin secretion and insulin sensitivity pattern is different in isolated impaired glucose tolerance and impaired fasting glucose: the risk factor in Impaired Glucose Tolerance for Atherosclerosis and Diabetes study. *Diabetes Care*, *26*(3), 868–874.
Hardy, A. B., Fox, J. E. M., Giglou, P. R., Wijesekara, N., Bhattacharjee, A., Sultan, S., … Wheeler, M. B. (2009). Characterization of Erg K+ channels in alpha- and beta-cells of mouse and human islets. *The Journal of Biological Chemistry*, *284*(44), 30441–30452. https://doi.org/10.1074/jbc.M109.040659
He, L., & Wu, L.-G. (2007). The debate on the kiss-and-run fusion at synapses. *Trends in Neurosciences*, *30*(9), 447–455. https://doi.org/10.1016/j.tins.2007.06.012
He, X., Lai, Q., Chen, C., Li, N., Sun, F., Huang, W., … Wang, C.-Y. (2018). Both conditional ablation and overexpression of E2 SUMO-conjugating enzyme (UBC9) in mouse pancreatic beta cells result in impaired beta cell function. *Diabetologia*, *61*(4), 881–895. https://doi.org/10.1007/s00125-017-4523-9
Heaslip, A. T., Nelson, S. R., Lombardo, A. T., Beck Previs, S., Armstrong, J., & Warshaw, D. M. (2014). Cytoskeletal Dependence of Insulin Granule Movement Dynamics in INS-1 Beta-Cells in Response to Glucose. *PLOS ONE*, *9*(10), e109082. Retrieved from

https://doi.org/10.1371/journal.pone.0109082
HELLMAN, B. (1959). The numerical distribution of the islets of Langerhans at different ages of the rat. *Acta Endocrinologica*, *32*, 63–77.
Henquin, J. C. (1977). Tetraethylammonium potentiation of insulin release and inhibition of rubidium efflux in pancreatic islets. *Biochemical and Biophysical Research Communications*, *77*(2), 551–556.
Henquin, J. C., Meissner, H. P., & Preissler, M. (1979). 9-Aminoacridine- and tetraethylammonium-induced reduction of the potassium permeability in pancreatic B-cells. Effects on insulin release and electrical properties. *Biochimica et Biophysica Acta*, *587*(4), 579–592.
Herrington, J., Sanchez, M., Wunderler, D., Yan, L., Bugianesi, R. M., Dick, I. E., … McManus, O. B. (2005). Biophysical and pharmacological properties of the voltage-gated potassium current of human pancreatic beta-cells. *The Journal of Physiology*, *567*(Pt 1), 159–175. https://doi.org/10.1113/jphysiol.2005.089375
Hodgkin, A. L., & Huxley, A. F. (1952, August). A quantitative description of membrane current and its application to conduction and excitation in nerve. *The Journal of Physiology*.
Hohmeier, H. E., & Newgard, C. B. (2004). Cell lines derived from pancreatic islets. *Molecular and Cellular Endocrinology*, *228*(1–2), 121–128. https://doi.org/10.1016/j.mce.2004.04.017
Hoppa, M. B., Collins, S., Ramracheya, R., Hodson, L., Amisten, S., Zhang, Q., … Rorsman, P. (2009). Chronic palmitate exposure inhibits insulin secretion by dissociation of Ca(2+) channels from secretory granules. *Cell Metabolism*, *10*(6), 455–465. https://doi.org/10.1016/j.cmet.2009.09.011
Hoppa, M. B., Jones, E., Karanauskaite, J., Ramracheya, R., Braun, M., Collins, S. C., … Genoud, C. (2012). Multivesicular exocytosis in rat pancreatic beta cells. *Diabetologia*, *55*(4), 1001–1012.
In't Veld, P., & Marichal, M. (2010). Microscopic anatomy of the human islet of Langerhans. *Advances in Experimental Medicine and Biology*, *654*, 1–19. https://doi.org/10.1007/978-90-481-3271-3_1
Ionescu-Tirgoviste, C., Gagniuc, P. A., Gubceac, E., Mardare, L., Popescu, I., Dima, S., & Militaru, M. (2015). A 3D map of the islet routes throughout the healthy human pancreas. *Scientific Reports*, *5*, 14634. https://doi.org/10.1038/srep14634
Isom, L. L., De Jongh, K. S., Patton, D. E., Reber, B. F., Offord, J., Charbonneau, H., … Catterall, W. A. (1992). Primary structure and functional expression of the beta 1 subunit of the rat brain sodium channel. *Science (New York, N.Y.)*, *256*(5058), 839–842.
Jacobson, D. A., Kuznetsov, A., Lopez, J. P., Kash, S., Ammala, C. E., & Philipson, L. H. (2007). Kv2.1 ablation alters glucose-induced islet electrical activity, enhancing insulin secretion. *Cell Metabolism*, *6*(3), 229–235. https://doi.org/10.1016/j.cmet.2007.07.010
Jacobson, D. A., Mendez, F., Thompson, M., Torres, J., Cochet, O., & Philipson, L. H. (2010). Calcium-activated and voltage-gated potassium channels of the pancreatic islet impart distinct and complementary roles during secretagogue induced electrical responses. *The Journal of Physiology*, *588*(Pt 18), 3525–3537. https://doi.org/10.1113/jphysiol.2010.190207
Jacobson, D. A., & Philipson, L. H. (2007). Action potentials and insulin secretion: new insights into the role of Kv channels. *Diabetes, Obesity & Metabolism*, *9 Suppl 2*, 89–98. https://doi.org/10.1111/j.1463-1326.2007.00784.x
Jacobson, K., Mouritsen, O. G., & Anderson, R. G. W. (2007). Lipid rafts: at a crossroad

between cell biology and physics. *Nature Cell Biology*, *9*(1), 7.
Jaqaman, K., Loerke, D., Mettlen, M., Kuwata, H., Grinstein, S., Schmid, S. L., & Danuser, G. (2008). Robust single-particle tracking in live-cell time-lapse sequences. *Nature Methods*, *5*(8), 695–702. https://doi.org/10.1038/nmeth.1237
Jensen, M. V, Haldeman, J. M., Zhang, H., Lu, D., Huising, M. O., Vale, W. W., … Newgard, C. B. (2013). Control of voltage-gated potassium channel Kv2.2 expression by pyruvate-isocitrate cycling regulates glucose-stimulated insulin secretion. *The Journal of Biological Chemistry*, *288*(32), 23128–23140. https://doi.org/10.1074/jbc.M113.491654
Johnson, B., Leek, A. N., Solé, L., Maverick, E. E., Levine, T. P., & Tamkun, M. M. (2018). Kv2 potassium channels form endoplasmic reticulum/plasma membrane junctions via interaction with VAPA and VAPB. *Proceedings of the National Academy of Sciences*. Retrieved from http://www.pnas.org/content/early/2018/06/22/1805757115.abstract
Johnston, N. R., Mitchell, R. K., Haythorne, E., Pessoa, M. P., Semplici, F., Ferrer, J., … Hodson, D. J. (2016). Beta Cell Hubs Dictate Pancreatic Islet Responses to Glucose. *Cell Metabolism*, *24*(3), 389–401. https://doi.org/10.1016/j.cmet.2016.06.020
Kahn, S. E., Cooper, M. E., & Del Prato, S. (2014). Pathophysiology and treatment of type 2 diabetes: perspectives on the past, present, and future. *Lancet (London, England)*, *383*(9922), 1068–1083. https://doi.org/10.1016/S0140-6736(13)62154-6
Kamb, A., Tseng-Crank, J., & Tanouye, M. A. (1988). Multiple products of the Drosophila Shaker gene may contribute to potassium channel diversity. *Neuron*, *1*(5), 421–430.
Kampmann, U., Madsen, L. R., Skajaa, G. O., Iversen, D. S., Moeller, N., & Ovesen, P. (2015, July). Gestational diabetes: A clinical update. *World Journal of Diabetes*. https://doi.org/10.4239/wjd.v6.i8.1065
Kasimova, M. A., Granata, D., & Carnevale, V. (2016). Voltage-Gated Sodium Channels: Evolutionary History and Distinctive Sequence Features. *Current Topics in Membranes*, *78*, 261–286. https://doi.org/10.1016/bs.ctm.2016.05.002
Kelly, R. P., Sutton, R., & Ashcroft, F. M. (1991). Voltage-activated calcium and potassium currents in human pancreatic beta-cells. *The Journal of Physiology*, *443*(1), 175–192.
Kim, A., Miller, K., Jo, J., Kilimnik, G., Wojcik, P., & Hara, M. (2009). Islet architecture: A comparative study. *Islets*, *1*(2), 129–136. https://doi.org/10.4161/isl.1.2.9480
Kimball, C. P., & Murlin, J. R. (1923). Aqueous extracts of pancreas III. Some precipitation reactions of insulin. *Journal of Biological Chemistry*, *58*(1), 337–346.
Kishi, A., Nakamura, T., Nishio, Y., Maegawa, H., & Kashiwagi, A. (2003). Sumoylation of Pdx1 is associated with its nuclear localization and insulin gene activation. *American Journal of Physiology. Endocrinology and Metabolism*, *284*(4), E830-40. https://doi.org/10.1152/ajpendo.00390.2002
Klein, O., Roded, A., Zur, N., Azouz, N. P., Pasternak, O., Hirschberg, K., … Fukuda, M. (2017). Rab5 is critical for SNAP23 regulated granule-granule fusion during compound exocytosis. *Scientific Reports*, *7*(1), 15315.
Kolic, J., & Johnson, J. D. (2016). Specialized Hub Beta Cells Trade Maximal Insulin Production for Perfect Timing. *Cell Metabolism*, *24*(3), 371–373. https://doi.org/10.1016/j.cmet.2016.08.022
Korade, Z., & Kenworthy, A. K. (2008). Lipid rafts, cholesterol, and the brain. *Neuropharmacology*, *55*(8), 1265–1273.
Kozakov, D., Hall, D. R., Xia, B., Porter, K. A., Padhorny, D., Yueh, C., … Vajda, S. (2017). The ClusPro web server for protein-protein docking. *Nature Protocols*, *12*(2), 255–278.

https://doi.org/10.1038/nprot.2016.169
Kruse, M., Schulze-Bahr, E., Corfield, V., Beckmann, A., Stallmeyer, B., Kurtbay, G., … Pongs, O. (2009). Impaired endocytosis of the ion channel TRPM4 is associated with human progressive familial heart block type I. *The Journal of Clinical Investigation*, *119*(9), 2737–2744. https://doi.org/10.1172/JCI38292
Kwan, E. P., & Gaisano, H. Y. (2005). Glucagon-like peptide 1 regulates sequential and compound exocytosis in pancreatic islet β-cells. *Diabetes*, *54*(9), 2734–2743.
Lacy, P., & Eitzen, G. (2008). Control of granule exocytosis in neutrophils. *Frontiers in Bioscience : A Journal and Virtual Library*, *13*, 5559–5570.
Larsson, H. P., Baker, O. S., Dhillon, D. S., & Isacoff, E. Y. (1996). Transmembrane movement of the shaker K+ channel S4. *Neuron*, *16*(2), 387–397.
Leung, Y. M., Kang, Y., Gao, X., Xia, F., Xie, H., Sheu, L., … Gaisano, H. Y. (2003). Syntaxin 1A binds to the cytoplasmic C terminus of Kv2.1 to regulate channel gating and trafficking. *The Journal of Biological Chemistry*, *278*(19), 17532–17538. https://doi.org/10.1074/jbc.M213088200
Leung, Y. M., Kwan, E. P., Ng, B., Kang, Y., & Gaisano, H. Y. (2007). SNAREing voltage-gated K+ and ATP-sensitive K+ channels: tuning beta-cell excitability with syntaxin-1A and other exocytotic proteins. *Endocrine Reviews*, *28*(6), 653–663. https://doi.org/10.1210/er.2007-0010
Li, M. (2015). Role of T-Type Ca2+ Channels in Basal Insulin Release. In S. W. Schaffer & M. Li (Eds.), *T-type Calcium Channels in Basic and Clinical Science* (pp. 137–150). Vienna: Springer Vienna. https://doi.org/10.1007/978-3-7091-1413-1_10
Li, M., Guo, D., Isales, C. M., Eizirik, D. L., Atkinson, M., She, J.-X., & Wang, C.-Y. (2005). SUMO wrestling with type 1 diabetes. *Journal of Molecular Medicine*, *83*(7), 504–513.
Li, X. N., Herrington, J., Petrov, A., Ge, L., Eiermann, G., Xiong, Y., … Zhou, Y.-P. (2013). The role of voltage-gated potassium channels Kv2.1 and Kv2.2 in the regulation of insulin and somatostatin release from pancreatic islets. *The Journal of Pharmacology and Experimental Therapeutics*, *344*(2), 407–416. https://doi.org/10.1124/jpet.112.199083
Liang, T., Qin, T., Xie, L., Dolai, S., Zhu, D., Prentice, K. J., … Gaisano, H. Y. (2017). New roles of syntaxin-1A in insulin granule exocytosis and replenishment. *Journal of Biological Chemistry*, *292*(6), 2203–2216.
Lim, S. T., Antonucci, D. E., Scannevin, R. H., & Trimmer, J. S. (2000). A novel targeting signal for proximal clustering of the Kv2.1 K+ channel in hippocampal neurons. *Neuron*, *25*(2), 385–397.
Liu, Y., Holmgren, M., Jurman, M. E., & Yellen, G. (1997). Gated access to the pore of a voltage-dependent K+ channel. *Neuron*, *19*(1), 175–184.
Lori, F., Dafna, S.-L., Uri, A., & Ilana, L. (2009). Voltage-gated Potassium Channel as a Facilitator of Exocytosis. *Annals of the New York Academy of Sciences*, *1152*(1), 87–92. https://doi.org/10.1111/j.1749-6632.2008.03997.x
Low, J. T., Zavortink, M., Mitchell, J. M., Gan, W. J., Do, O. H., Schwiening, C. J., … Thorn, P. (2014). Insulin secretion from beta cells in intact mouse islets is targeted towards the vasculature. *Diabetologia*, *57*(8), 1655–1663. https://doi.org/10.1007/s00125-014-3252-6
Lvov, A., Greitzer, D., Berlin, S., Chikvashvili, D., Tsuk, S., Lotan, I., & Michaelevski, I. (2009). Rearrangements in the relative orientation of cytoplasmic domains induced by a membrane-anchored protein mediate modulations in Kv channel gating. *The Journal of Biological Chemistry*, *284*(41), 28276–28291. https://doi.org/10.1074/jbc.M109.028761

Lyon, J., Manning Fox, J. E., Spigelman, A. F., Kim, R., Smith, N., O'Gorman, D., … MacDonald, P. E. (2016). Research-focused isolation of human islets from donors with and without diabetes at the Alberta Diabetes Institute IsletCore. *Endocrinology*, *157*(2), 560–569. https://doi.org/10.1210/en.2015-1562

MacDonald, P. E. (2011). Signal integration at the level of ion channel and exocytotic function in pancreatic beta-cells. *American Journal of Physiology. Endocrinology and Metabolism*, *301*(6), E1065-9. https://doi.org/10.1152/ajpendo.00426.2011

MacDonald, P. E. (2014). Controlling insulin secretion: An exciting TASK. *Endocrinology*, *155*(10), 3729–3731. https://doi.org/10.1210/en.2014-1667

MacDonald, P. E. (2018). A post-translational balancing act: the good and the bad of SUMOylation in pancreatic islets. *Diabetologia*, *61*(4), 775–779. https://doi.org/10.1007/s00125-017-4543-5

MacDonald, P. E., Braun, M., Galvanovskis, J., & Rorsman, P. (2006). Release of small transmitters through kiss-and-run fusion pores in rat pancreatic beta cells. *Cell Metabolism*, *4*(4), 283–290. https://doi.org/10.1016/j.cmet.2006.08.011

MacDonald, P. E., Ha, X. F., Wang, J., Smukler, S. R., Sun, A. M., Gaisano, H. Y., … Wheeler, M. B. (2001). Members of the Kv1 and Kv2 Voltage-Dependent K^+ Channel Families Regulate Insulin Secretion. *Molecular Endocrinology*, *15*(8), 1423–1435. https://doi.org/10.1210/mend.15.8.0685

MacDonald, P. E., Joseph, J. W., & Rorsman, P. (2005). Glucose-sensing mechanisms in pancreatic -cells. *Philosophical Transactions of the Royal Society B: Biological Sciences*, *360*(1464), 2211–2225. https://doi.org/10.1098/rstb.2005.1762

MacDonald, P. E., Salapatek, A. M. F., & Wheeler, M. B. (2003). Temperature and redox state dependence of native Kv2.1 currents in rat pancreatic β-cells. *The Journal of Physiology*, *546*(3), 647–653. https://doi.org/10.1113/jphysiol.2002.035709

MacDonald, P. E., Sewing, S., Wang, J., Joseph, J. W., Smukler, S. R., Sakellaropoulos, G., … Wheeler, M. B. (2002). Inhibition of Kv2.1 voltage-dependent K+ channels in pancreatic beta-cells enhances glucose-dependent insulin secretion. *The Journal of Biological Chemistry*, *277*(47), 44938–44945. https://doi.org/10.1074/jbc.M205532200

MacDonald, P. E., Wang, G., Tsuk, S., Dodo, C., Kang, Y., Tang, L., … Gaisano, H. Y. (2002). Synaptosome-associated protein of 25 kilodaltons modulates Kv2.1 voltage-dependent K(+) channels in neuroendocrine islet beta-cells through an interaction with the channel N terminus. *Molecular Endocrinology (Baltimore, Md.)*, *16*(11), 2452–2461. https://doi.org/10.1210/me.2002-0058

Mahajan, R., Gerace, L., & Melchior, F. (1998, January). Molecular Characterization of the SUMO-1 Modification of RanGAP1 and Its Role in Nuclear Envelope Association . *The Journal of Cell Biology*.

Mandikian, D., Bocksteins, E., Parajuli, L. K., Bishop, H. I., Cerda, O., Shigemoto, R., & Trimmer, J. S. (2014). Cell type-specific spatial and functional coupling between mammalian brain Kv2.1 K+ channels and ryanodine receptors. *The Journal of Comparative Neurology*, *522*(15), 3555–3574. https://doi.org/10.1002/cne.23641

Mandikian, D., Cerda, O., Sack, J. T., & Trimmer, J. S. (2011). A SUMO-Phospho tag team for wrestling with potassium channel gating. *The Journal of General Physiology*, *137*(5), 435–439. https://doi.org/10.1085/jgp.201110648

Manning Fox, J. E., Hajmrle, C., & Macdonald, P. E. (2012). Novel roles of SUMO in pancreatic beta-cells: thinking outside the nucleus. *Canadian Journal of Physiology and*

Pharmacology, *90*(6), 765–770. https://doi.org/10.1139/y11-134
Matthews, E. K., & Sakamoto, Y. (1975). Electrical characteristics of pancreatic islet cells. *The Journal of Physiology*, *246*(2), 421–437.
McCoy, J. G., & Nimigean, C. M. (2012). Structural correlates of selectivity and inactivation in potassium channels. *Biochimica et Biophysica Acta*, *1818*(2), 272–285. https://doi.org/10.1016/j.bbamem.2011.09.007
Meglasson, M. D., & Matschinsky, F. M. (1984). New perspectives on pancreatic islet glucokinase. *The American Journal of Physiology*, *246*(1 Pt 1), E1-13. https://doi.org/10.1152/ajpendo.1984.246.1.E1
Meissner, H. P., Henquin, J. C., & Preissler, M. (1978). Potassium dependence of the membrane potential of pancreatic B-cells. *FEBS Letters*, *94*(1), 87–89.
Meissner, H. P., & Schmelz, H. (1974). Membrane potential of beta-cells in pancreatic islets. *Pflugers Archiv : European Journal of Physiology*, *351*(3), 195–206.
Melchior, F., Schergaut, M., & Pichler, A. (2003). SUMO: ligases, isopeptidases and nuclear pores. *Trends in Biochemical Sciences*, *28*(11), 612–618. https://doi.org/10.1016/j.tibs.2003.09.002
Menting, J. G., Yang, Y., Chan, S. J., Phillips, N. B., Smith, B. J., Whittaker, J., … Lawrence, M. C. (2014). Protective hinge in insulin opens to enable its receptor engagement. *Proceedings of the National Academy of Sciences*, *111*(33), E3395 LP-E3404. Retrieved from http://www.pnas.org/content/111/33/E3395.abstract
Michaelevski, I., Chikvashvili, D., Tsuk, S., Singer-Lahat, D., Kang, Y., Linial, M., … Lotan, I. (2003). Direct interaction of target SNAREs with the Kv2.1 channel. Modal regulation of channel activation and inactivation gating. *The Journal of Biological Chemistry*, *278*(36), 34320–34330. https://doi.org/10.1074/jbc.M304943200
Milner, R. D., & Hales, C. N. (1967). The role of calcium and magnesium in insulin secretion from rabbit pancreas studied in vitro. *Diabetologia*, *3*(1), 47–49.
Misonou, H., Mohapatra, D. P., Menegola, M., & Trimmer, J. S. (2005). Calcium- and metabolic state-dependent modulation of the voltage-dependent Kv2.1 channel regulates neuronal excitability in response to ischemia. *The Journal of Neuroscience : The Official Journal of the Society for Neuroscience*, *25*(48), 11184–11193. https://doi.org/10.1523/JNEUROSCI.3370-05.2005
Motulsky, H. J., & Brown, R. E. (2006). Detecting outliers when fitting data with nonlinear regression - a new method based on robust nonlinear regression and the false discovery rate. *BMC Bioinformatics*, *7*, 123. https://doi.org/10.1186/1471-2105-7-123
Murray, D. H., & Tamm, L. K. (2009). Clustering of syntaxin-1A in model membranes is modulated by phosphatidylinositol 4,5-bisphosphate and cholesterol. *Biochemistry*, *48*(21), 4617–4625. https://doi.org/10.1021/bi9003217
Mustfa, S. A., Singh, M., Suhail, A., Mohapatra, G., Verma, S., Chakravorty, D., … Srikanth, C. V. (2017). SUMOylation pathway alteration coupled with downregulation of SUMO E2 enzyme at mucosal epithelium modulates inflammation in inflammatory bowel disease. *Open Biology*, *7*(6). Retrieved from http://rsob.royalsocietypublishing.org/content/7/6/170024.abstract
Noda, M., Shimizu, S., Tanabe, T., Takai, T., Kayano, T., Ikeda, T., … Minamino, N. (1984). Primary structure of Electrophorus electricus sodium channel deduced from cDNA sequence. *Nature*, *312*(5990), 121–127.
Noma, A. (1983). ATP-regulated K+ channels in cardiac muscle. *Nature*, *305*, 147. Retrieved

from http://dx.doi.org/10.1038/305147a0
O'Connell, K. M. S., Loftus, R., & Tamkun, M. M. (2010). Localization-dependent activity of the Kv2.1 delayed-rectifier K+ channel. *Proceedings of the National Academy of Sciences of the United States of America*, *107*(27), 12351–12356. https://doi.org/10.1073/pnas.1003028107
O'Connor, M. D., Landahl, H., & Grodsky, G. M. (1980). Comparison of storage- and signal-limited models of pancreatic insulin secretion. *The American Journal of Physiology*, *238*(5), R378-89. https://doi.org/10.1152/ajpregu.1980.238.5.R378
Ohara-Imaizumi, M., Nakamichi, Y., Tanaka, T., Ishida, H., & Nagamatsu, S. (2002). Imaging exocytosis of single insulin secretory granules with evanescent wave microscopy: distinct behavior of granule motion in biphasic insulin release. *The Journal of Biological Chemistry*, *277*(6), 3805–3808. https://doi.org/10.1074/jbc.C100712200
Ohara-Imaizumi, M., Nishiwaki, C., Nakamichi, Y., Kikuta, T., Nagai, S., & Nagamatsu, S. (2004). Correlation of syntaxin-1 and SNAP-25 clusters with docking and fusion of insulin granules analysed by total internal reflection fluorescence microscopy. *Diabetologia*, *47*(12), 2200–2207. https://doi.org/10.1007/s00125-004-1579-0
Ohara-Imaizumi, M., Ohtsuka, T., Matsushima, S., Akimoto, Y., Nishiwaki, C., Nakamichi, Y., … Nagamatsu, S. (2005). ELKS, a protein structurally related to the active zone-associated protein CAST, is expressed in pancreatic beta cells and functions in insulin exocytosis: interaction of ELKS with exocytotic machinery analyzed by total internal reflection fluorescence m. *Molecular Biology of the Cell*, *16*(7), 3289–3300. https://doi.org/10.1091/mbc.e04-09-0816
Omann, G. M., & Axelrod, D. (1996). Membrane-proximal calcium transients in stimulated neutrophils detected by total internal reflection fluorescence. *Biophysical Journal*, *71*(5), 2885–2891. https://doi.org/10.1016/S0006-3495(96)79485-7
Orskov, F., & Orskov, I. (1992). Escherichia coli serotyping and disease in man and animals. *Canadian Journal of Microbiology*, *38*(7), 699–704.
Ostenson, C.-G., Gaisano, H., Sheu, L., Tibell, A., & Bartfai, T. (2006). Impaired gene and protein expression of exocytotic soluble N-ethylmaleimide attachment protein receptor complex proteins in pancreatic islets of type 2 diabetic patients. *Diabetes*, *55*(2), 435–440.
Pace, C. S., & Price, S. (1972). Electrical responses of pancreatic islet cells to secretory stimuli. *Biochemical and Biophysical Research Communications*, *46*(4), 1557–1563.
Palfrey, H. C., & Artalejo, C. R. (2003). Secretion: kiss and run caught on film. *Current Biology*, *13*(10), R397–R399.
Paolisso, G., Scheen, A., d'Onofrio, F., & Lefebvre, P. (1990). Magnesium and glucose homeostasis. *Diabetologia*, *33*(9), 511–514.
Plant, L. D., Dementieva, I. S., Kollewe, A., Olikara, S., Marks, J. D., & Goldstein, S. A. N. (2010). One SUMO is sufficient to silence the dimeric potassium channel K2P1. *Proceedings of the National Academy of Sciences of the United States of America*, *107*(23), 10743–10748. https://doi.org/10.1073/pnas.1004712107
Plant, L. D., Dowdell, E. J., Dementieva, I. S., Marks, J. D., & Goldstein, S. A. N. (2011). SUMO modification of cell surface Kv2.1 potassium channels regulates the activity of rat hippocampal neurons. *The Journal of General Physiology*, *137*(5), 441–454. https://doi.org/10.1085/jgp.201110604
Plant, L. D., Marks, J. D., & Goldstein, S. A. (2016). SUMOylation of NaV1.2 channels mediates the early response to acute hypoxia in central neurons. *ELife*, *5*.

https://doi.org/10.7554/eLife.20054
Prentki, M., & Nolan, C. J. (2006, July). Islet β cell failure in type 2 diabetes. *Journal of Clinical Investigation*. https://doi.org/10.1172/JCI29103
Qin, T., Liang, T., Zhu, D., Kang, Y., Xie, L., Dolai, S., … Gaisano, H. Y. (2017). Munc18b Increases Insulin Granule Fusion, Restoring Deficient Insulin Secretion in Type-2 Diabetes Human and Goto-Kakizaki Rat Islets with Improvement in Glucose Homeostasis. *EBioMedicine*, *16*, 262–274. https://doi.org/10.1016/j.ebiom.2017.01.030
Quianzon, C. C., & Cheikh, I. (2012). History of insulin. *Journal of Community Hospital Internal Medicine Perspectives*. https://doi.org/10.3402/jchimp.v2i2.18701
Rajan, S., Plant, L. D., Rabin, M. L., Butler, M. H., & Goldstein, S. A. N. (2005). Sumoylation silences the plasma membrane leak K+ channel K2P1. *Cell*, *121*(1), 37–47. https://doi.org/10.1016/j.cell.2005.01.019
Ramakrishnan, N. A., Drescher, M. J., & Drescher, D. G. (2012, May). The SNARE complex in neuronal and sensory cells. *Molecular and Cellular Neurosciences*. https://doi.org/10.1016/j.mcn.2012.03.009
Renstrom, E., Eliasson, L., & Rorsman, P. (1997). Protein kinase A-dependent and -independent stimulation of exocytosis by cAMP in mouse pancreatic B-cells. *The Journal of Physiology*, *502 (Pt 1*, 105–118.
Ritchie, J. M., & Rogart, R. B. (1977, January). Density of sodium channels in mammalian myelinated nerve fibers and nature of the axonal membrane under the myelin sheath. *Proceedings of the National Academy of Sciences of the United States of America*.
Riz, M., Braun, M., & Pedersen, M. G. (2014). Mathematical modeling of heterogeneous electrophysiological responses in human beta-cells. *PLoS Computational Biology*, *10*(1), e1003389. https://doi.org/10.1371/journal.pcbi.1003389
Röder, P. V, Wu, B., Liu, Y., & Han, W. (2016, March). Pancreatic regulation of glucose homeostasis. *Experimental & Molecular Medicine*. https://doi.org/10.1038/emm.2016.6
Rorsman, P., & Braun, M. (2013). Regulation of insulin secretion in human pancreatic islets. *Annual Review of Physiology*, *75*, 155–179. https://doi.org/10.1146/annurev-physiol-030212-183754
Rorsman, P., Eliasson, L., Renstrom, E., Gromada, J., Barg, S., & Gopel, S. (2000). The Cell Physiology of Biphasic Insulin Secretion. *News in Physiological Sciences : An International Journal of Physiology Produced Jointly by the International Union of Physiological Sciences and the American Physiological Society*, *15*, 72–77.
Rorsman, P., & Trube, G. (1985). Glucose dependent K+-channels in pancreatic beta-cells are regulated by intracellular ATP. *Pflugers Archiv : European Journal of Physiology*, *405*(4), 305–309.
Rosario, L. M., Barbosa, R. M., Antunes, C. M., Silva, A. M., Abrunhosa, A. J., & Santos, R. M. (1993). Bursting electrical activity in pancreatic beta-cells: evidence that the channel underlying the burst is sensitive to Ca2+ influx through L-type Ca2+ channels. *Pflugers Archiv : European Journal of Physiology*, *424*(5–6), 439–447.
Rosenbluth, J. (1976). Intramembranous particle distribution at the node of Ranvier and adjacent axolemma in myelinated axons of the frog brain. *Journal of Neurocytology*, *5*(6), 731–745.
Rosengren, A. H., Braun, M., Mahdi, T., Andersson, S. A., Travers, M. E., Shigeto, M., … Eliasson, L. (2012). Reduced insulin exocytosis in human pancreatic beta-cells with gene variants linked to type 2 diabetes. *Diabetes*, *61*(7), 1726–1733. https://doi.org/10.2337/db11-1516

Rouille, Y., Martin, S., & Steiner, D. F. (1995). Differential processing of proglucagon by the subtilisin-like prohormone convertases PC2 and PC3 to generate either glucagon or glucagon-like peptide. *The Journal of Biological Chemistry*, *270*(44), 26488–26496.
Routh, V. H., Hao, L., Santiago, A. M., Sheng, Z., & Zhou, C. (2014). Hypothalamic glucose sensing: making ends meet . *Frontiers in Systems Neuroscience* . Retrieved from https://www.frontiersin.org/article/10.3389/fnsys.2014.00236
Rutter, G. A., & Tsuboi, T. (2004). Kiss and run exocytosis of dense core secretory vesicles. *Neuroreport*, *15*(1), 79–81.
Saito, K., Iwama, N., & Takahashi, T. (1978). Morphometrical analysis on topographical difference in size distribution, number and volume of islets in the human pancreas. *The Tohoku Journal of Experimental Medicine*, *124*(2), 177–186.
Saitoh, H., & Hinchey, J. (2000). Functional heterogeneity of small ubiquitin-related protein modifiers SUMO-1 versus SUMO-2/3. *The Journal of Biological Chemistry*, *275*(9), 6252–6258.
Sajman, J., Trus, M., Atlas, D., & Sherman, E. (2017). The L-type Voltage-Gated Calcium Channel co-localizes with Syntaxin 1A in nano-clusters at the plasma membrane. *Scientific Reports*, *7*(1), 11350. https://doi.org/10.1038/s41598-017-10588-4
Salunkhe, V. A., Esguerra, J. L. S., Ofori, J. K., Mollet, I. G., Braun, M., Stoffel, M., … Eliasson, L. (2015). Modulation of microRNA-375 expression alters voltage-gated Na(+) channel properties and exocytosis in insulin-secreting cells. *Acta Physiologica (Oxford, England)*, *213*(4), 882–892. https://doi.org/10.1111/apha.12460
Salzer, J. L. (2003). Polarized domains of myelinated axons. *Neuron*, *40*(2), 297–318.
Sarmiere, P. D., Weigle, C. M., & Tamkun, M. M. (2008). The Kv2.1 K+ channel targets to the axon initial segment of hippocampal and cortical neurons in culture and in situ. *BMC Neuroscience*, *9*, 112. https://doi.org/10.1186/1471-2202-9-112
Scannevin, R. H., Murakoshi, H., Rhodes, K. J., & Trimmer, J. S. (1996). Identification of a cytoplasmic domain important in the polarized expression and clustering of the Kv2.1 K+ channel. *The Journal of Cell Biology*, *135*(6 Pt 1), 1619–1632.
Scarlett, J. M., & Schwartz, M. W. (2015). Gut-brain mechanisms controlling glucose homeostasis. *F1000Prime Reports*. https://doi.org/10.12703/P7-12
Schwartz, M. W., & Porte, D. (2005). Diabetes, Obesity, and the Brain. *Science*, *307*(5708), 375 LP-379.
Shao, C., & Cobb, M. H. (2009). Sumoylation regulates the transcriptional activity of MafA in pancreatic beta cells. *The Journal of Biological Chemistry*, *284*(5), 3117–3124. https://doi.org/10.1074/jbc.M806286200
Sharma, P., Yamada, S., Lualdi, M., Dasso, M., & Kuehn, M. R. (2013). Senp1 is essential for desumoylating Sumo1-modified proteins but dispensable for Sumo2 and Sumo3 deconjugation in the mouse embryo. *Cell Reports*, *3*(5), 1640–1650. https://doi.org/10.1016/j.celrep.2013.04.016
Shen, C., Rathore, S. S., Yu, H., Gulbranson, D. R., Hua, R., Zhang, C., … Shen, J. (2015). The trans-SNARE-regulating function of Munc18-1 is essential to synaptic exocytosis. *Nature Communications*, *6*, 8852. Retrieved from http://dx.doi.org/10.1038/ncomms9852
Sherwin, R. S. (1980). Role of Liver in Glucose Homeostasis. *Diabetes Care*, *3*(2), 261 LP-265.
Shibasaki, T., Takahashi, H., Miki, T., Sunaga, Y., Matsumura, K., Yamanaka, M., … Seino, S. (2007). Essential role of Epac2/Rap1 signaling in regulation of insulin granule dynamics by cAMP. *Proceedings of the National Academy of Sciences of the United States of America*,

104(49), 19333–19338. https://doi.org/10.1073/pnas.0707054104
Simon, S. M., & Llinas, R. R. (1985). Compartmentalization of the submembrane calcium activity during calcium influx and its significance in transmitter release. *Biophysical Journal*, *48*(3), 485–498. https://doi.org/10.1016/S0006-3495(85)83804-2
Singer-Lahat, D., Sheinin, A., Chikvashvili, D., Tsuk, S., Greitzer, D., Friedrich, R., … Lotan, I. (2007). K+ channel facilitation of exocytosis by dynamic interaction with syntaxin. *The Journal of Neuroscience : The Official Journal of the Society for Neuroscience*, *27*(7), 1651–1658. https://doi.org/10.1523/JNEUROSCI.4006-06.2007
Speca, D. J., Ogata, G., Mandikian, D., Bishop, H. I., Wiler, S. W., Eum, K., … Trimmer, J. S. (2014, April). Deletion of the Kv2.1 delayed rectifier potassium channel leads to neuronal and behavioral hyperexcitability. *Genes, Brain, and Behavior*. https://doi.org/10.1111/gbb.12120
Speier, S., Nyqvist, D., Cabrera, O., Yu, J., Molano, R. D., Pileggi, A., … Berggren, P.-O. (2008). Noninvasive in vivo imaging of pancreatic islet cell biology. *Nature Medicine*, *14*, 574. Retrieved from http://dx.doi.org/10.1038/nm1701
Steiner, D. F., & Oyer, P. E. (1967, February). THE BIOSYNTHESIS OF INSULIN AND A PROBABLE PRECURSOR OF INSULIN BY A HUMAN ISLET CELL ADENOMA. *Proceedings of the National Academy of Sciences of the United States of America*.
Su, J., Yu, H., Lenka, N., Hescheler, J., & Ullrich, S. (2001). The expression and regulation of depolarization-activated K+ channels in the insulin-secreting cell line INS-1. *Pflugers Archiv : European Journal of Physiology*, *442*(1), 49–56. https://doi.org/10.1007/s004240000508
Subach, F. V, Patterson, G. H., Manley, S., Gillette, J. M., Lippincott-Schwartz, J., & Verkhusha, V. V. (2009). Photoactivatable mCherry for high-resolution two-color fluorescence microscopy. *Nature Methods*, *6*(2), 153–159. https://doi.org/10.1038/nmeth.1298
Südhof, T. C. (2012, July). The Presynaptic Active Zone. *Neuron*. https://doi.org/10.1016/j.neuron.2012.06.012
Südhof, T. C., & Rothman, J. E. (2009). Membrane Fusion: Grappling with SNARE and SM Proteins. *Science*, *323*(5913), 474 LP-477. Retrieved from http://science.sciencemag.org/content/323/5913/474.abstract
Sutherland, E. W. (1948). Origin and distribution of the hyperglycemic-glycogenolytic factor of the pancreas.
Szabat, M., Modi, H., Ramracheya, R., Girbinger, V., Chan, F., Lee, J. T. C., … Johnson, J. D. (2015). High-content screening identifies a role for Na(+) channels in insulin production. *Royal Society Open Science*, *2*(12), 150306. https://doi.org/10.1098/rsos.150306
Tamarina, N. A., Wang, Y., Mariotto, L., Kuznetsov, A., Bond, C., Adelman, J., & Philipson, L. H. (2003). Small-conductance calcium-activated K+ channels are expressed in pancreatic islets and regulate glucose responses. *Diabetes*, *52*(8), 2000–2006.
Tamkun, M. M., O'connell, K. M. S., & Rolig, A. S. (2007). A cytoskeletal-based perimeter fence selectively corrals a sub-population of cell surface Kv2.1 channels. *Journal of Cell Science*, *120*(Pt 14), 2413–2423. https://doi.org/10.1242/jcs.007351
Tang, L. T.-H., Craig, T. J., & Henley, J. M. (2015). SUMOylation of synapsin Ia maintains synaptic vesicle availability and is reduced in an autism mutation. *Nature Communications*, *6*, 7728.
Thomann, D., Rines, D. R., Sorger, P. K., & Danuser, G. (2002). Automatic fluorescent tag detection in 3D with super-resolution: application to the analysis of chromosome

movement. *Journal of Microscopy*, *208*(Pt 1), 49–64.
Tinker, A., Aziz, Q., & Thomas, A. (2014). The role of ATP-sensitive potassium channels in cellular function and protection in the cardiovascular system. *British Journal of Pharmacology*, *171*(1), 12–23.
Toft-Bertelsen, T. L., Ziomkiewicz, I., Houy, S., Pinheiro, P. S., & Sørensen, J. B. (2016, November). Regulation of Ca(2+) channels by SNAP-25 via recruitment of syntaxin-1 from plasma membrane clusters. (T. F. J. Martin, Ed.), *Molecular Biology of the Cell*. https://doi.org/10.1091/mbc.E16-03-0184
Togashi, K., Hara, Y., Tominaga, T., Higashi, T., Konishi, Y., Mori, Y., & Tominaga, M. (2006). TRPM2 activation by cyclic ADP-ribose at body temperature is involved in insulin secretion. *The EMBO Journal*, *25*(9), 1804–1815.
Trimmer, J. S. (1991). Immunological identification and characterization of a delayed rectifier K+ channel polypeptide in rat brain. *Proceedings of the National Academy of Sciences of the United States of America*, *88*(23), 10764–10768.
Tucker, S. J., Gribble, F. M., Proks, P., Trapp, S., Ryder, T. J., Haug, T., … Ashcroft, F. M. (1998, June). Molecular determinants of KATP channel inhibition by ATP. *The EMBO Journal*. https://doi.org/10.1093/emboj/17.12.3290
Ueda, K., Komine, J., Matsuo, M., Seino, S., & Amachi, T. (1999, February). Cooperative binding of ATP and MgADP in the sulfonylurea receptor is modulated by glibenclamide. *Proceedings of the National Academy of Sciences of the United States of America*.
Ullrich, A., Bohme, M. A., Schoneberg, J., Depner, H., Sigrist, S. J., & Noe, F. (2015). Dynamical Organization of Syntaxin-1A at the Presynaptic Active Zone. *PLoS Computational Biology*, *11*(9), e1004407. https://doi.org/10.1371/journal.pcbi.1004407
Ungar, D., & Hughson, F. M. (2003). SNARE protein structure and function. *Annual Review of Cell and Developmental Biology*, *19*, 493–517. https://doi.org/10.1146/annurev.cellbio.19.110701.155609
Urbina, F. L., Gomez, S. M., & Gupton, S. L. (2018). Spatiotemporal organization of exocytosis emerges during neuronal shape change, 1–16.
Urrego, D., Tomczak, A. P., Zahed, F., Stühmer, W., & Pardo, L. A. (2014, March). Potassium channels in cell cycle and cell proliferation. *Philosophical Transactions of the Royal Society B: Biological Sciences*. https://doi.org/10.1098/rstb.2013.0094
van den Bogaart, G., Meyenberg, K., Risselada, H. J., Amin, H., Willig, K. I., Hubrich, B. E., … Jahn, R. (2011). Membrane protein sequestering by ionic protein-lipid interactions. *Nature*, *479*(7374), 552–555. https://doi.org/10.1038/nature10545
Vergari, E., Plummer, G., Dai, X., & MacDonald, P. E. (2012). DeSUMOylation controls insulin exocytosis in response to metabolic signals. *Biomolecules*, *2*(2), 269–281. https://doi.org/10.3390/biom2020269
Wagner, T. F. J., Loch, S., Lambert, S., Straub, I., Mannebach, S., Mathar, I., … Philipp, S. E. (2008). Transient receptor potential M3 channels are ionotropic steroid receptors in pancreatic β cells. *Nature Cell Biology*, *10*(12), 1421.
Waxman, S. G., Black, J. A., Kocsis, J. D., & Ritchie, J. M. (1989, February). Low density of sodium channels supports action potential conduction in axons of neonatal rat optic nerve. *Proceedings of the National Academy of Sciences of the United States of America*.
Wen, X., Saltzgaber, G. W., & Thoreson, W. B. (2017). Kiss-and-Run Is a Significant Contributor to Synaptic Exocytosis and Endocytosis in Photoreceptors . *Frontiers in Cellular Neuroscience* . Retrieved from

https://www.frontiersin.org/article/10.3389/fncel.2017.00286
Wheeler, M. B., Sheu, L., Ghai, M., Bouquillon, A., Grondin, G., Weller, U., … Gaisano, H. Y. (1996). Characterization of SNARE protein expression in beta cell lines and pancreatic islets. *Endocrinology*, *137*(4), 1340–1348. https://doi.org/10.1210/endo.137.4.8625909
White, M. F. (2003). Insulin Signaling in Health and Disease. *Science*, *302*(5651), 1710 LP-1711. Retrieved from http://science.sciencemag.org/content/302/5651/1710.abstract
Wilkinson, K. A., Nishimune, A., & Henley, J. M. (2008, May). Analysis of SUMO-1 modification of neuronal proteins containing consensus SUMOylation motifs. *Neuroscience Letters*. https://doi.org/10.1016/j.neulet.2008.03.029
Williamson, D. J., Owen, D. M., Rossy, J., Magenau, A., Wehrmann, M., Gooding, J. J., & Gaus, K. (2011). Pre-existing clusters of the adaptor Lat do not participate in early T cell signaling events. *Nature Immunology*, *12*(7), 655–662. https://doi.org/10.1038/ni.2049
Wiser, O., Trus, M., Hernández, A., Renström, E., Barg, S., Rorsman, P., & Atlas, D. (1999). The voltage sensitive Lc-type Ca²⁺ channel is functionally coupled to the exocytotic machinery. *Proceedings of the National Academy of Sciences*, *96*(1), 248 LP-253. Retrieved from http://www.pnas.org/content/96/1/248.abstract
Wolf-Goldberg, T., Michaelevski, I., Sheu, L., Gaisano, H. Y., Chikvashvili, D., & Lotan, I. (2006). Target soluble N-ethylmaleimide-sensitive factor attachment protein receptors (t-SNAREs) differently regulate activation and inactivation gating of Kv2.2 and Kv2.1: Implications on pancreatic islet cell Kv channels. *Molecular Pharmacology*, *70*(3), 818–828. https://doi.org/10.1124/mol.105.021717
Wong, M. Y., Liu, C., Wang, S. S. H., Roquas, A. C. F., Fowler, S. C., & Kaeser, P. S. (2018). Liprin-alpha3 controls vesicle docking and exocytosis at the active zone of hippocampal synapses. *Proceedings of the National Academy of Sciences of the United States of America*, *115*(9), 2234–2239. https://doi.org/10.1073/pnas.1719012115
Woods, S. C., Lotter, E. C., McKay, L. D., & Porte, D. J. (1979). Chronic intracerebroventricular infusion of insulin reduces food intake and body weight of baboons. *Nature*, *282*(5738), 503–505.
Xia, F., Gao, X., Kwan, E., Lam, P. P. L., Chan, L., Sy, K., … Tsushima, R. G. (2004). Disruption of pancreatic beta-cell lipid rafts modifies Kv2.1 channel gating and insulin exocytosis. *The Journal of Biological Chemistry*, *279*(23), 24685–24691. https://doi.org/10.1074/jbc.M314314200
Xia, F., Xie, L., Mihic, A., Gao, X., Chen, Y., Gaisano, H. Y., & Tsushima, R. G. (2008). Inhibition of Cholesterol Biosynthesis Impairs Insulin Secretion and Voltage-Gated Calcium Channel Function in Pancreatic β-Cells. *Endocrinology*, *149*(10), 5136–5145.
Xia, X.-M., Ding, J. P., & Lingle, C. J. (1999). Molecular basis for the inactivation of Ca2+-and voltage-dependent BK channels in adrenal chromaffin cells and rat insulinoma tumor cells. *Journal of Neuroscience*, *19*(13), 5255–5264.
Xiong, D., Li, T., Dai, H., Arena, A. F., Plant, L. D., & Goldstein, S. A. N. (2017). SUMOylation determines the voltage required to activate cardiac IKs channels. *Proceedings of the National Academy of Sciences of the United States of America*, *114*(32), E6686–E6694. https://doi.org/10.1073/pnas.1706267114
Yan, L., Figueroa, D. J., Austin, C. P., Liu, Y., Bugianesi, R. M., Slaughter, R. S., … Kohler, M. G. (2004). Expression of voltage-gated potassium channels in human and rhesus pancreatic islets. *Diabetes*, *53*(3), 597–607.
Yang, P., Hu, S., Yang, F., Guan, X.-Q., Wang, S.-Q., Zhu, P., … Yu, Q.-L. (2014). Sumoylation

modulates oxidative stress relevant to the viability and functionality of pancreatic beta cells. *American Journal of Translational Research*, *6*(4), 353.

Yang, Y. H. C., Vilin, Y. Y., Roberge, M., Kurata, H. T., & Johnson, J. D. (2014). Multiparameter screening reveals a role for Na+ channels in cytokine-induced beta-cell death. *Molecular Endocrinology (Baltimore, Md.)*, *28*(3), 406–417. https://doi.org/10.1210/me.2013-1257

Yasuda, T., Shibasaki, T., Minami, K., Takahashi, H., Mizoguchi, A., Uriu, Y., … Seino, S. (2010). Rim2alpha determines docking and priming states in insulin granule exocytosis. *Cell Metabolism*, *12*(2), 117–129. https://doi.org/10.1016/j.cmet.2010.05.017

Yuan, T., Lu, J., Zhang, J., Zhang, Y., & Chen, L. (2015). Spatiotemporal detection and analysis of exocytosis reveal fusion "hotspots" organized by the cytoskeleton in endocrine cells. *Biophysical Journal*, *108*(2), 251–260. https://doi.org/10.1016/j.bpj.2014.11.3462

Zhang, Y., Liu, Y., Qu, J., Hardy, A., Zhang, N., Diao, J., … Wheeler, M. B. (2009, October). Functional Characterization of HCN Channels in Rat Pancreatic β Cells. *The Journal of Endocrinology*. https://doi.org/10.1677/JOE-09-0068

Zhang, Y., McKay, S. E., Bewley, B., & Kaczmarek, L. K. (2008). Repetitive firing triggers clustering of Kv2.1 potassium channels in Aplysia neurons. *The Journal of Biological Chemistry*, *283*(16), 10632–10641. https://doi.org/10.1074/jbc.M800253200

Zhu, D., Xie, L., Karimian, N., Liang, T., Kang, Y., Huang, Y.-C., & Gaisano, H. Y. (2015). Munc18c mediates exocytosis of pre-docked and newcomer insulin granules underlying biphasic glucose stimulated insulin secretion in human pancreatic beta-cells. *Molecular Metabolism*, *4*(5), 418–426. https://doi.org/10.1016/j.molmet.2015.02.004

Zhu, X., Hu, R., Brissova, M., Stein, R. W., Powers, A. C., Gu, G., & Kaverina, I. (2015). Microtubules negatively regulate insulin secretion in pancreatic β cells. *Developmental Cell*, *34*(6), 656–668. https://doi.org/10.1016/j.devcel.2015.08.020